



اوتيو تكنولوجي مارا
UNIVERSITI
TEKNOLOGI
MARA

Possible Physical Mechanism between Solar Activity and Earthquake Events

Mohamad Huzaimy Jusoh

Applied Electromagnetic Research Group

Faculty of Electrical Engineering

Universiti Teknologi MARA

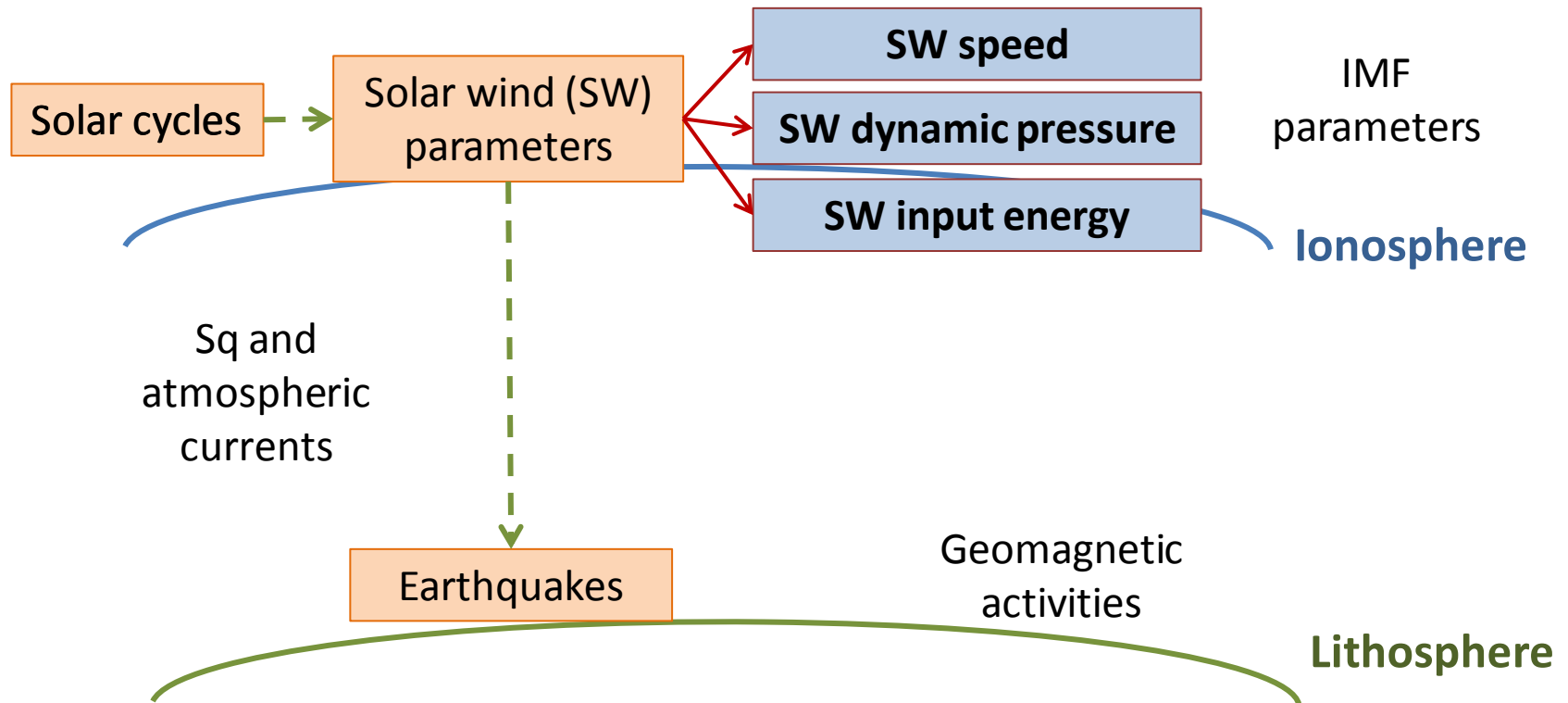
MALAYSIA

CONTENTS

1. Introduction
2. Motivations
3. Results
 - 3.1 Variations of solar cycle and earthquakes
 - 3.2 Solar wind parameters associated with earthquakes
4. Discussion: Possible physical mechanisms
5. Current research activities
6. Conclusion

1. Introduction: Solar activity and Seismicity

- A comprehensive analysis for possible correlation of solar activity and seismicity requires a large database for both extraterrestrial and terrestrial parameters.

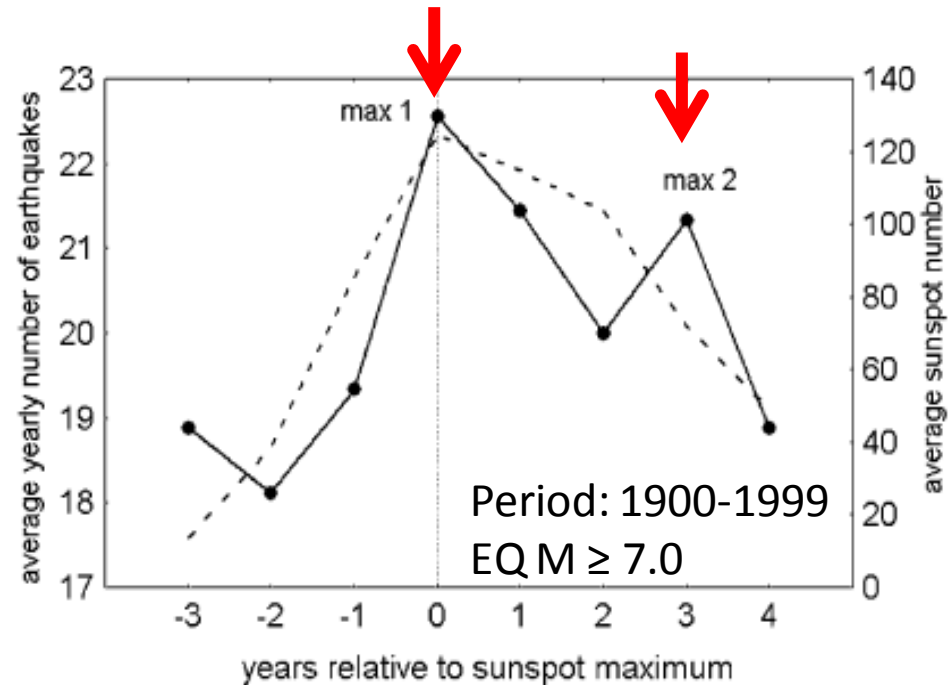
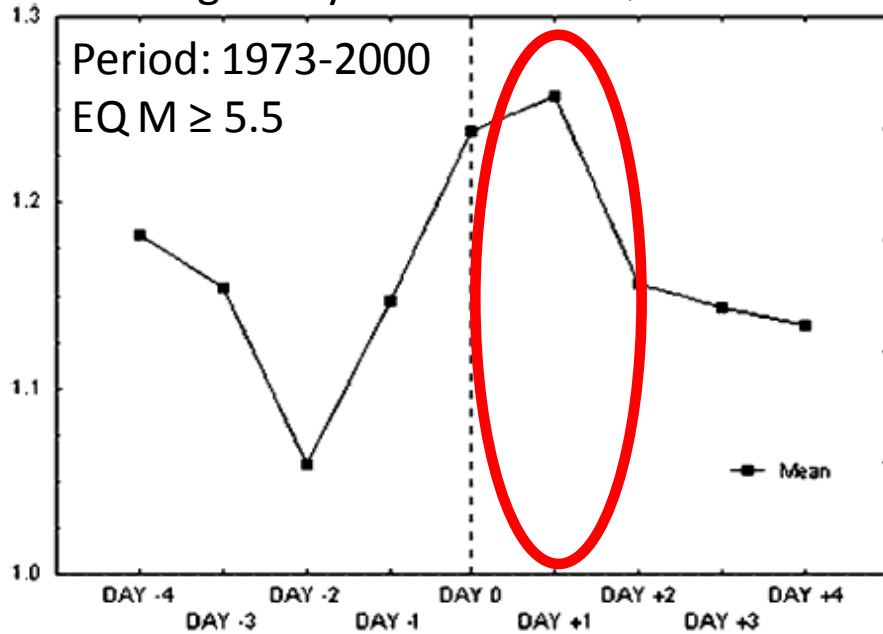


2. Motivation (Previous studies)

2.1 Trends of global seismicity and solar activity

[S. Odintsov et al., 2005]

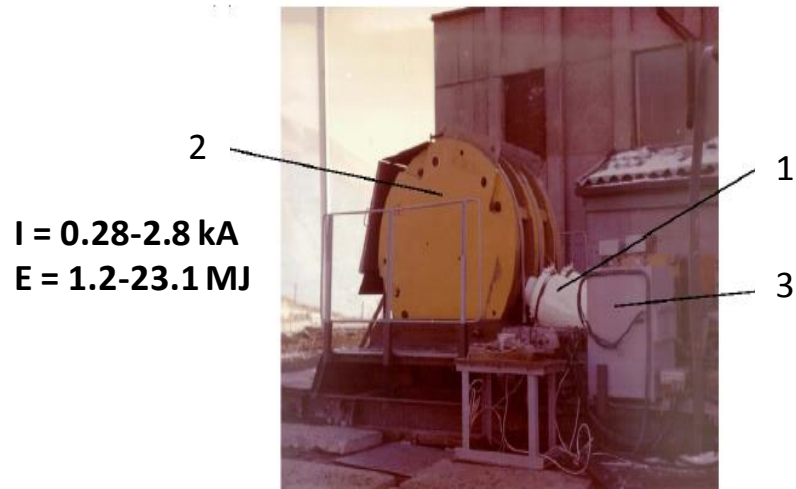
Average daily number of EQ with HSSW



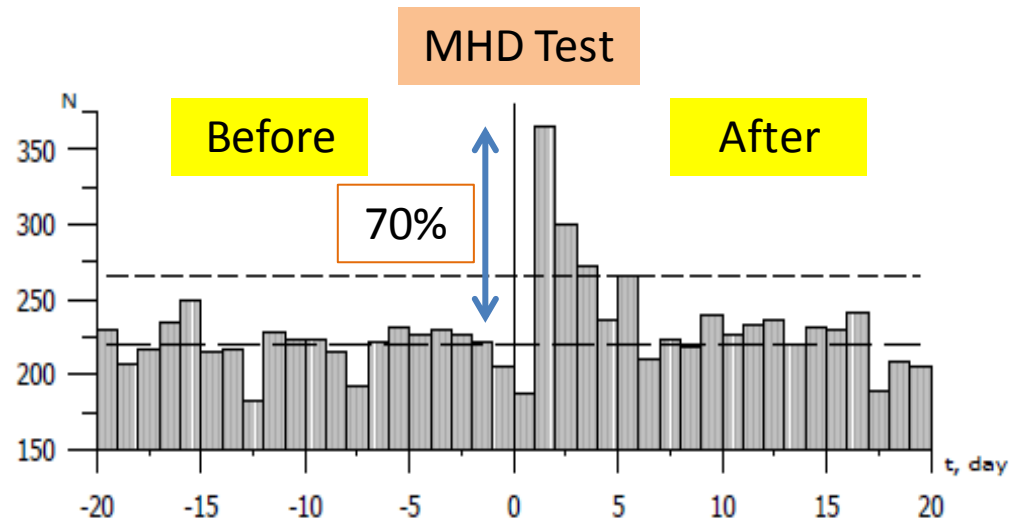
- Average number of EQ with high speed solar wind (HSSW) maximum 1 day after the arrival of HSSW.
- Analysis on average yearly EQ with SSN shows 2-peak trends; 1 coinciding with max SC and another 1 during descending SC.
- Suggested 2 possible corresponding factor of EQ; coronal mass ejections (max SC) and HSSW (CH) (descending SC).

2.2 Induced Earthquakes under the effect of High Energy Electromagnetic Pulses

[Nikolai T. Tarasov and Nadezhda V. Tarasova, 2004]



Pulsed MHD generator installed at Bishkek geophysical proving ground (Kyrgysia, Northern Tien-Shan); 1 – solid propellant plasma generators; 2 – magnet system; 3 – electric switching equipment



Variation of average daily earthquake number of Northern Tien Shan and adjacent areas before ($t < 0$) and after ($t > 0$) MHD generator firing run at Bishkek proving ground.

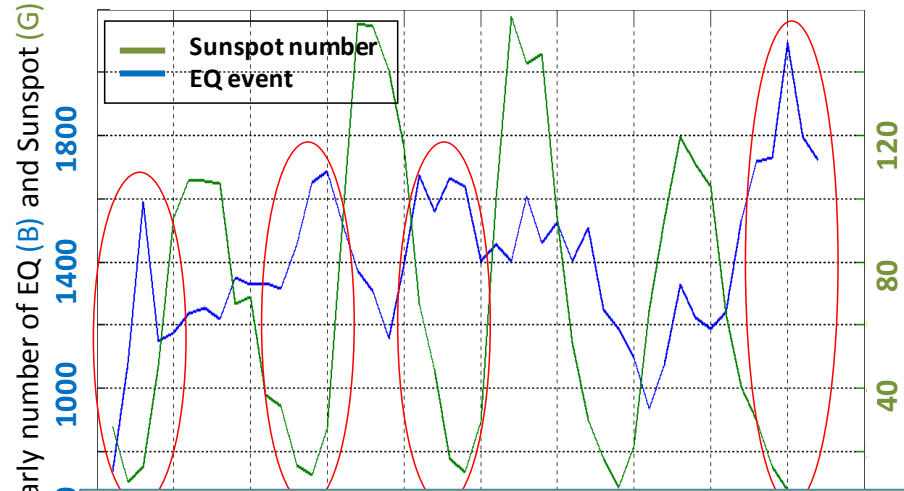
- The induced EQs increased nearly 70% within 2-6 days after MHD generator runs.
- The EQs triggered are shallow depth (5-25 km) and $M \leq 5.0$

3. Results

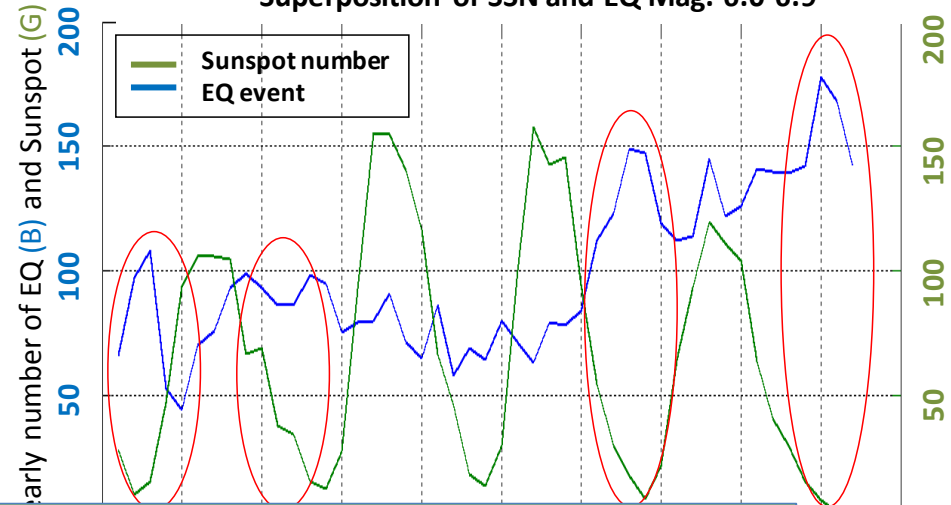
Num.	Result
3.1	Variation of Earthquake Occurrence with Solar Cycle (SC)
3.2	Solar wind parameters associated with earthquakes
3.2.1	Relationship of EQ with HSSW
3.2.2	Relationship of Earthquakes with Solar Wind Input Energy, ϵ (epsilon)

3.1.1 Occurrences of Earthquakes with Solar cycles (SC 20-23)

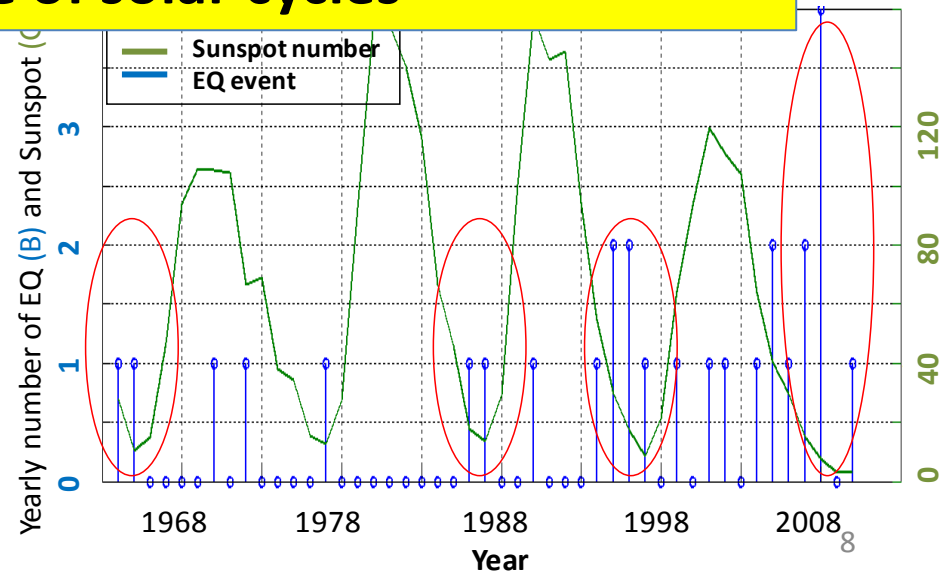
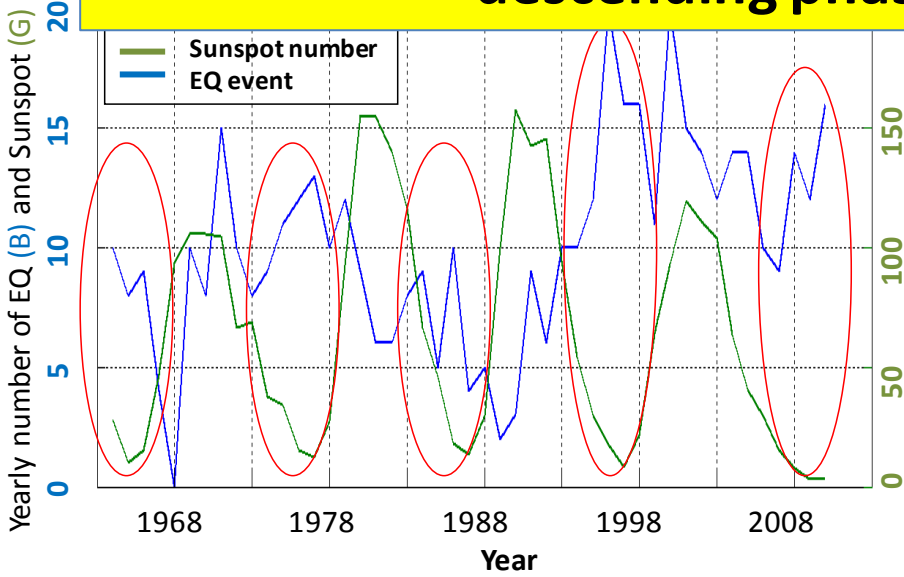
Superposition of Sunspot number and EQ Mag. 5.0-5.9



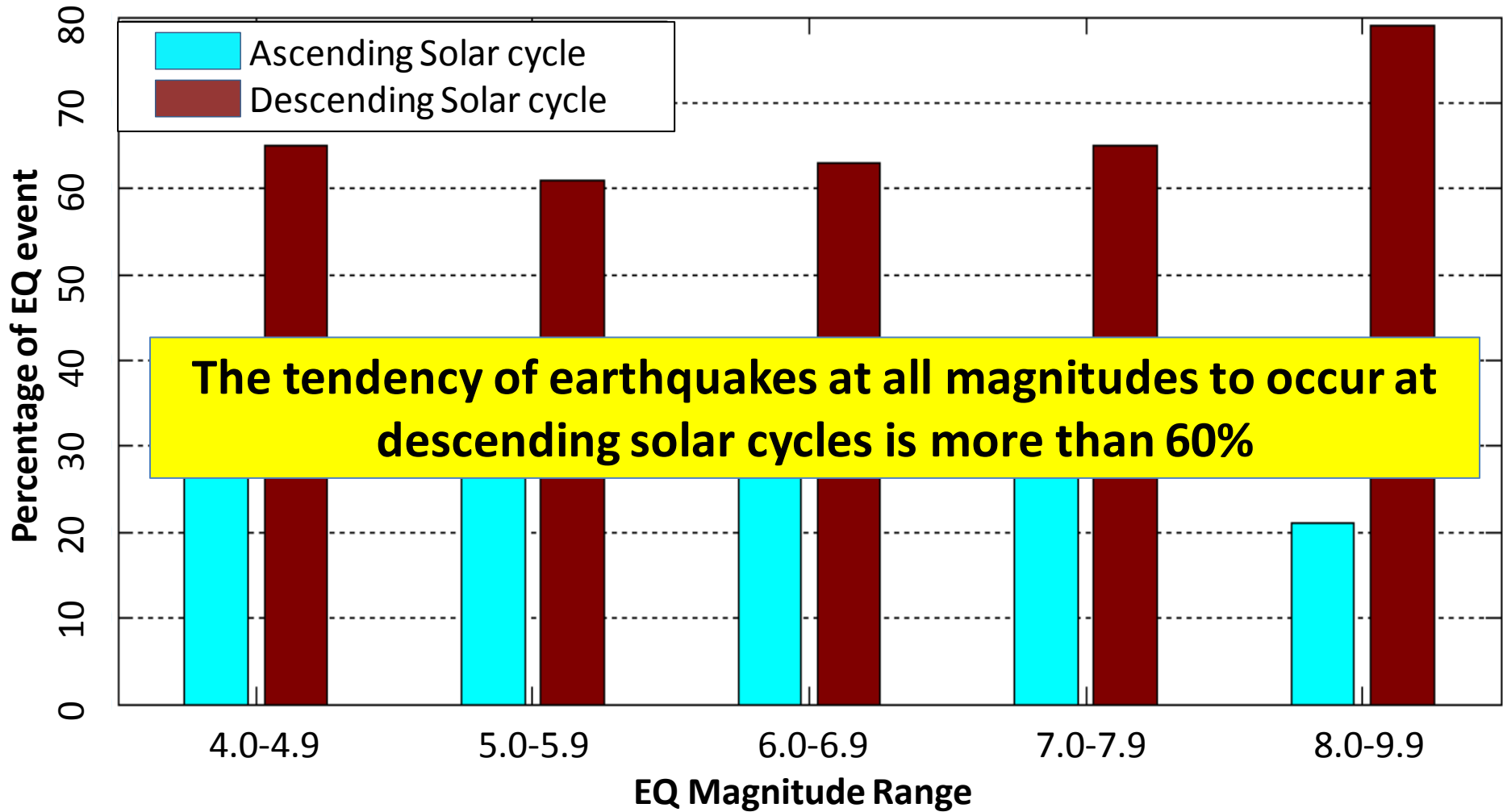
Superposition of SSN and EQ Mag. 6.0-6.9



Higher number of earthquake events tend to occur during descending phase of solar cycles



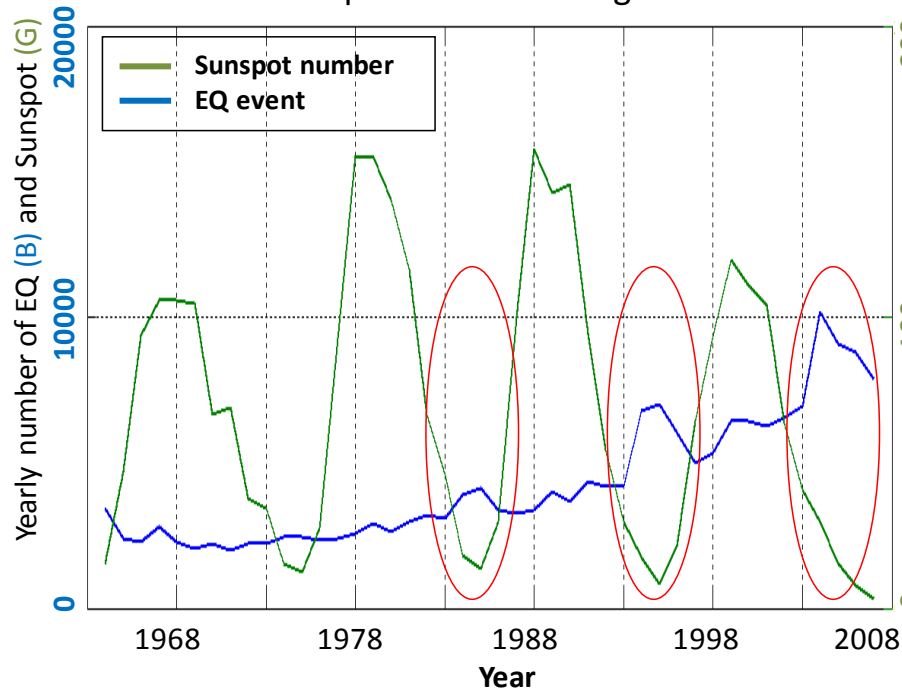
3.1.2 Percentage of EQ Occurrence during Different Phases of Solar Cycles 20 to 23



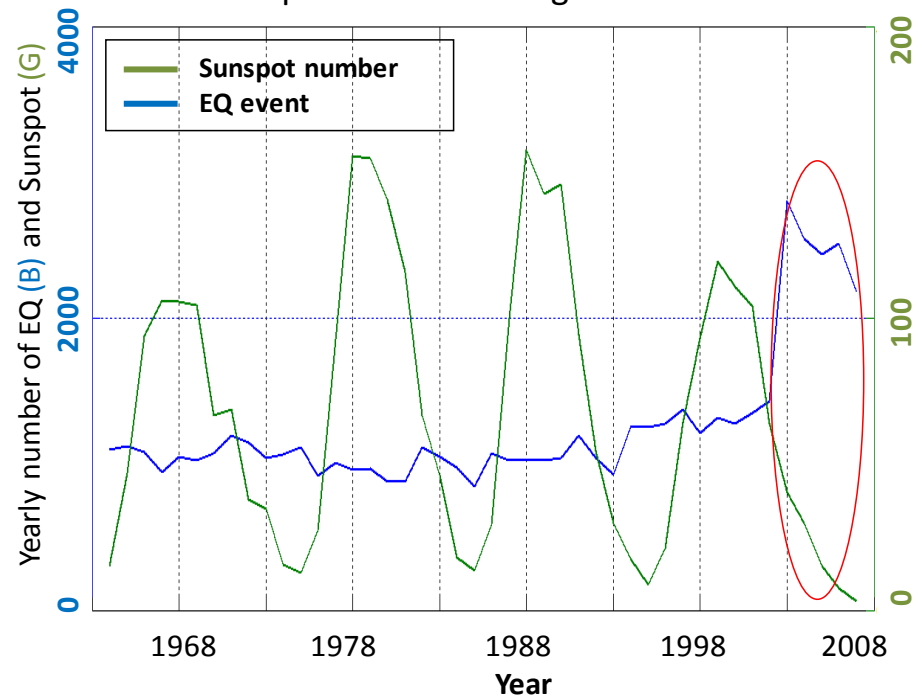
Total	Event =	255,567	66,776	4,767	487	28

3.1.3 Variation of Earthquake depth with Solar cycle

Earthquake at epicenter depth < 40 km with sunspot number during SC 20-23



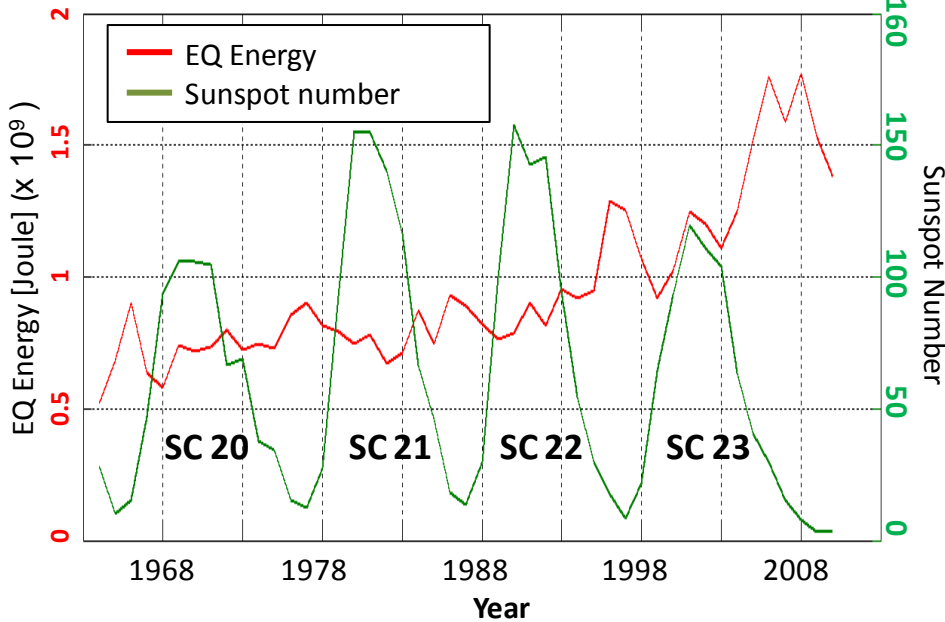
Earthquake at epicenter depth 40-100 km with sunspot number during SC 20-23



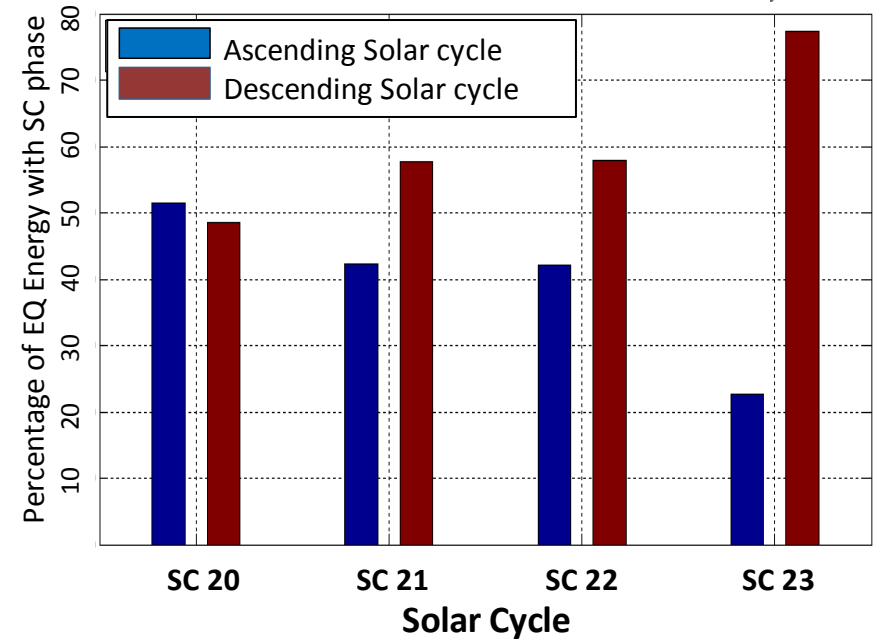
- Number of EQ (both epicenter depth ranges) shows increasing trend.
- Number of shallow earthquake appears higher during lower sunspot number especially during minimum phases of SC 21-23.
- No significant corresponding between SC phases and EQ at epicenter depth 40-100 km except during minimum phase of SC 23.

3.1.4 Energy Released in Global Earthquakes

EQ energy released during SC 20-23



Comparison of EQ energy and SC phases



Jusoh and Yumoto, 2011

- The earthquake energy calculated based on seismic energy method [Kanamori, 1977]:

$$\text{Log } E = 1.5M + 4.7$$

E: EQ energy [Joule]

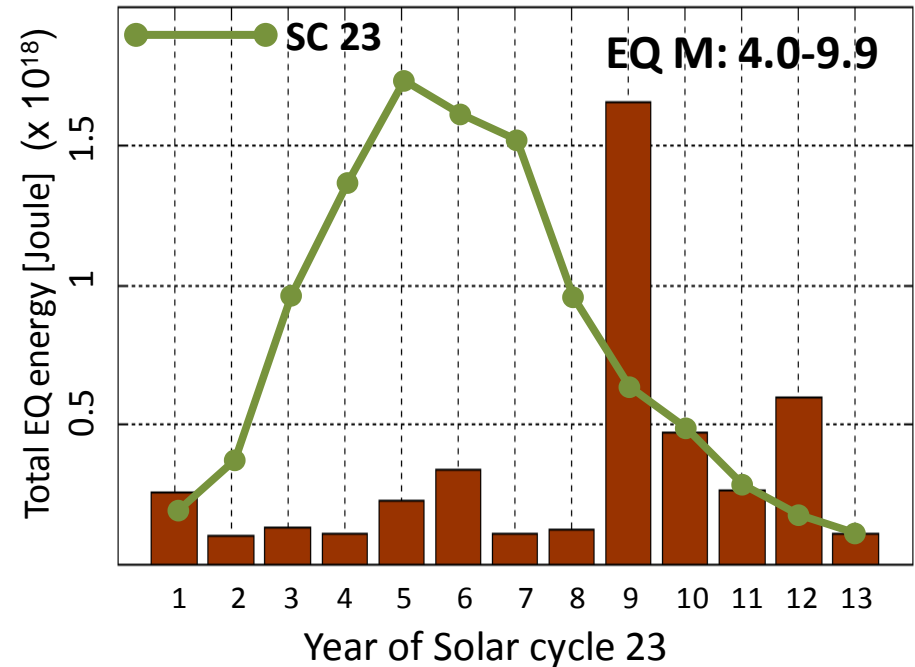
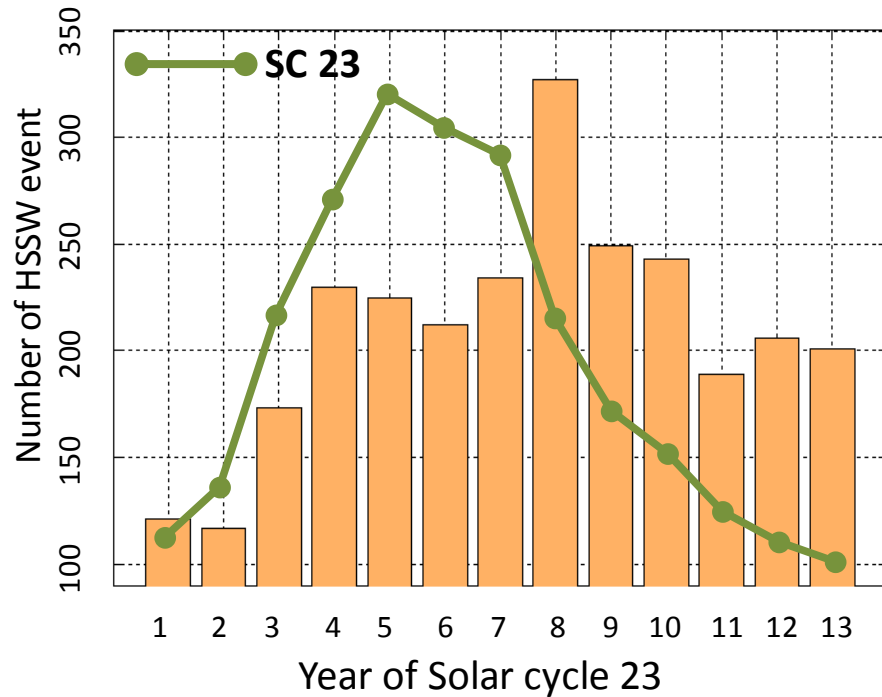
M: EQ magnitude

- In general, EQ energy shows increasing trend.
- It can be seen clearly the amount of released energy from earthquake events are significantly higher during descending phases of solar cycles.

3. Results

Num.	Result
3.1	Variation of Earthquake Occurrence with Solar Cycle (SC)
3.2	Solar wind parameters associated with earthquakes
3.2.1	Relationship of EQ with HSSW
3.2.2	Relationship of Earthquakes with Solar Wind Input Energy, ϵ (epsilon)

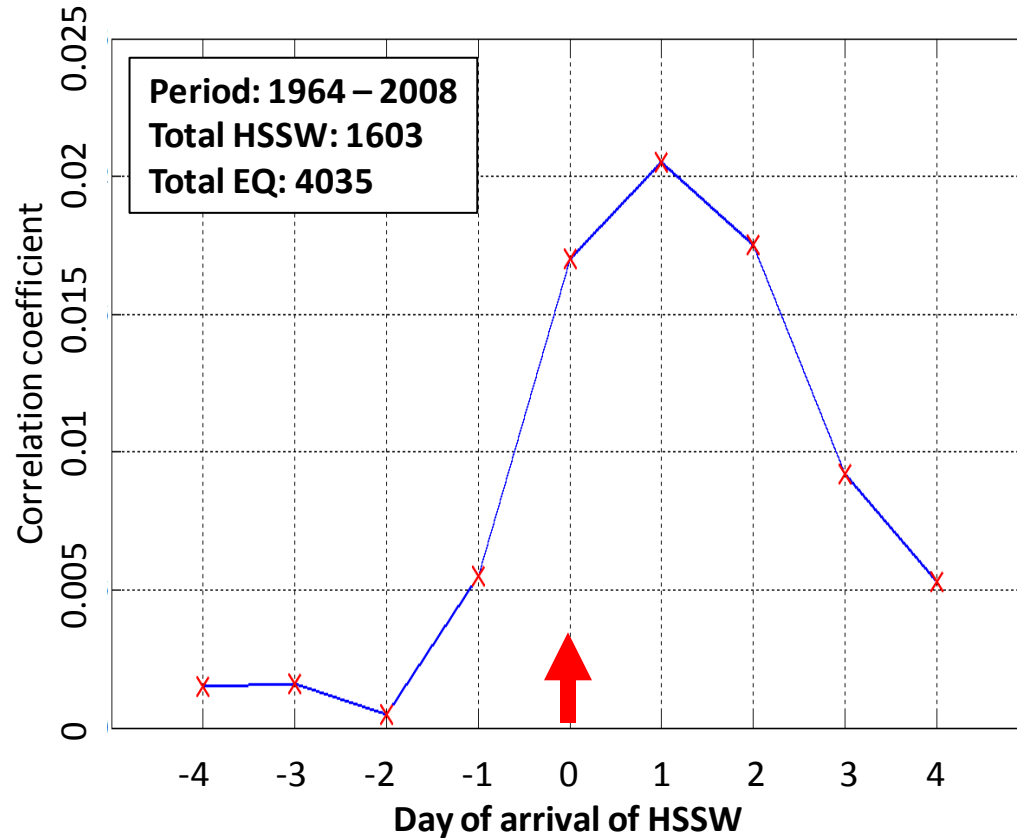
3.2.1 High Speed Solar Wind Events (HSSW) (SC 23)



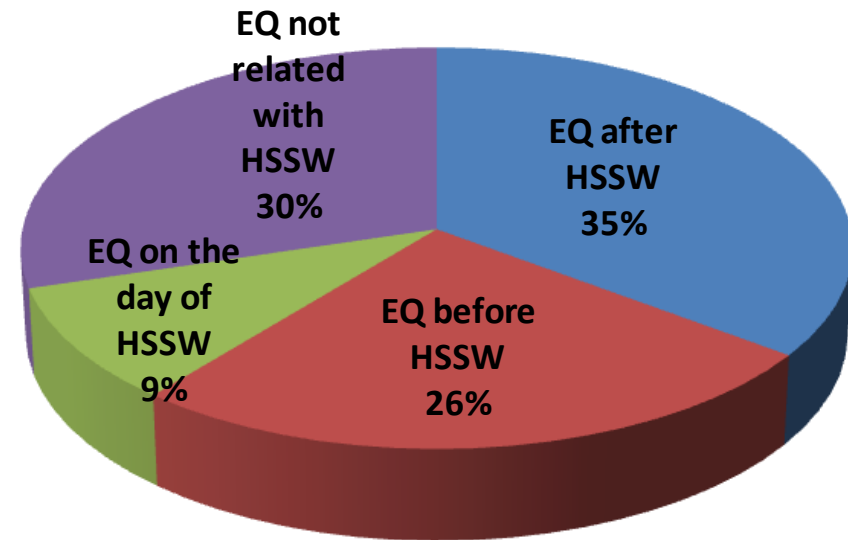
- ◆ Higher number of HSSW events occurred during descending phase of SC 23
- ◆ The amount of earthquake released energy is higher during descending phase of SC 23; the same trend with HSSW event.

3.2.1 High Speed Solar Wind and Earthquakes (M=5.0-9.9)

Occurrence of Great EQ with respect to HSSW



Percentage of Earthquake with respect to HSSW



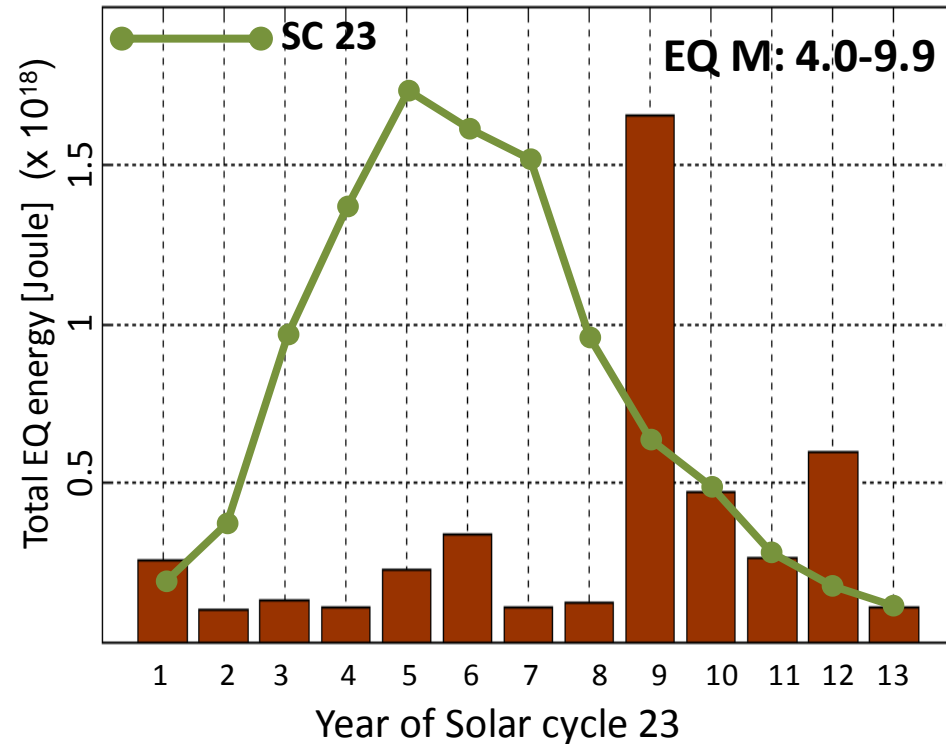
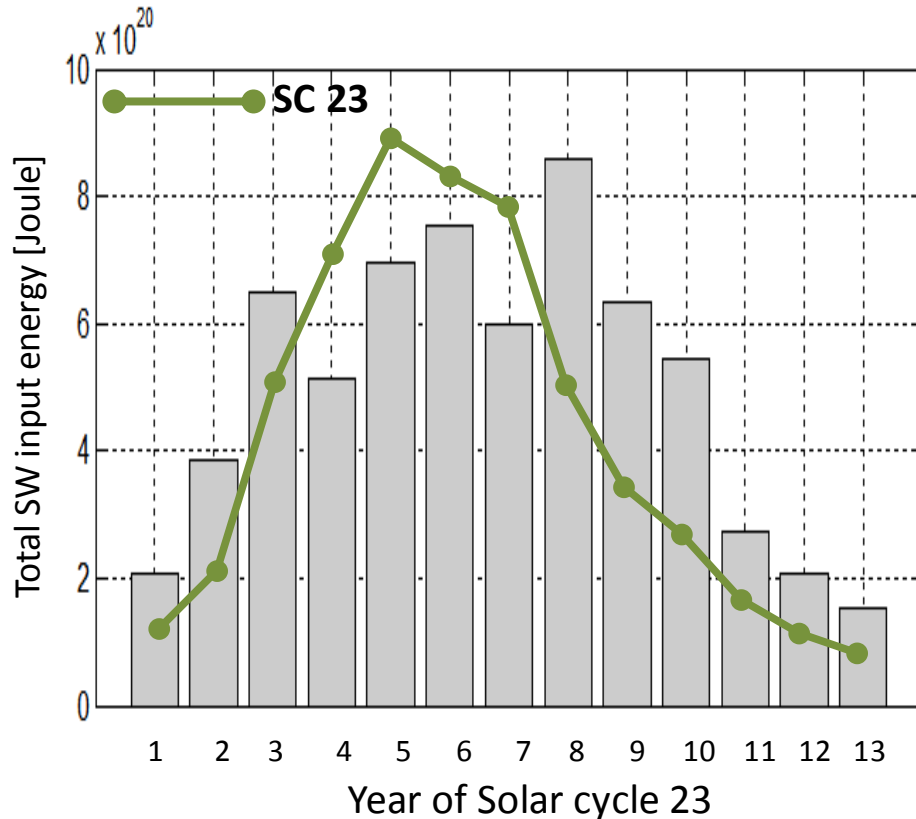
Jusoh and Yumoto, 2011

- Even though the values of correlation coefficients are low, the period of 1 day after the arrival of HSSW shows highest corresponding with the seismic events

3. Results

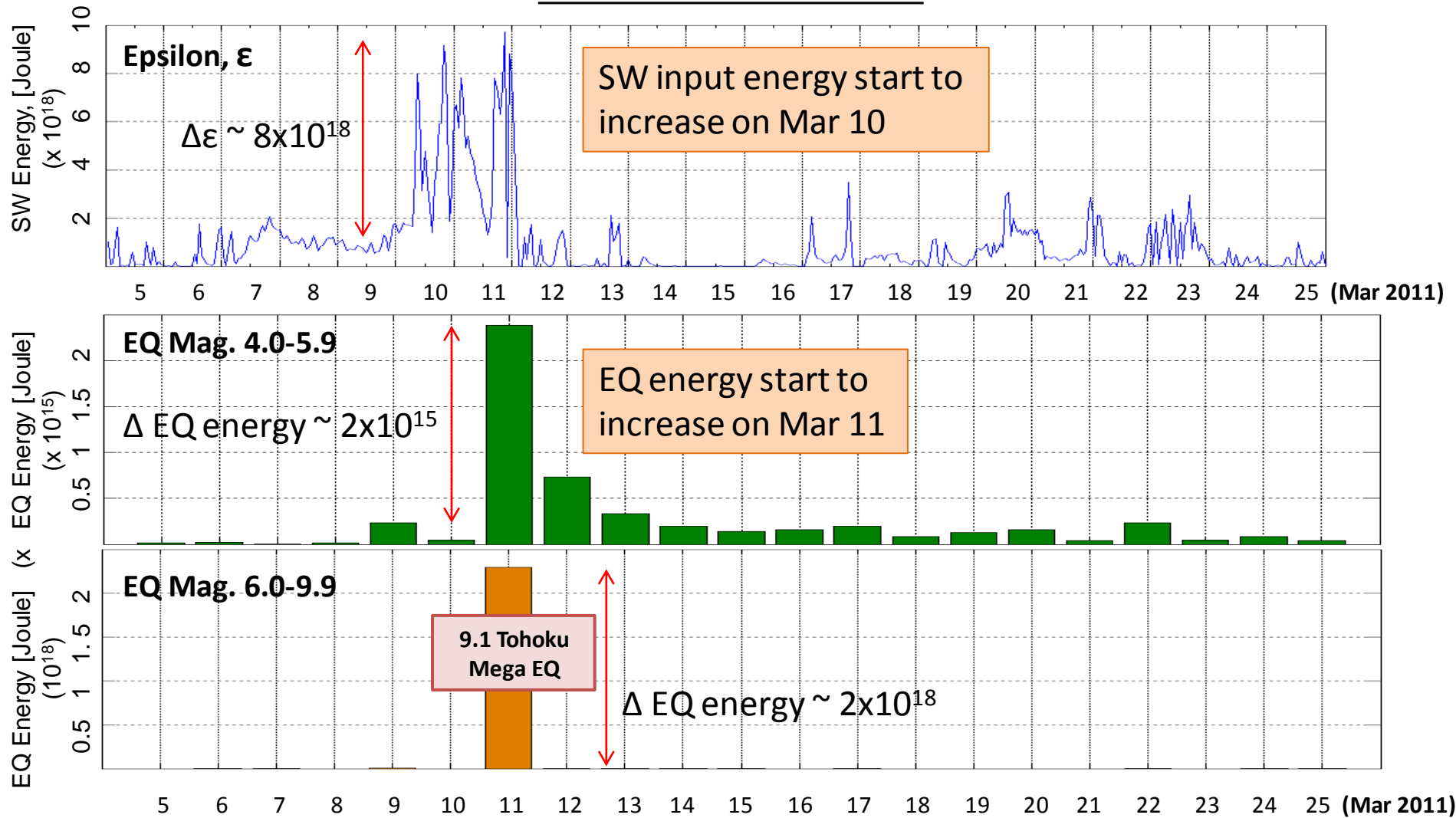
Num.	Result
3.1	Variation of Earthquake Occurrence with Solar Cycle (SC)
3.2	Solar wind parameters associated with earthquakes
3.2.1	Relationship of EQ with HSSW
3.2.2	Relationship of Earthquakes with Solar Wind Input Energy, ϵ (epsilon)

3.2.3 Annual solar wind input energy variation (SC 23)



- ◆ Higher amplitude of solar wind input energy occurred during descending phase of SC 23
- ◆ The amount of earthquake released energy is higher during descending phase of SC 23; the same trend with solar wind input energy .

3.2.3 Relationship of Solar Wind Input Energy with EQ: 5 – 25 March 2011



- The amount of SW input energy is very big as compared with the EQ energy
 ➔ It could be sufficient to be one of the energy source of earthquakes.

4. Discussion: Possible Physical mechanism

- Our analysis shows earthquake events correspond well with higher solar wind parameters.

BUT

- How the effect of solar wind can be transferred into mechanical energy and possibly trigger the earthquake?
- We examined 2 possible coupling mechanisms:
 1. Ground magnetic pulsation (Ultra Low Frequency)
 2. Lorentz force

4.1 Possible physical mechanism: Ground magnetic pulsation

Table 1: IAGA classification of ULF waves in 1964

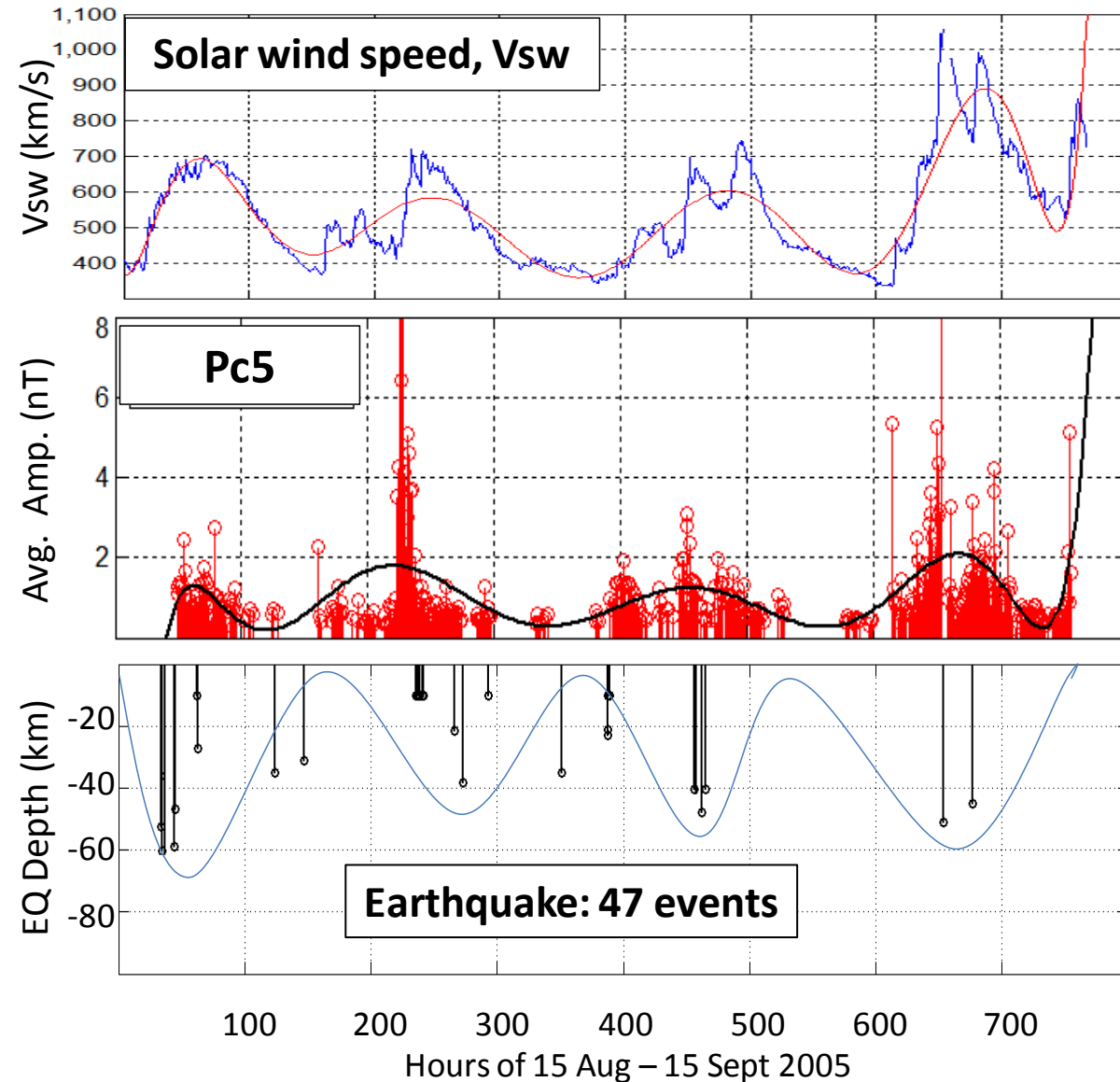
CONTINUOUS						IRREGULAR	
	Pc 1	Pc 2	Pc 3	Pc 4	Pc 5	Pi 1	Pi 2
Period (sec)	0.2-5	5-10	10-45	45-150	150-600	1-40	40-150
Frequency (mHz)	200-5000	100-200	22-100	6.7-22	1.7-6.7	25-1000	6.7-25

Table2 : Dependence of the skin depth in the lithosphere

Skin depth δ (km)		Conductivity σ (S/m)			
		10^{-1}	10^{-2}	10^{-3}	
T (Period)	sec	10	5.03	15.91	50.32
		45	10.68	33.76	106.76
		150	19.4	61.64	194.92
	min	50	87.18	275.66	871.73
		150	150.99	477.46	1509.88

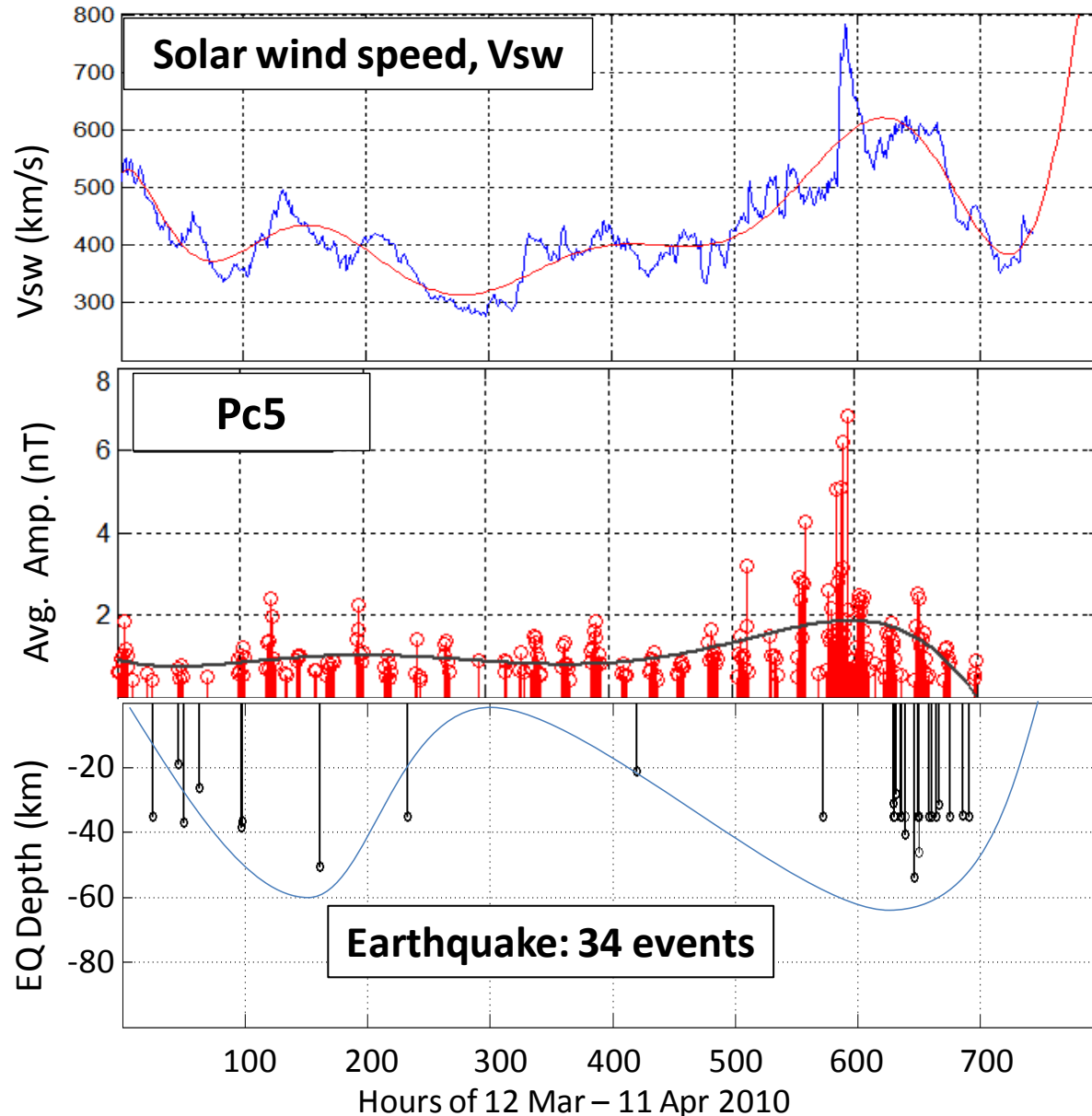
Yumoto et al., 2009

4.1.1 Relationship of Vsw and magnetic pulsations (Pc5) at North Japan (15 Aug-15 Sept 2005)



- ◆ EQ events (30-60 km epicenter depth) tend to occur during period of high Pc5 amplitude
- ◆ Variation of Pc5 amplitude shows good correlation with solar wind speed [*Rae et. al, 2005*].

4.1.2 Relationship of Vsw and magnetic pulsations (Pc5) at North Sumatra (12 Mar – 11 Apr 2010)

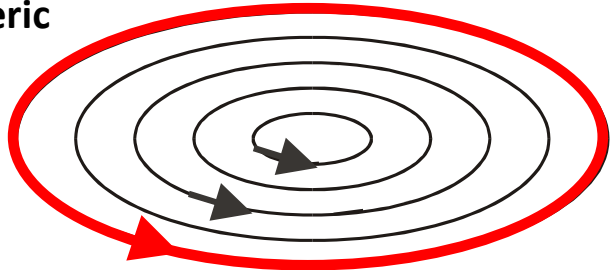


- ◆ EQ events (30-60 km epicenter depth) tend to occur during period of high Pc5 amplitude
- ◆ Variation of Pc5 amplitude shows good correlation with solar wind speed [Rae et. al, 2005].

4.2 Possible physical mechanism: Lorentz Force

This concept explains the consequences of electromagnetic forces (Lorentz force) between electric charges and currents [G. Duma and Y. Ruzhin, 2003].

Ionospheric current system



Basic electro-dynamic principles:

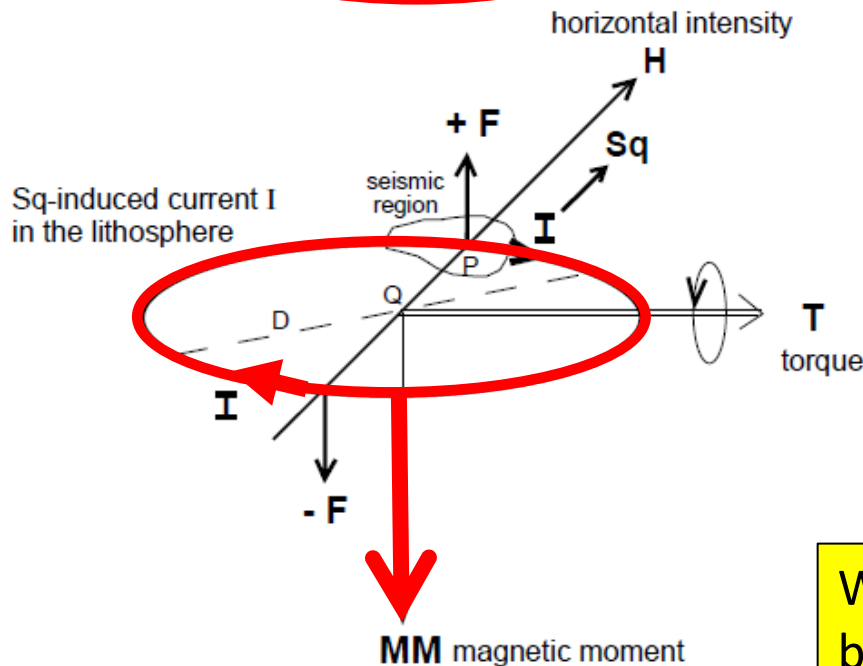
$$MM = \mu_0 * I * (D^2 * (\pi/4))$$

MM: magnetic moment [Am²]

μ_0 : permeability of free space

I: Electric current [A]

D: diameter of enclosed area [m]



$$T = MM \times H$$

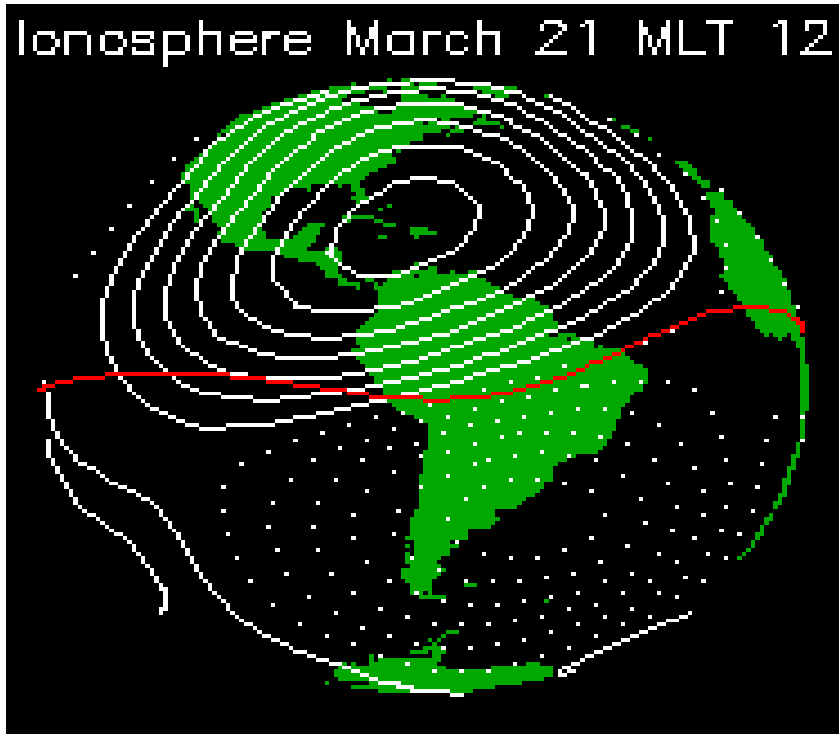
T: torque [Joule]

H: geomagnetic horizontal intensity [A/m]

We introduces the possible connection between solar wind input energy and the forces transferred into the lithosphere.

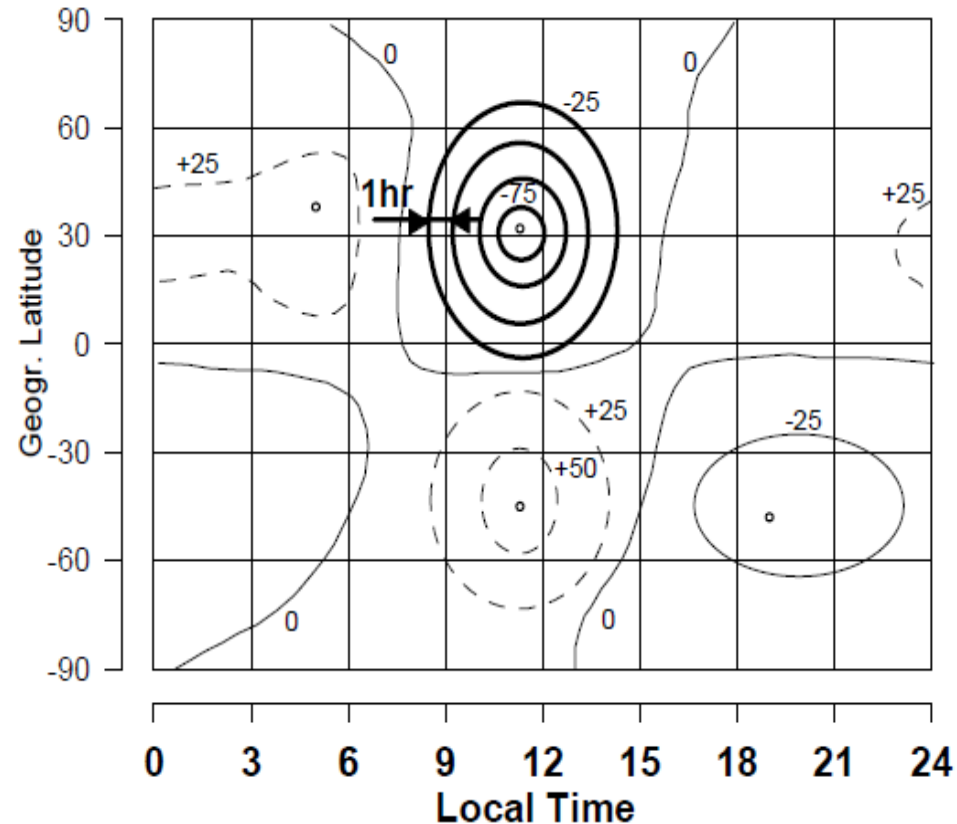
4.2 Ionospheric (Sq) current system

Ionospheric (Sq) current system



Source: <http://denali.gsfc.nasa.gov/research>

Simplified induced ionospheric current system in the Earth's interior [Matsushita, 1968]



Total induced underground current is 45% from the total ionospheric current.
[Yamazaki et. al 2011].

4.3 Estimation of torque at different solar wind input energy, ϵ

Solar wind input energy [Joule]	Average Ionospheric current kA (Induced I)	Magnetic moment [10^{10} Am^2]	Torque (T) [10^{12} Joule]	Force, F [kNm ⁻²]	Equivalent magnitude (Log E = 4.7 + 1.5M)
$\epsilon < 10^{17}$	40 (18)	6.4	1.7	486	5.0
$\epsilon: 10^{17} \sim 10^{18}$	80 (36)	12.8	3.5	972	5.2
$\epsilon > 10^{18}$	120 (54)	19	5.1	1500	5.4

$D = 3000 \text{ km}$

D is estimation distance between the center of current vortex and Ashibetsu station

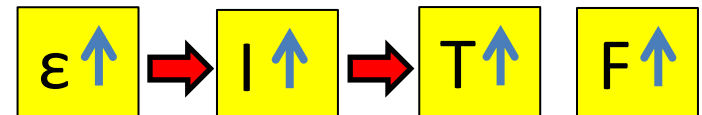
$H = 27\,000 \text{ nT}$

H is average horizontal component of magnetic data extracted from MAGDAS at Ashibetsu (ASB) station

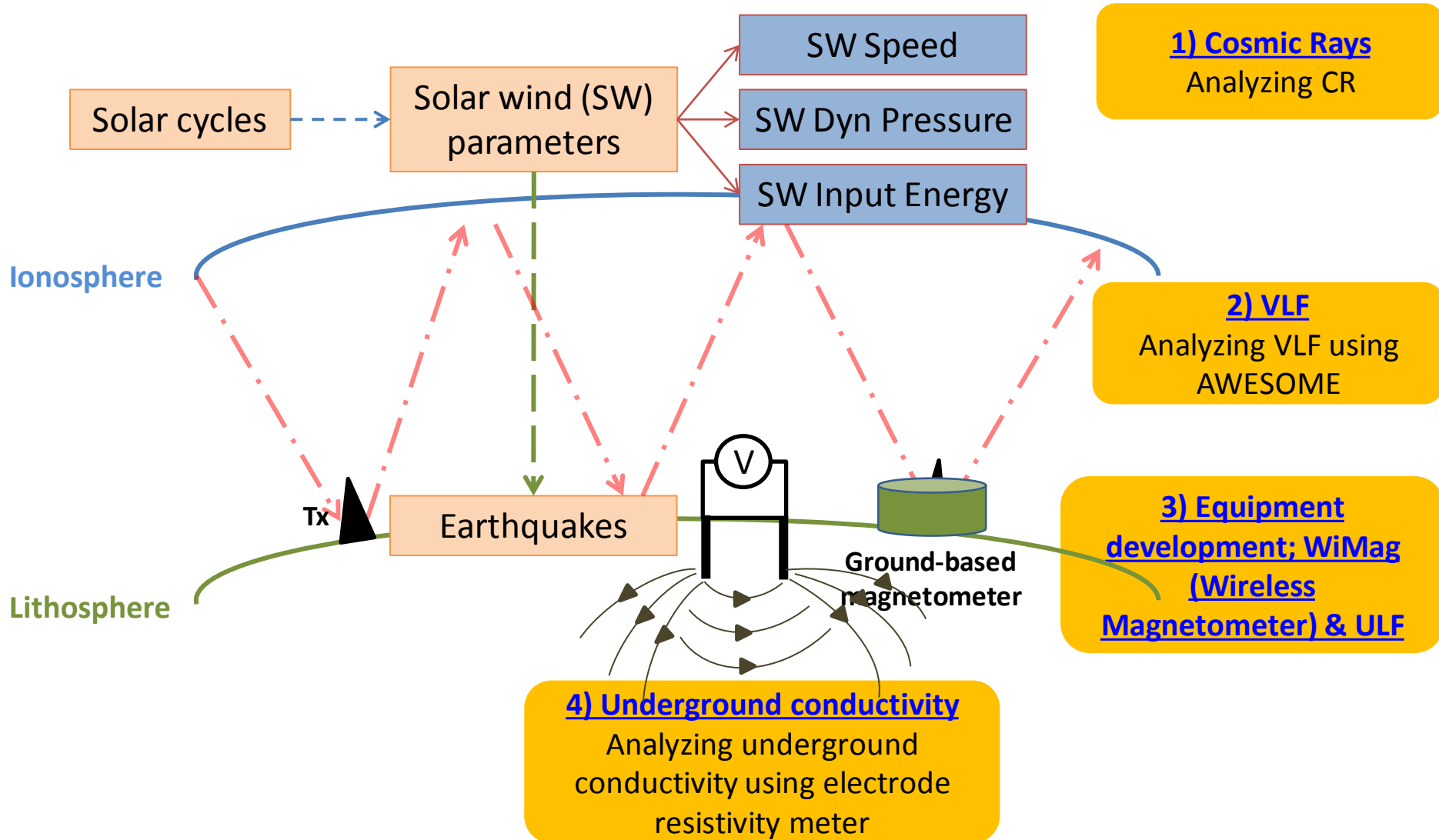
$$MM = \mu_0 * I * (D^2 * (\pi/4))$$

$$T = MM \times H$$

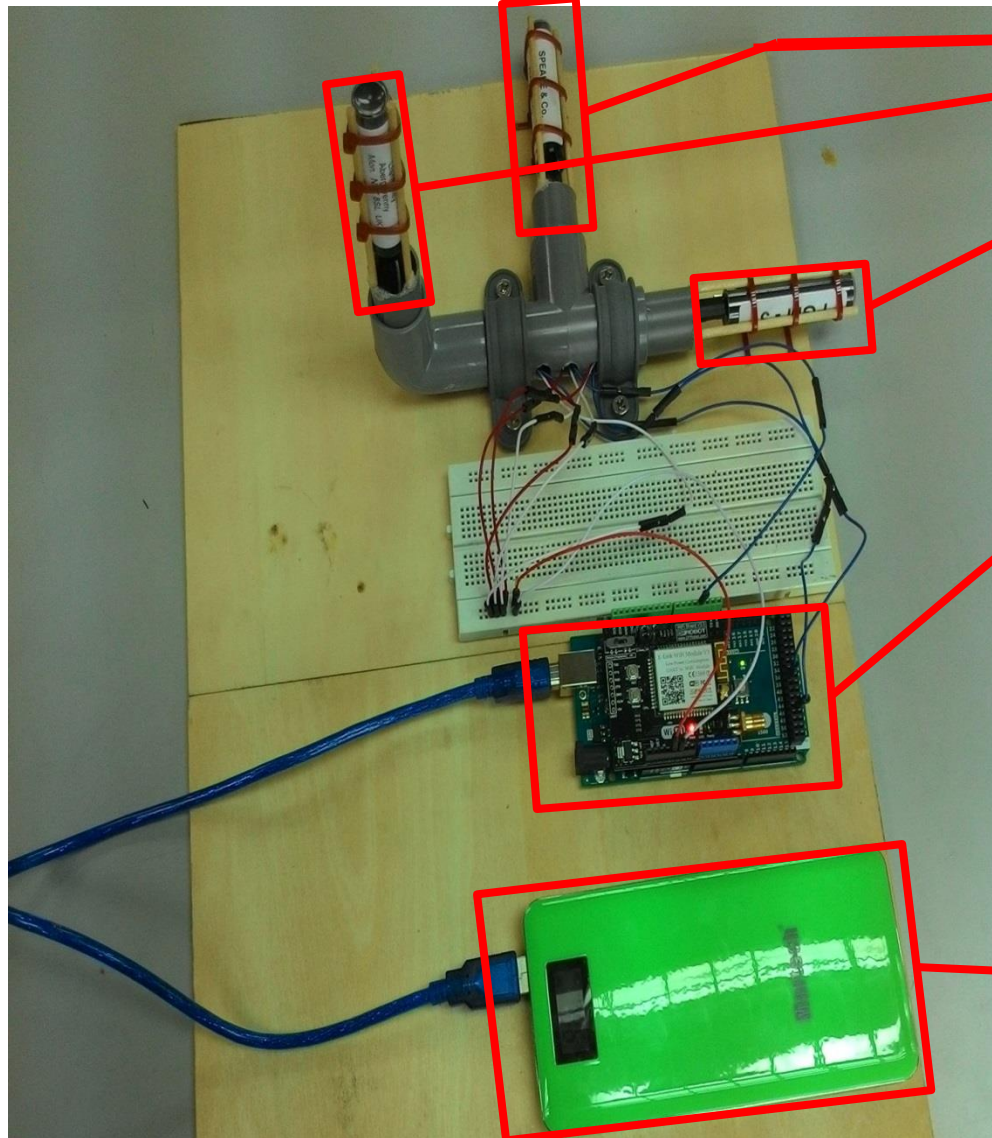
$$F = \int J \times H$$



5. Current Progress of Research Work



5.1 Development of Wireless Magnetometer (WiMag): Hardware setup (DUT)

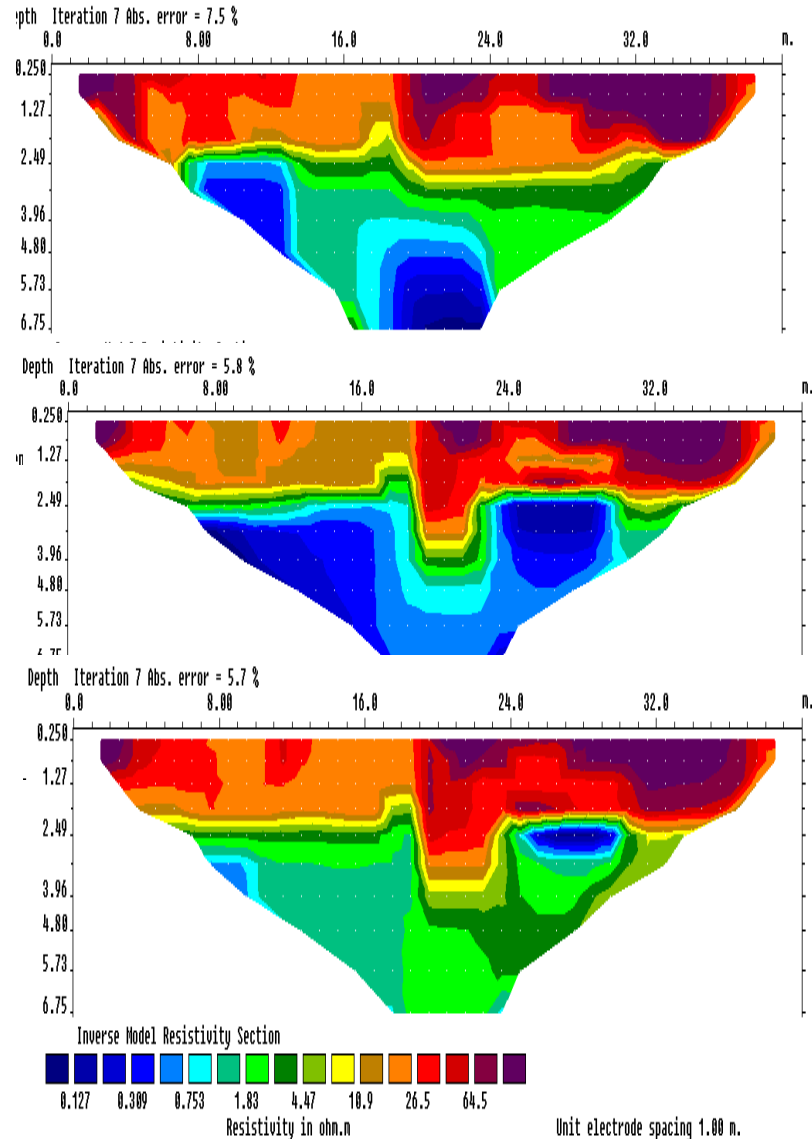
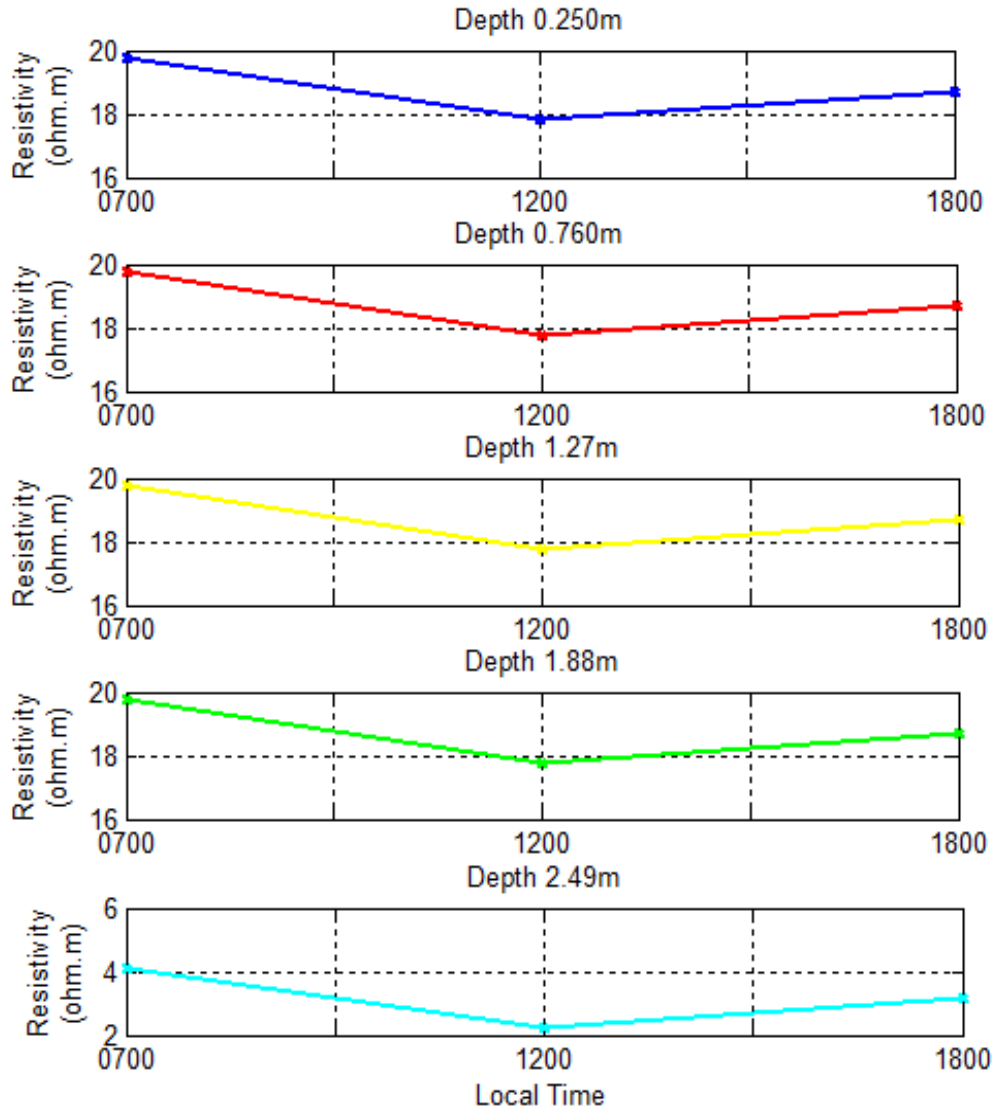


Fluxgate Sensors

Microcontroller development board:
AVR ATmega2560 (main microcontroller for hardware peripherals)
&
AVR ATmega16U (serial processing and main microcontroller burning)
+
IEEE802.11 b/g/n wireless module

5.0V with selectable current mode (1.0A/2.1A) 10Ah Rechargeable Cell

5.2 Underground resistivity-preliminary results

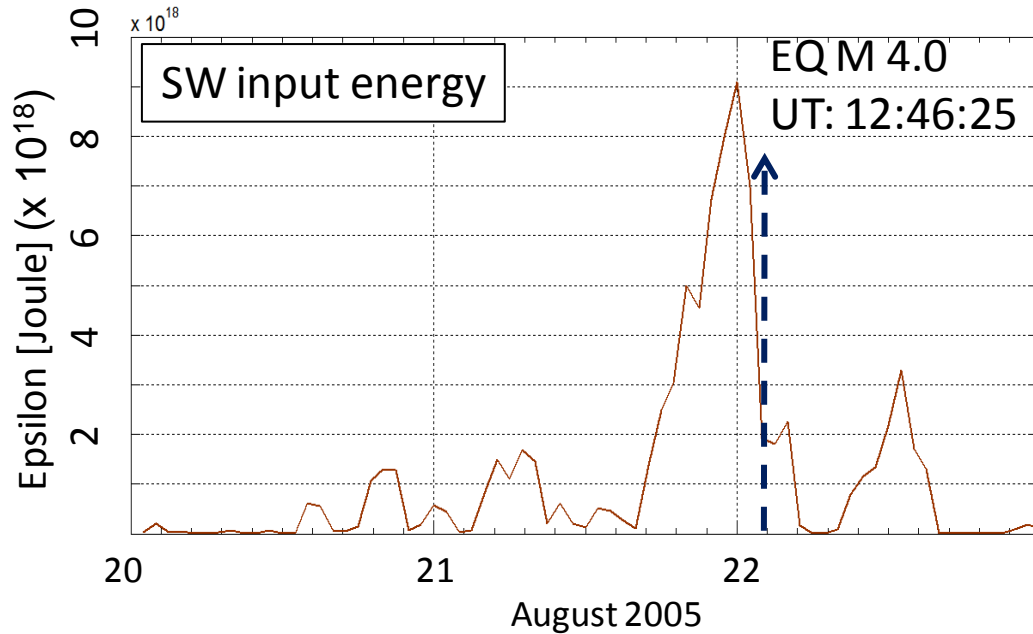


5. Conclusion

1. The overall analysis shows earthquakes of all magnitude tend to occur more frequently during descending solar cycle, when the solar wind parameters (solar wind speed, dynamic pressure and input energy) are high.
2. However, one solar wind event does not trigger one earthquake.
3. Geomagnetic pulsations and Lorentz force produced by induced currents can be possible connecting agents between the solar wind and the seismic activity.

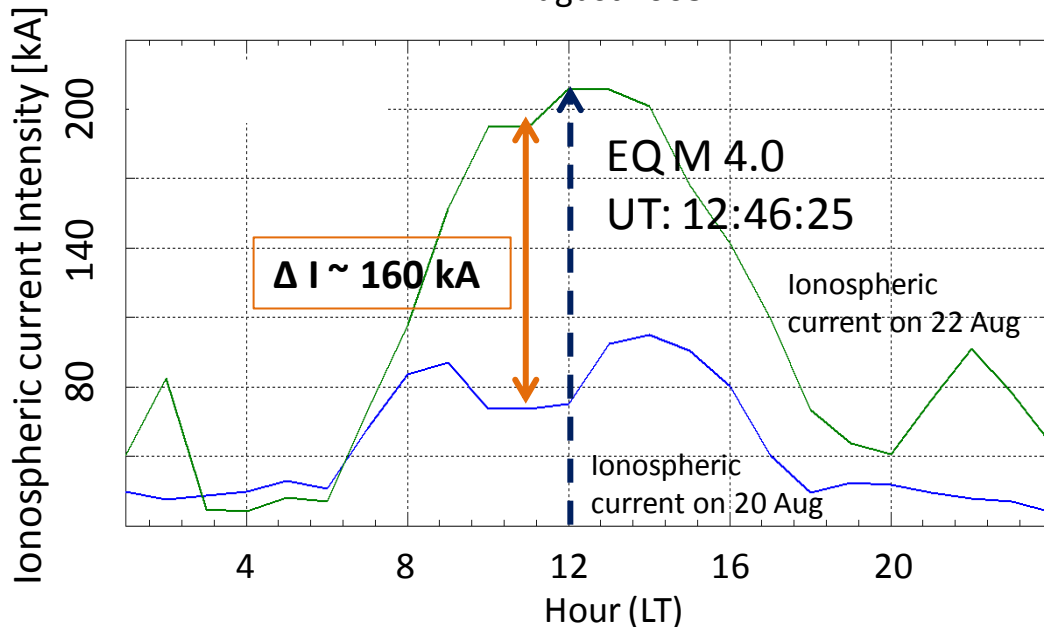
THANK YOU

4.3 Influence of SW input energy on Sq current



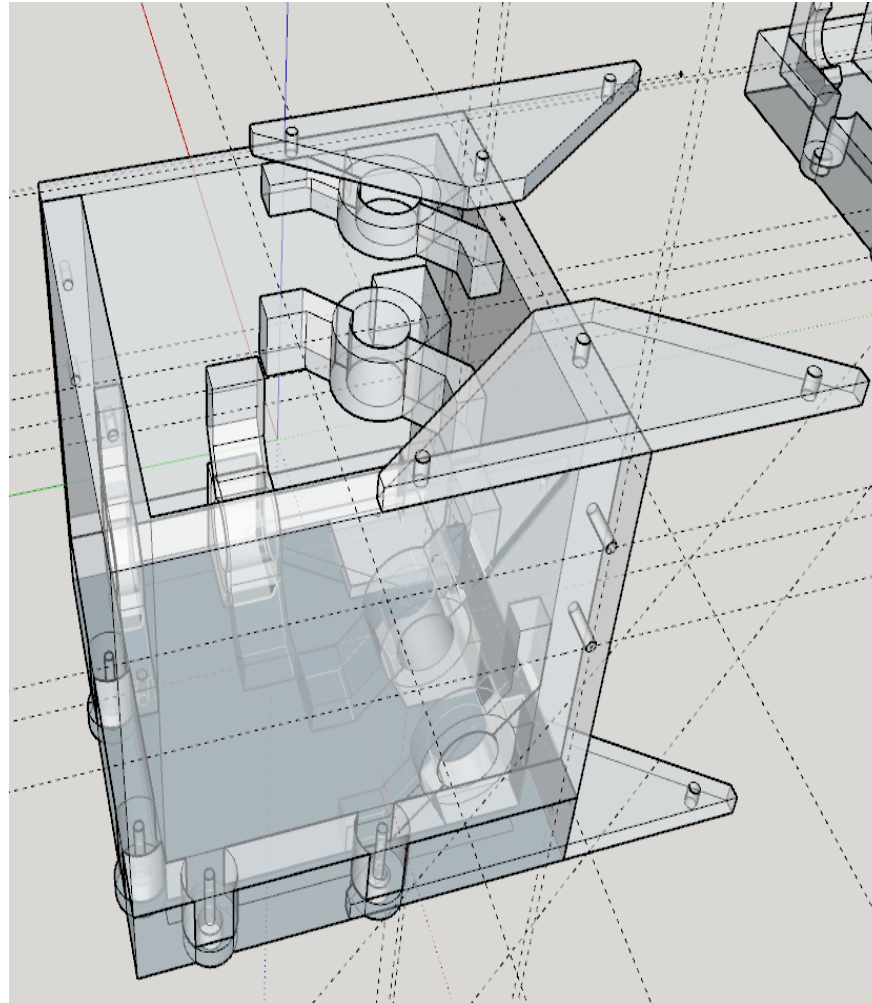
High solar wind input energy could cause higher ionospheric current. [Akasofu, 1981]

Higher SW input energy occurred on 22 August 2005



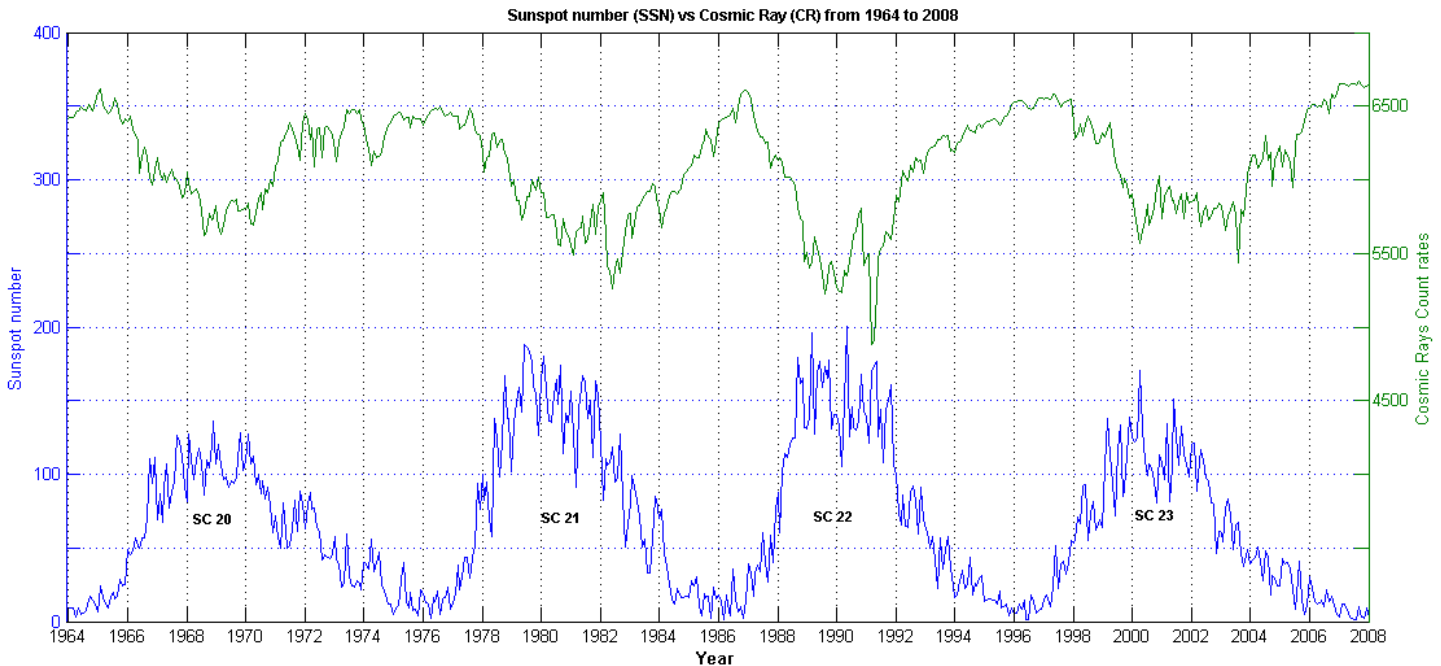
➤ Ionospheric current during quiet time on 20 August 2005 (Blue) increased 3 times when higher SW input energy detected on 22 August 2005 (Green).

In progress-3D design for WiMag enclosure



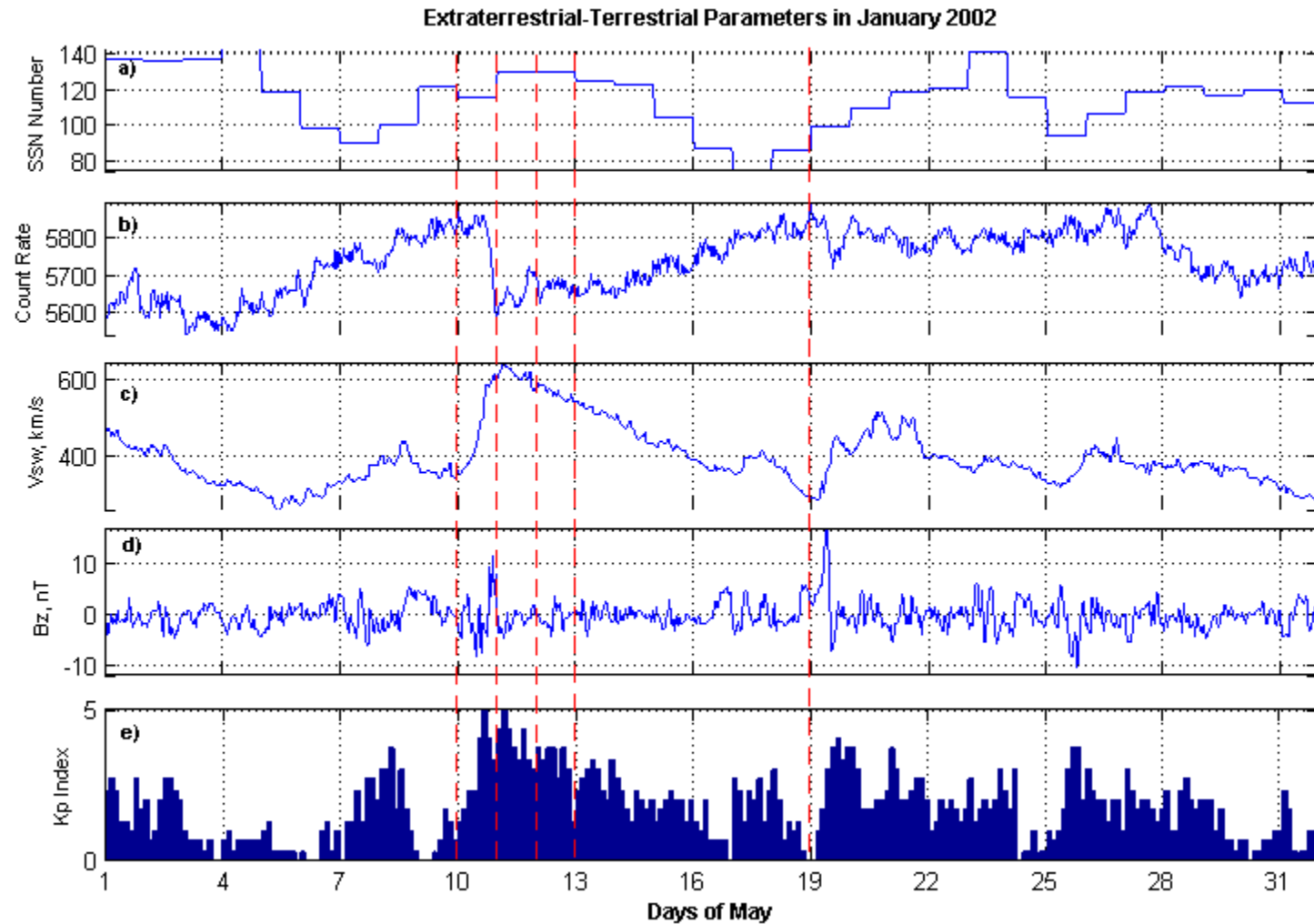
CR: Cosmic Rays

2. Experimental data & Results

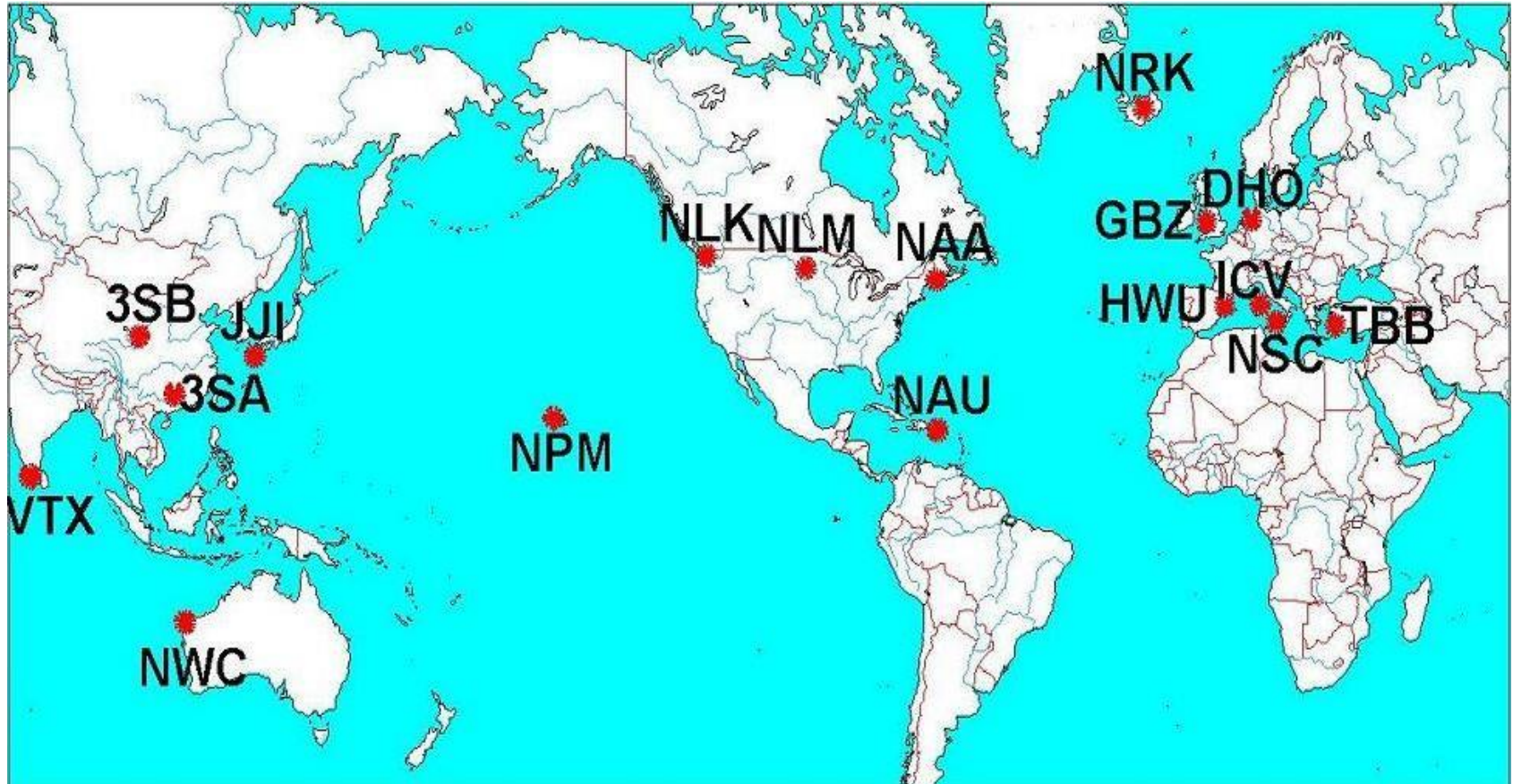


Monthly sunspot number and cosmic rays intensity from 1964 to 2008 that covers Solar Cycle (SC) 20 – 23.

CR: Cosmic Rays



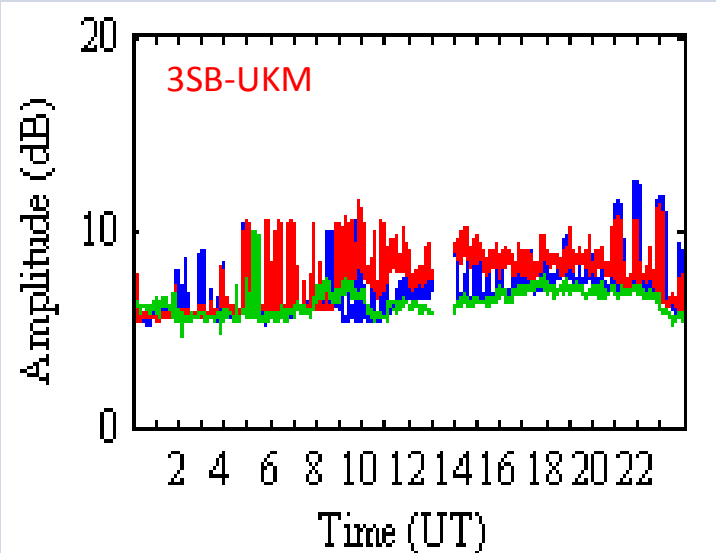
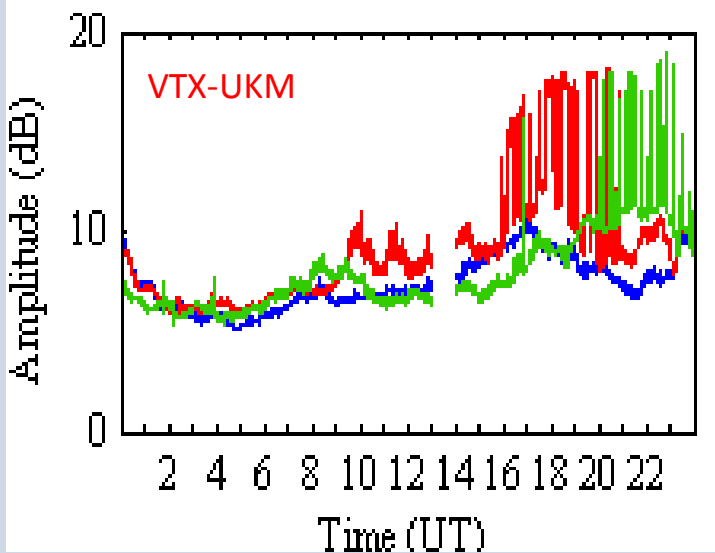
VLF: Very Low Frequency



Map of AWESOME VLF transmitters around the globe

VLF: Very Low Frequency

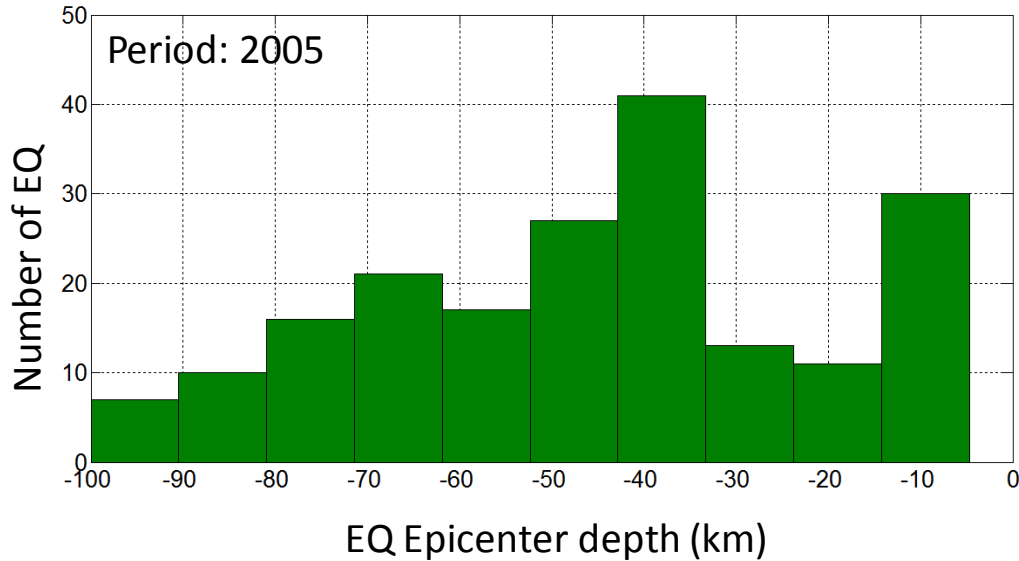
2. Experimental data & Result

Transmitter Station, Tx	Datong (3SB), China (39.6°N, 103.33°E)	Katabomman (VTX), India (8.47°N, 77.4°E)
<p>Quiet: 15 March 2010</p> <p>Weak: 12 March 2010</p> <p>Moderate: 6 April 2010</p>	 <p>3SB-UKM</p>	 <p>VTX-UKM</p>



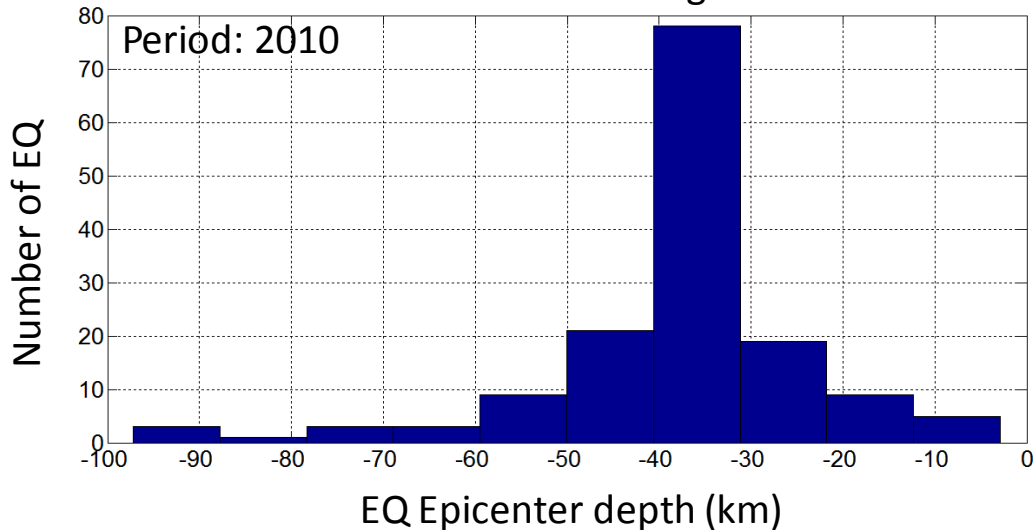
Earthquake epicenter depth

North Japan region



For both regions, most of EQ events occurred at around 30 - 60 km epicenter depth

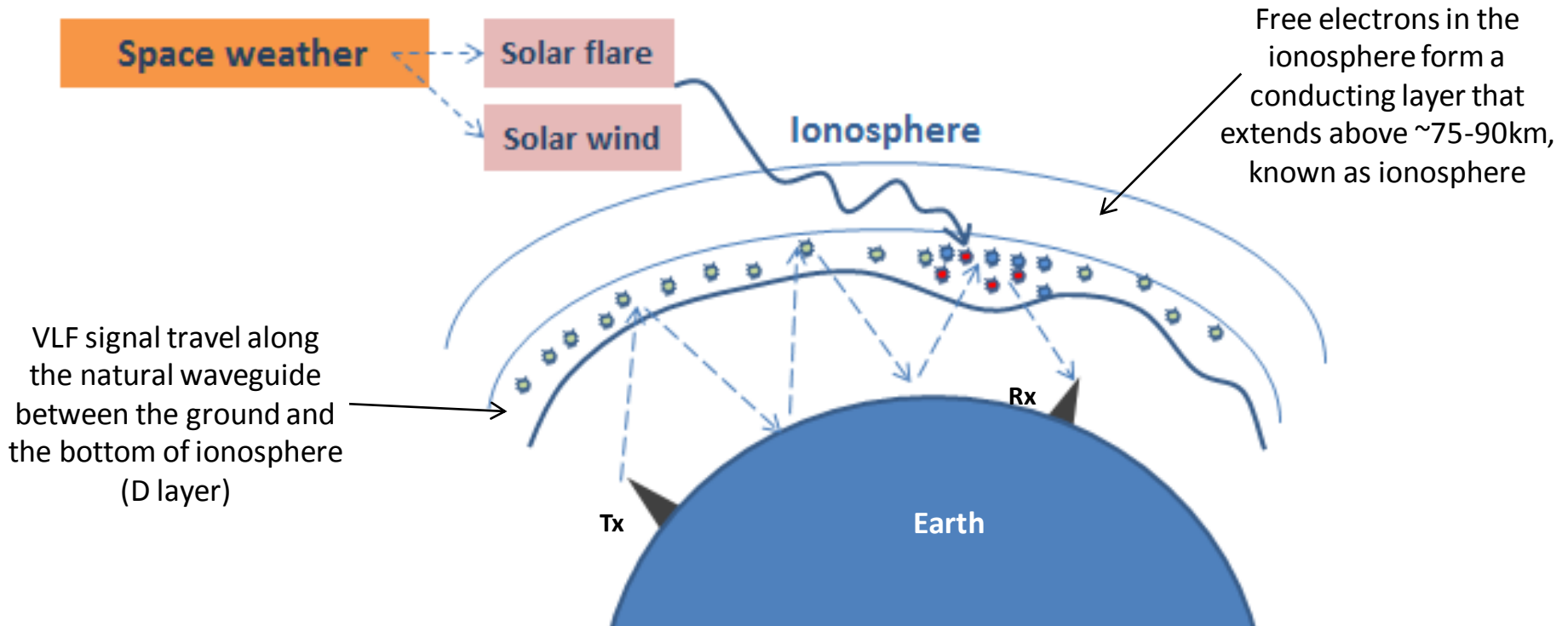
North Sumatra region



Skin depth δ (km)			Conductivity σ (S/m)		
			10^{-1}	10^{-2}	10^{-3}
T (Period)	sec	10	5.03	15.91	50.32
		45	10.68	33.76	106.76
		150	19.4	61.64	194.92
	min	50	87.18	275.66	871.73
		150	151	477.5	1509.9

Continuous Pulsations			
	Pc 3	Pc 4	Pc 5
Period (sec)	10-45	45-150	150-600
Freq. (mHz)	22-100	6.7-22	1.7-6.7

VLF: Very Low Frequency



- Earth's surface and free electron in the lower ionosphere.
- VLF transmissions propagate along the natural waveguide between transmitter, Tx and receiver, Rx.
- The amplitude and phase of the signal can be studied to derive the conditions of lower ionosphere due to space weather events

Data

- **Solar data (includes solar wind parameters)**

Obtained from the Goddard Space Flight Center, NASA via the OMNIWeb Data Explorer and the Space Physics Data Facility

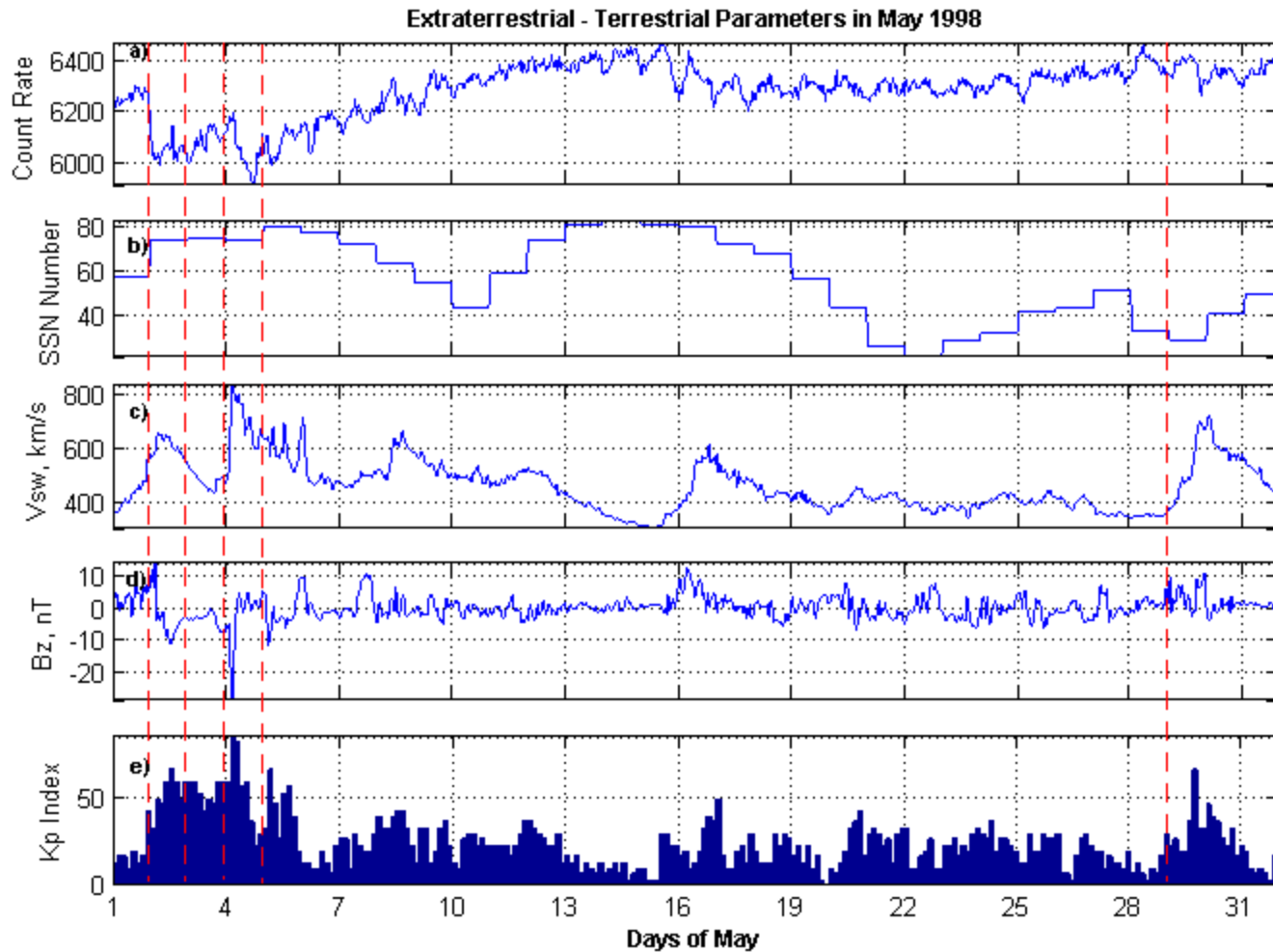
- **Earthquake events**

Extracted from the Advanced National Seismic System (ANSS) database

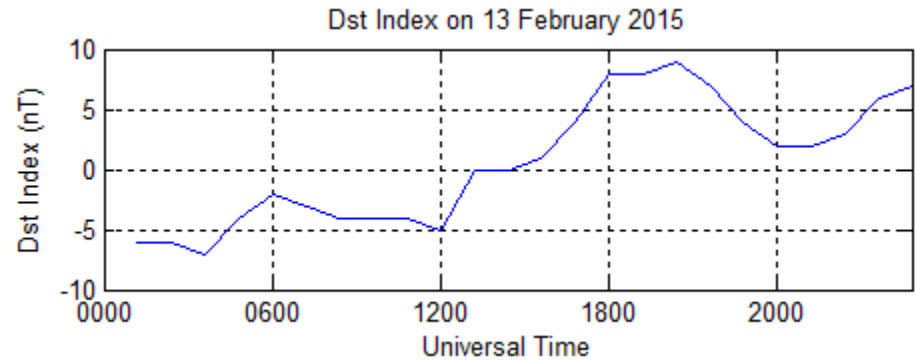
- **Geomagnetic data**

Extracted from Magnetic Data Acquisition System (MAGDAS)/Circum Pan Magnetic Network (CPMN), Kyushu University (PI: Prof. Yumoto)

CR: Cosmic Rays

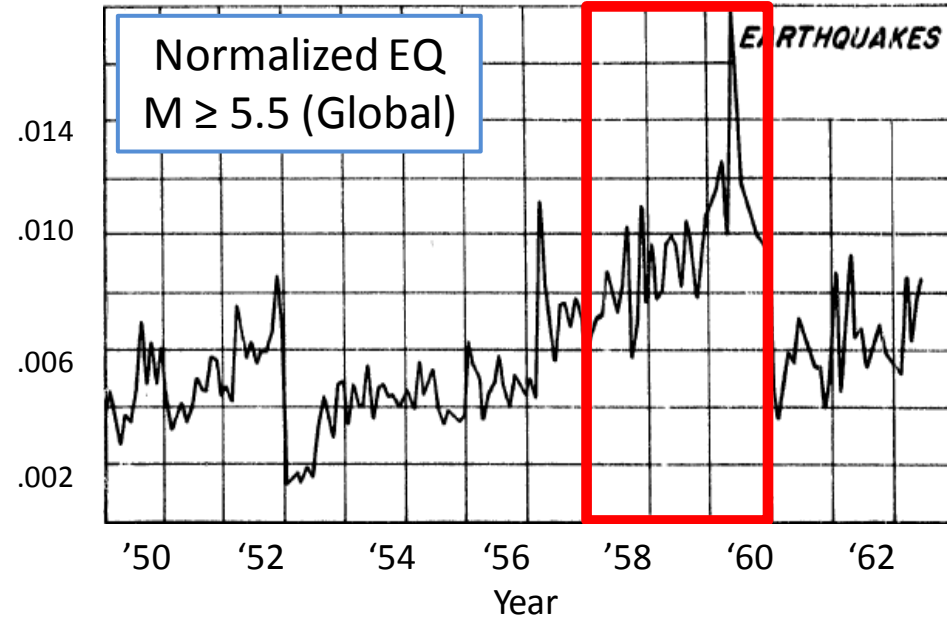
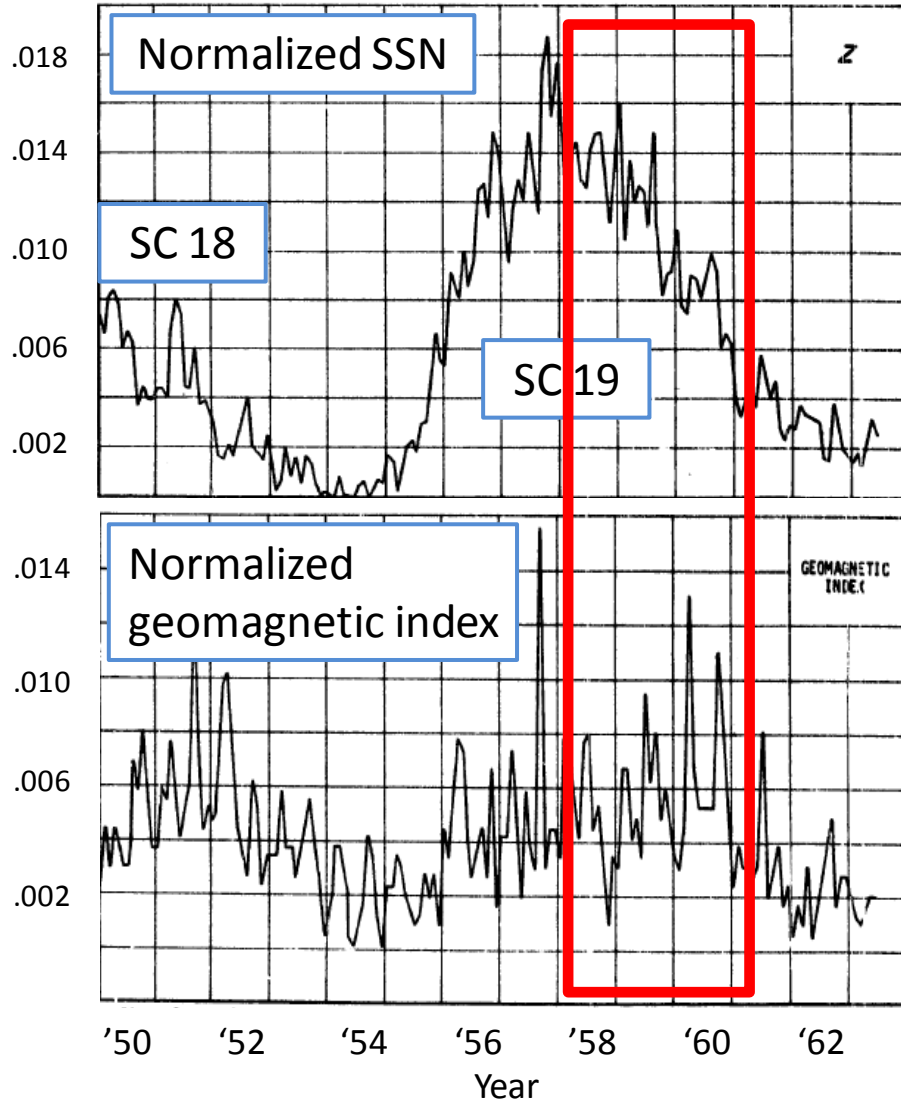


Experiment setup



- Configuration: Wenner array
- Instrument: ABEM Terrameter LS
- Duration: 10 minutes
- Field work: Resistivity
- Distance: 40m
- Depth: 6m
- Coordinate: 6.031303, 116.121047
- Date: 13 February 2015

2.1 Relationship of earthquake (EQ), sunspot numbers (SSN) and geomagnetic index [John F. Simpson, 1967]



- The normalized geomagnetic index (Kp) and EQ reached peak at 1960; same period of declining Solar cycle (SC) 19
- The geomagnetic index also shows its peak during declining phase of SC 18
- Proposed the surges of telluric currents during geomagnetic storm as coupling mechanism.

Objectives of study

➔ To date, previous researchers have done the investigations on relationship of:

- Global EQ and solar cycle (SC 18-19) [*Simpson, 1967, Belov et al., 2009*]
- EQ and High speed solar wind during SC 21-22 [*Odintsov et al., 2005*]
- Global geomagnetic activities & Sq current [*Duma et al., 2002, Odintsov et al., 2007*]

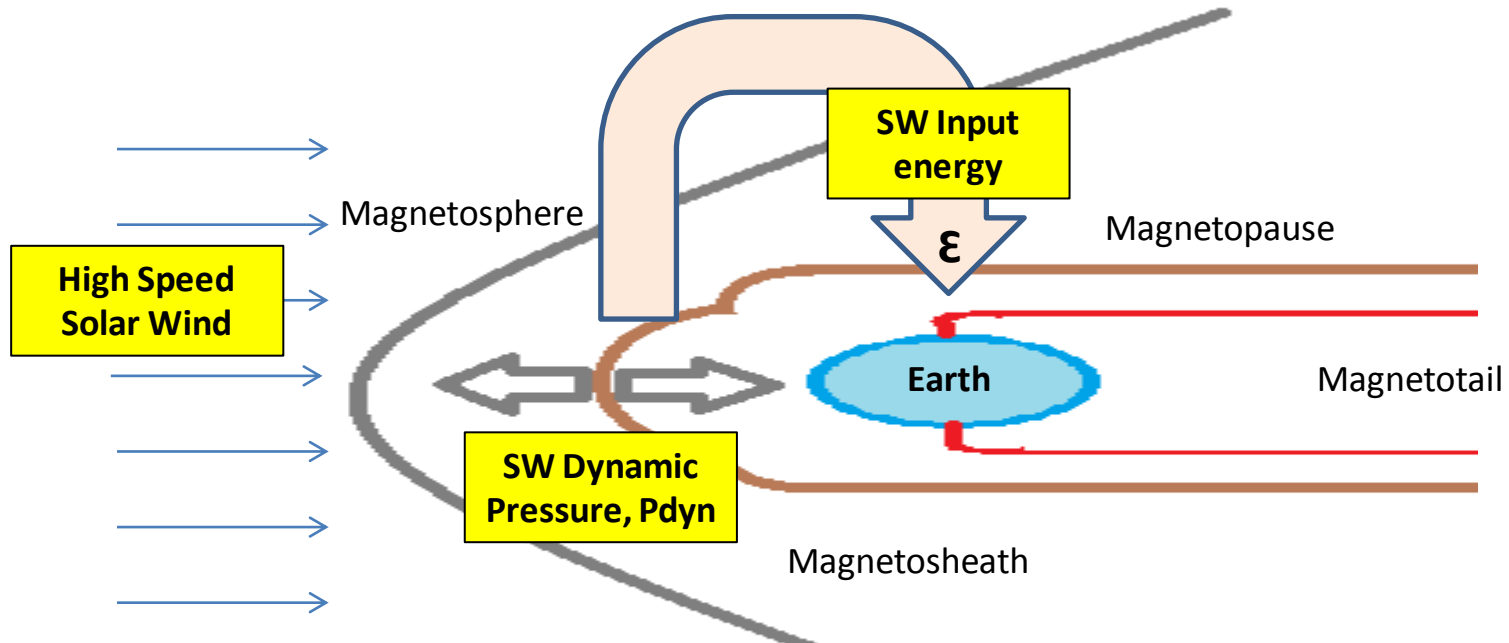
How does the solar parameter can influence the earthquake (EQ) events?

- To investigate the possible solar – seismicity coupling, we have to:
 1. Re-examine the relationship between **global EQ** and high speed solar wind with longer time period (4 solar cycles; SC 20-23).
 2. Examine the relationship of **local EQ** and its released energy at longer time period (4 solar cycles).
 3. Examine possible relationship between EQ and solar wind dynamic pressure, and solar wind input energy.
 4. Examine geomagnetic pulsations as connecting parameters between solar and EQ events.

3. Results

Num.	Result
3.1	Variation of Earthquake Occurrence with Solar Cycle (SC)
3.2	Solar wind parameters associated with earthquakes
3.2.1	Relationship of EQ with HSSW
3.2.2	Relationship of EQs with High Solar Wind Dynamic Pressure
3.2.3	Relationship of Earthquakes with Solar Wind Input Energy, ϵ (epsilon)

Solar Wind Parameters – Earth's Coupling



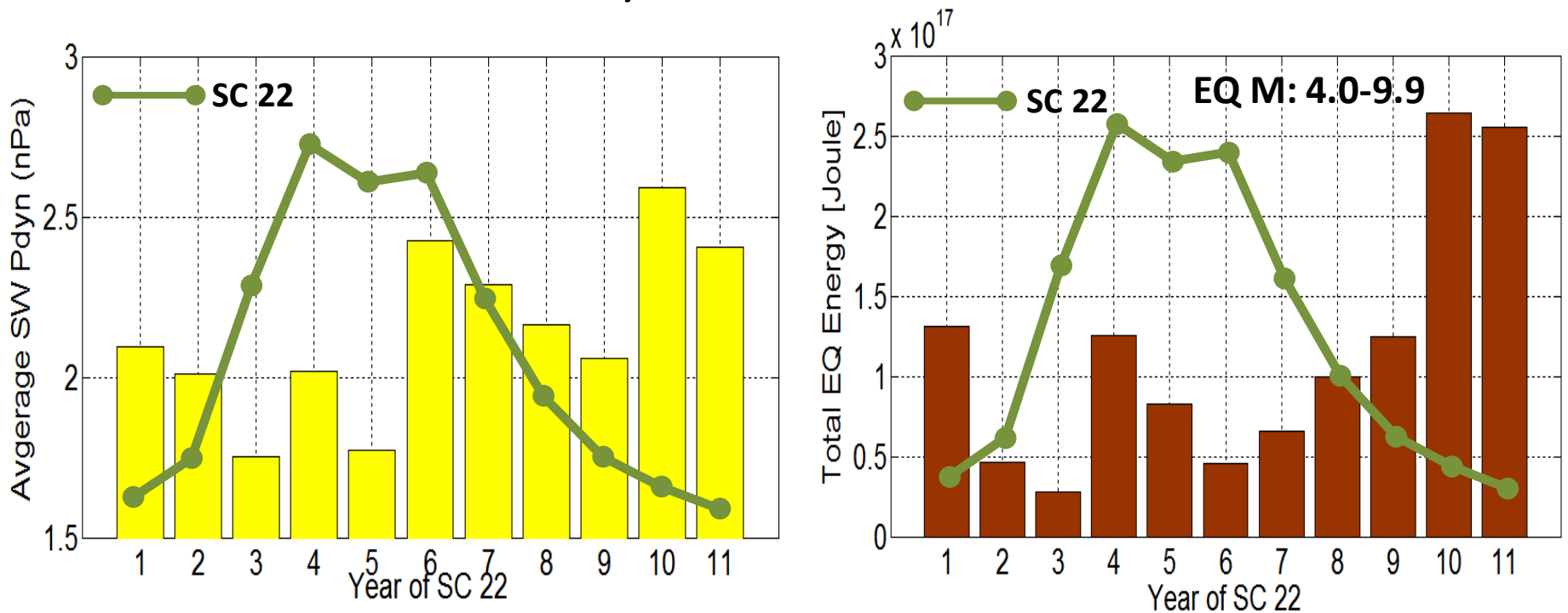
$$\text{SW Pdyn} = 1.6726 * \text{exp-6} * N * V_{\text{sw}}^2$$

[nPa]

Where: N = Proton density and Vsw = Solar wind speed
Can be extracted directly from OMNI database

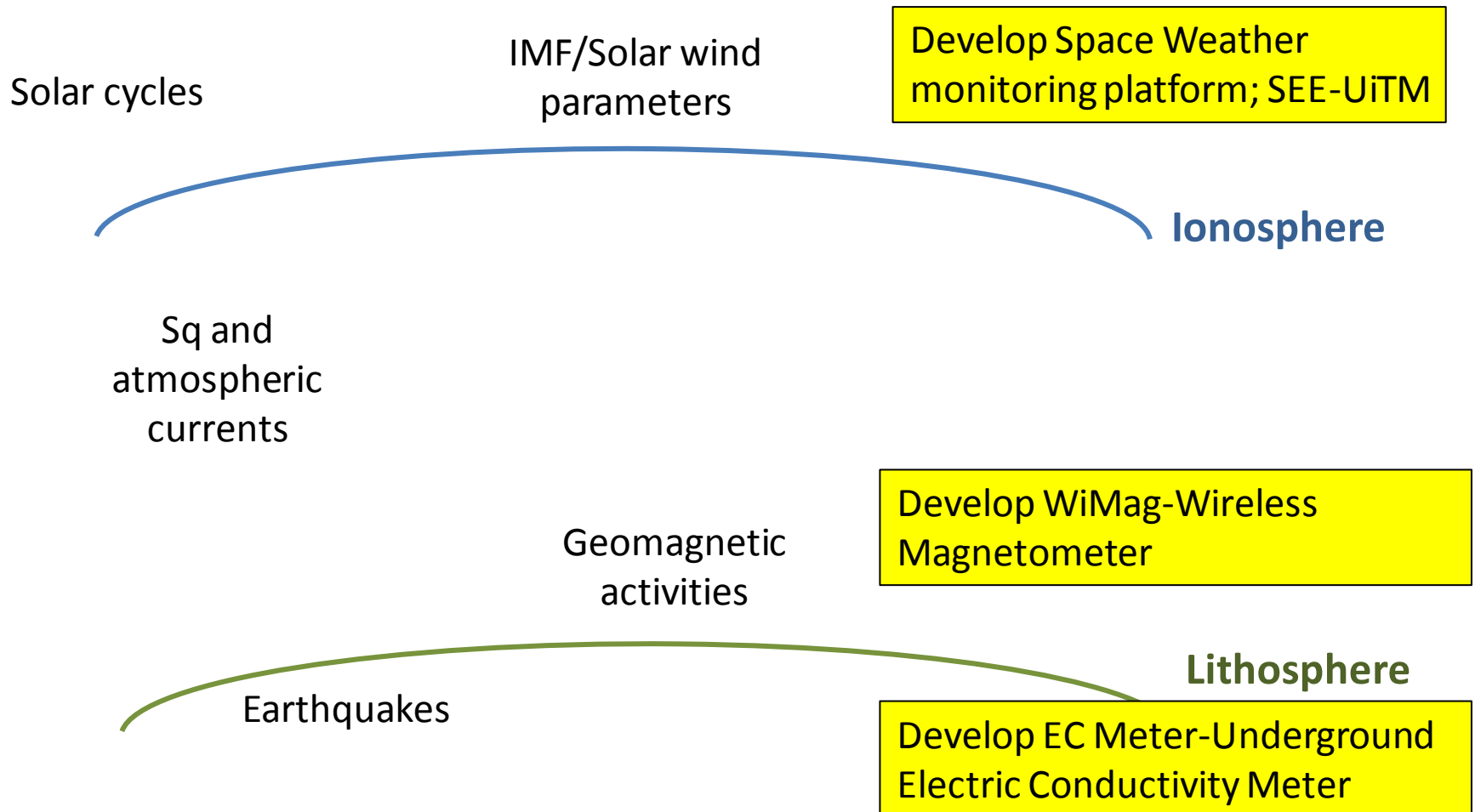
Artistic rendition of Earth's magnetopause

3.2.2 Relationship of EQs with High Solar Wind Dynamic Pressure



- ◆ Higher amplitude of solar wind dynamic pressure occurred during descending phase of SC 22
- ◆ The amount of earthquake released energy is higher during descending phase of SC 22; the same trend with solar wind dynamic pressure.

Current progress of research works (1)



Current progress of research works (2)

- Outreach Program

<http://seeuitm.wix.com/seeuitm>



Research students:

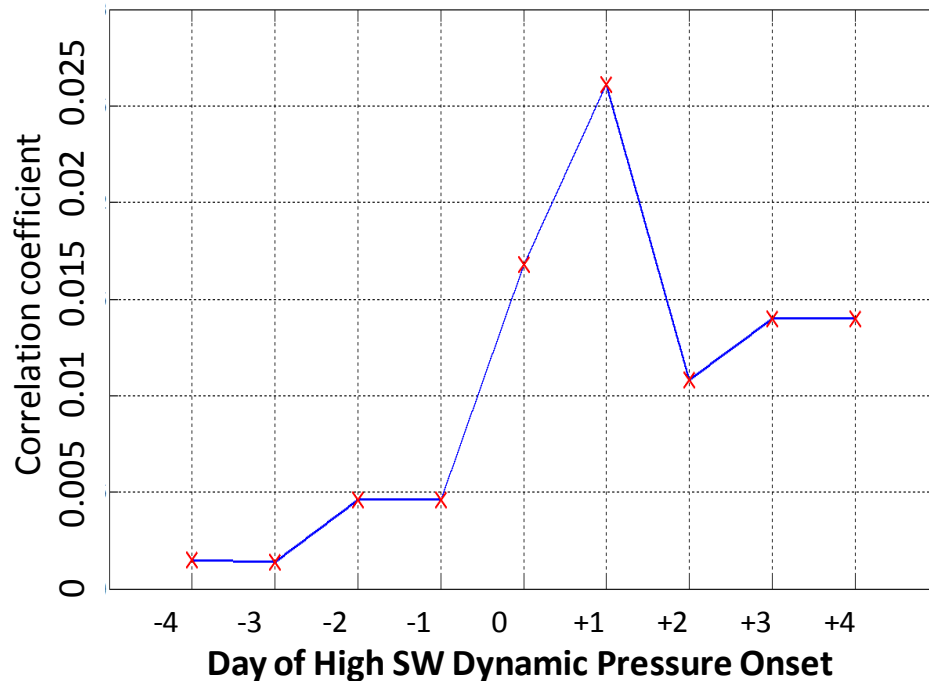
- 8 FYPs
- 6 Postgraduates

Research collaborations:

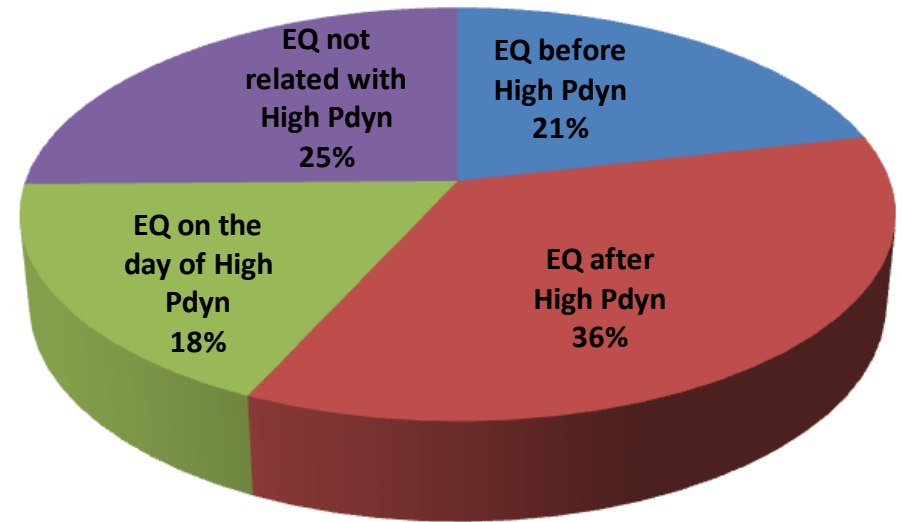
1. International Center for Space Weather Science and Education (ICSWSE), Kyushu University, Japan.
2. National Space Agency, (ANGKASA), Malaysia
3. Universiti Kebangsaan Malaysia (UKM)
4. Universiti Malaysia Sabah (UMS)

3.2.2 Day to day variation of High Solar Wind Dynamic Pressure with Earthquakes Magnitude 5.0-9.9

Correlation of High SW Pdyn and EQ
(Mag. 5.0-9.9) during SC 23



Average Fraction Correlation of Solar Wind High Dynamic Pressure and Earthquake



Total EQ: 1067 events

Total High Pdyn: 968 events

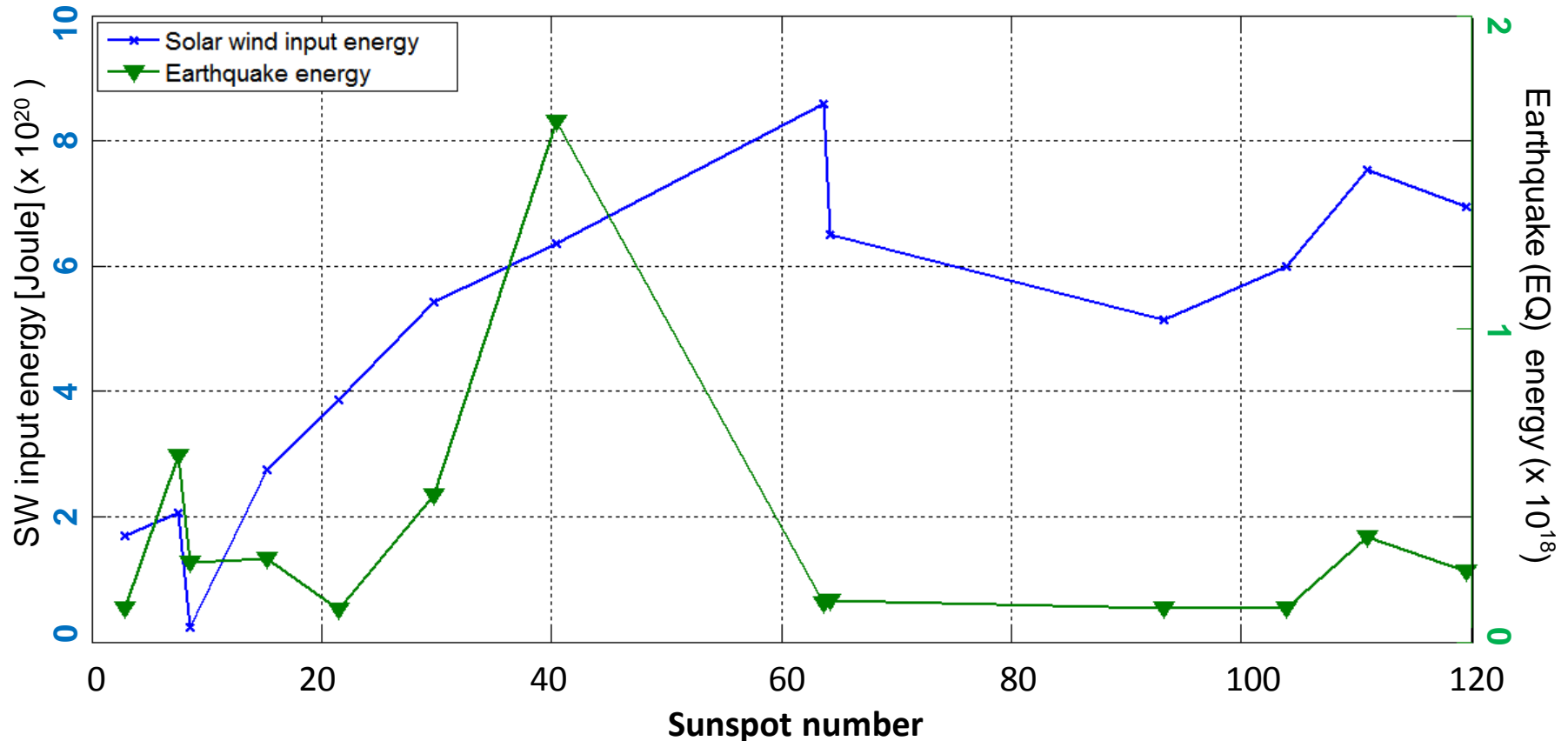
Total EQ: 112 events

Total High Pdyn: 316 events

Jusoh et. al, 2012

- Highest correlation coefficient detected 1 day after the day of high SW Pdyn.
- 54 % of EQ events occurred on the day and within 4 days after the arrival of high SW Pdyn.

3.2.3 Variation of annual solar wind input energy and earthquake energy (epicenter depth < 40 km) during SC 23



- SW input energy keep increasing when SSN increase to 63 and keep stable above 5×10^{20} Joule
- EQ energy shows a single peak at SSN 40 before drop to below 0.25×10^{18} Joule at SSN greater than 60

Summary of results

3.1 Variation of Earthquake Occurrence with Solar Cycle

➔ Both local and global earthquake activity at all magnitudes (4.0-9.9) tend to occur more frequently in the descending phase of solar cycles (SC 20-23).

3.2 Solar wind parameters associated with earthquakes

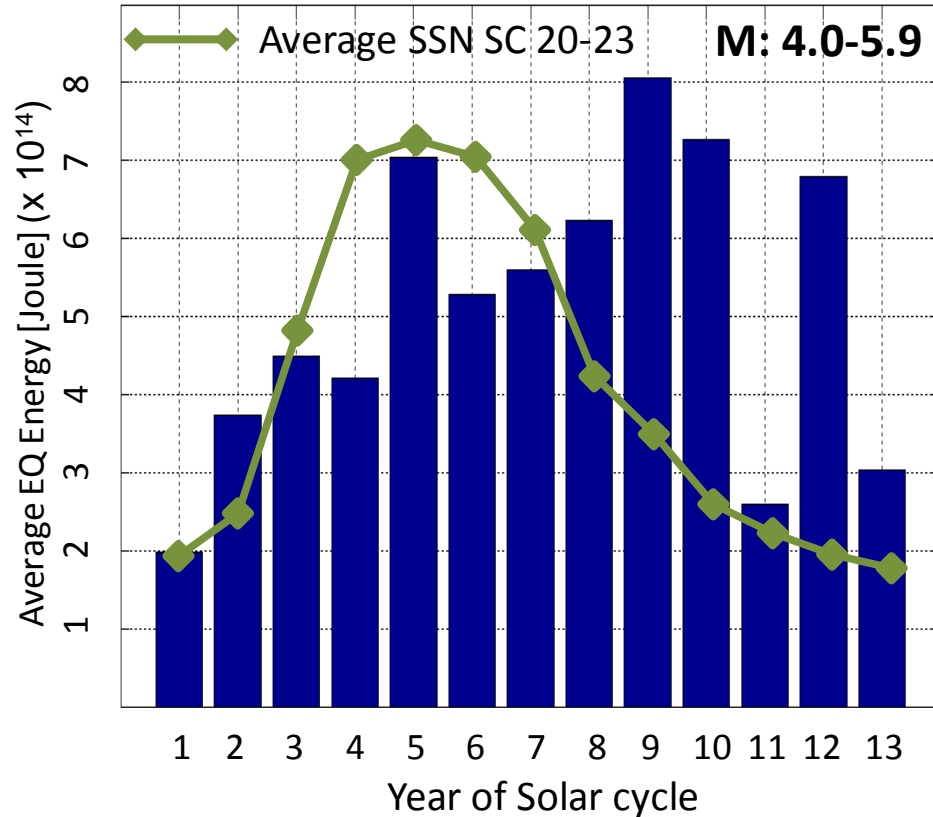
➔ Global earthquakes tend to occur during higher number/amplitude of high speed solar wind, solar wind dynamic pressure and solar wind input energy.

Future recommendations

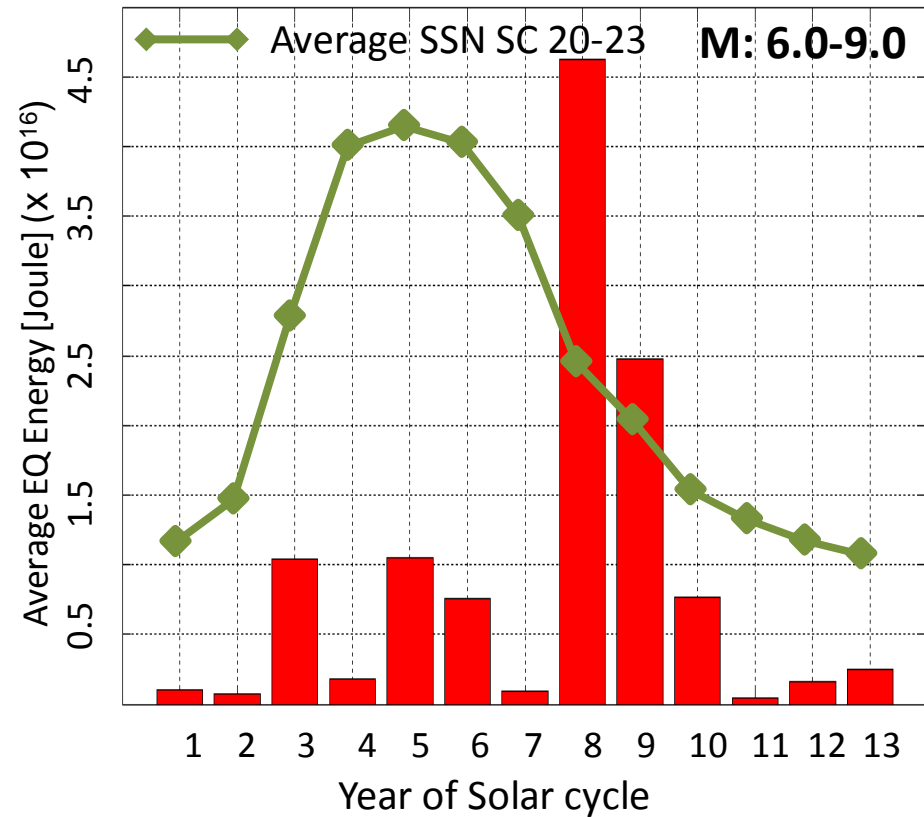
1. Investigate the occurrence of earthquake with the effect of solar tides
2. Consider more earthquake events at different seismic active areas with longer time period of observation
3. The physical coupling mechanism on solar – seismicity coupling needs further details clarification and analysis by developing a special model.

3.1.5 Distribution of Regional EQ Energy: Japan

Japan EQ (M: 4.0-5.9)



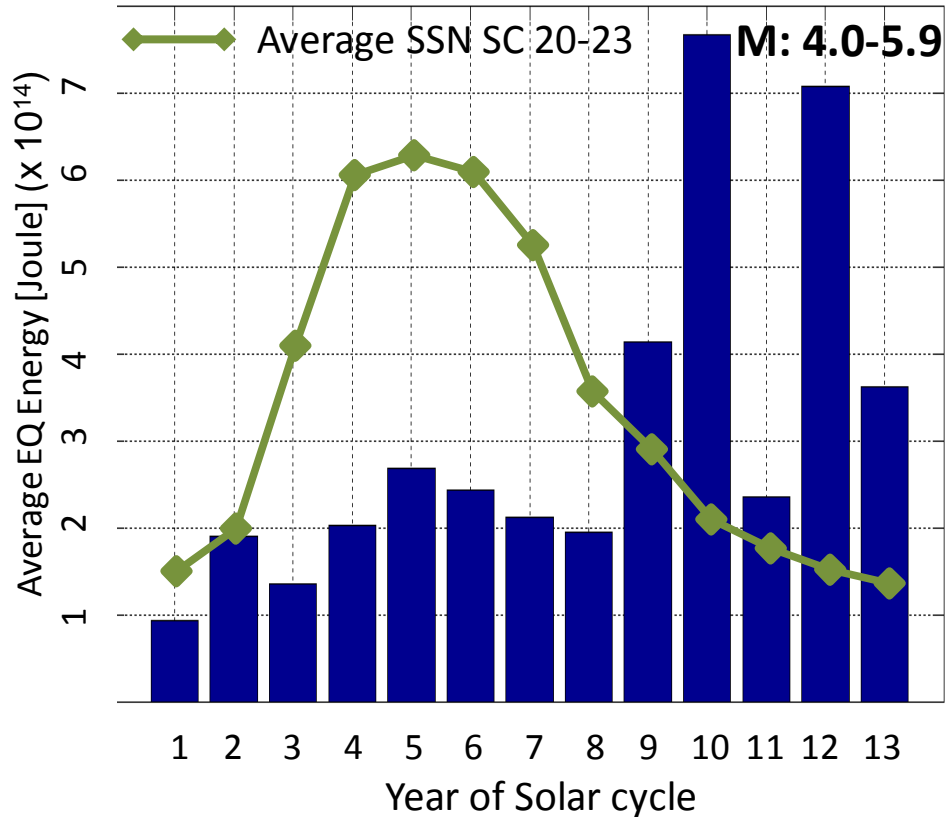
Japan EQ (M: 6.0-9.0)



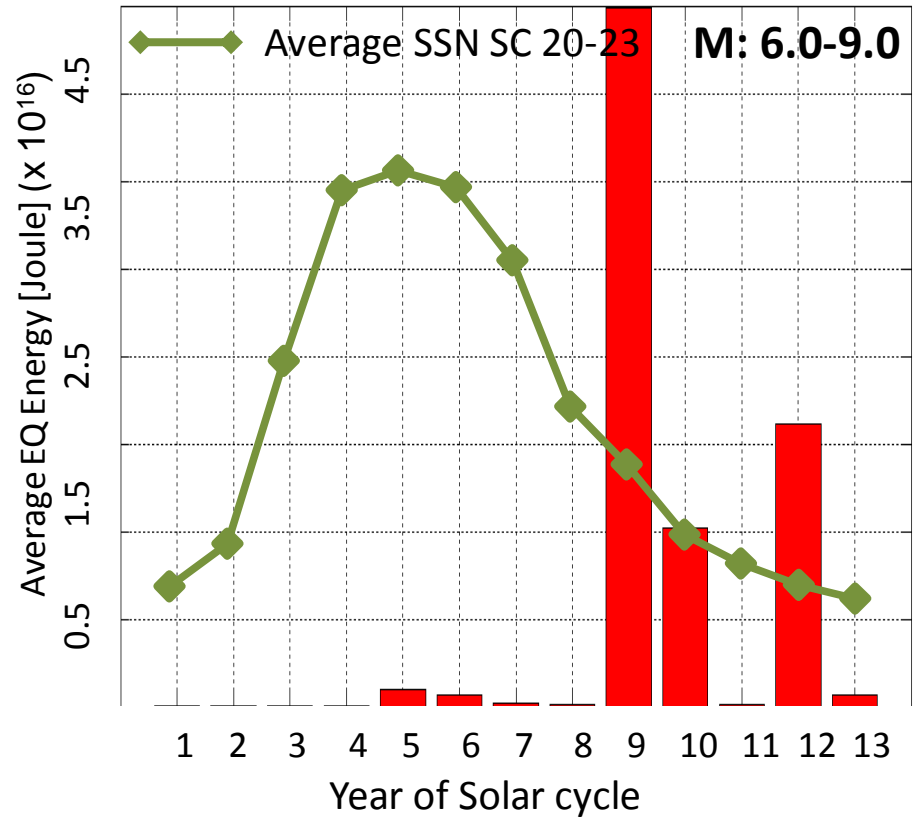
◆ Most of EQ energy (both magnitude ranges) released during the descending phase of solar cycle .

3.1.6 Distribution of Regional EQ Energy: Sumatra

Sumatra EQ (M: 4.0-5.9)



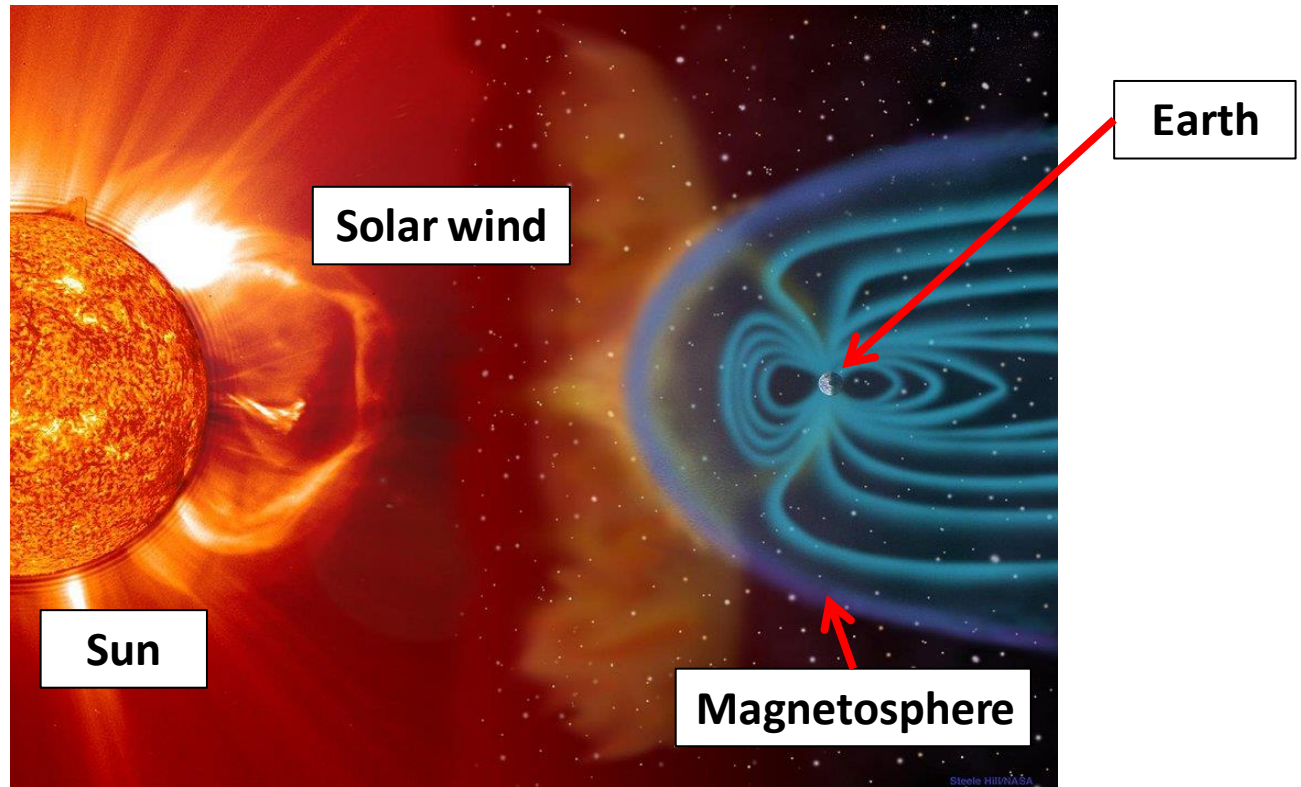
Sumatra EQ (M: 6.0-9.0)



Most of EQ energy (both magnitude ranges) released during the descending phase of solar cycle .

1. Introduction: Space and Earth's Electromagnetism

The Earth's magnetic field extends far into space. It is called the magnetosphere.”



When the magnetic particles from the sun, called “solar wind”, strike this magnetosphere, we see a phenomenon called...

Aurora



Courtesy of NASA



hoto by Yuichi Takasaka



hoto by Norihisa Sakamoto



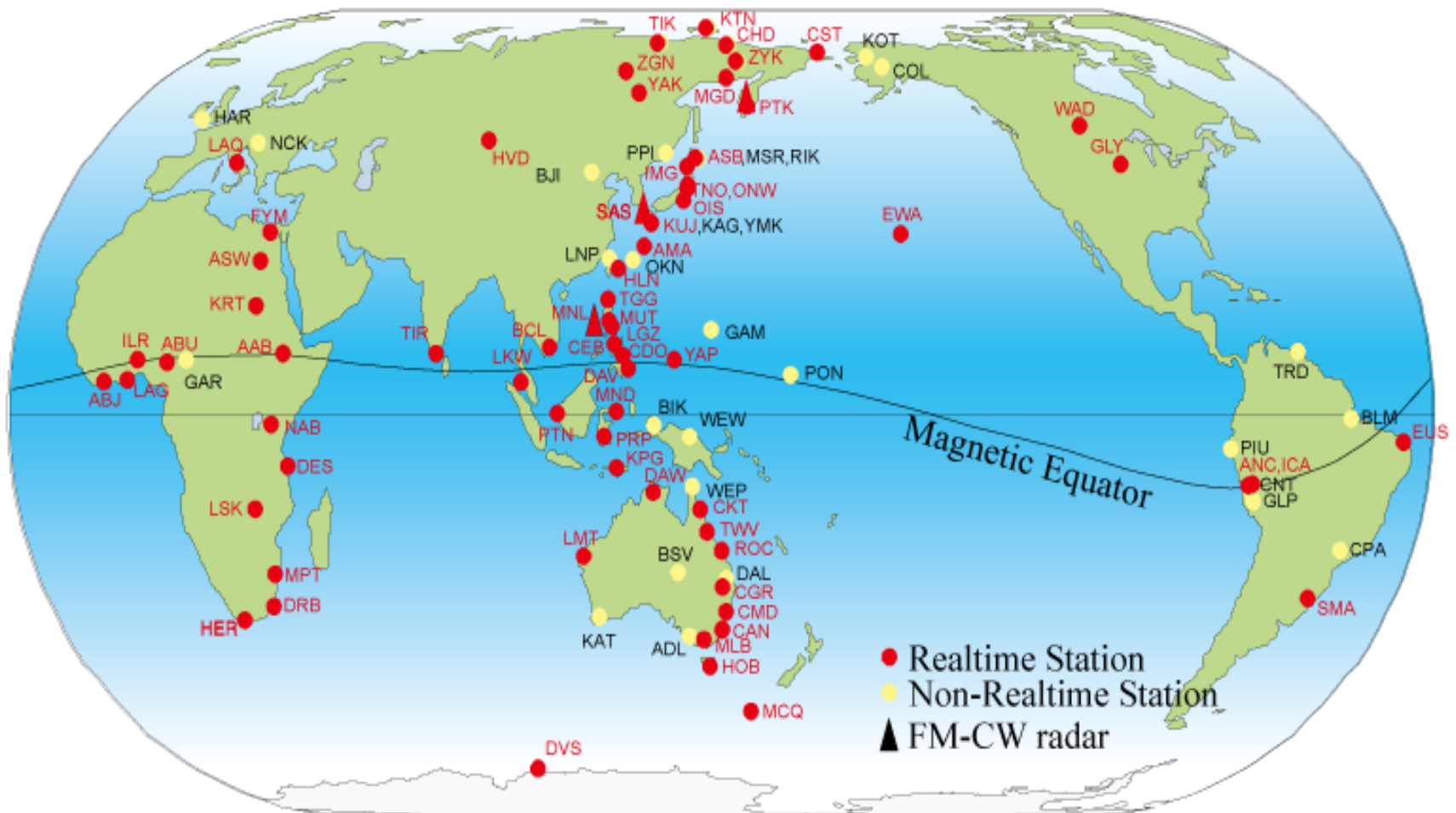
Photos by Rikubetsu Astronomical Observatory

Magnetometer array, developed by Kyushu University

MAGDAS/CPMN

2011

(MAGnetic Data Acquisition System/Circum-pan Pacific Magnetometer Network)



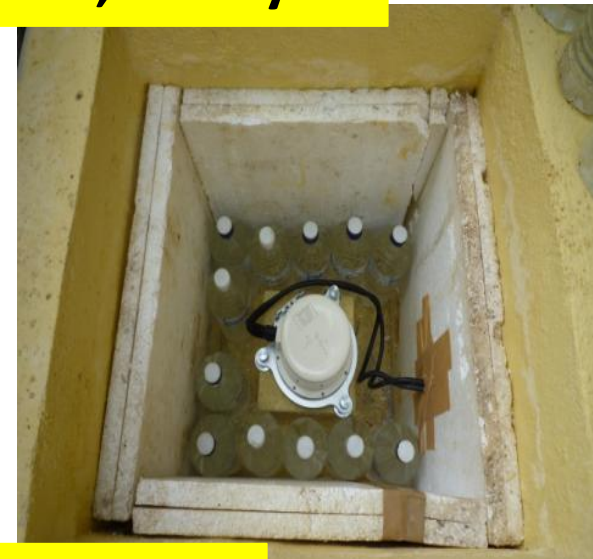
MAGDAS installation at Ica, Peru



Geomagnetic experiment at Bermuda Island

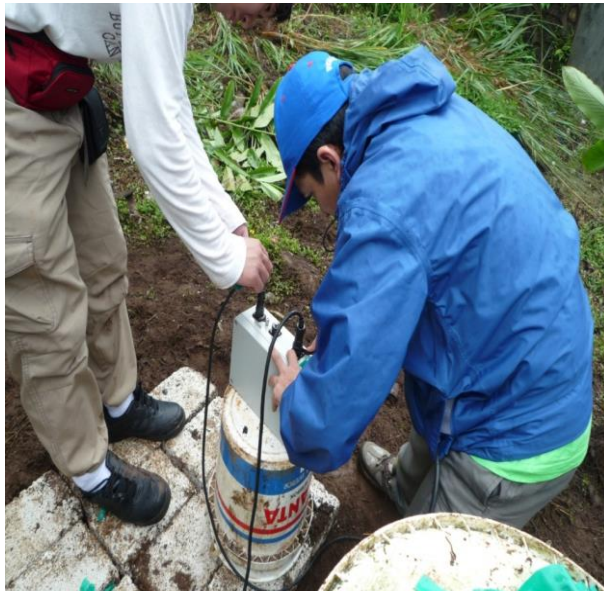


MAGDAS installation at Langkawi Island, Malaysia



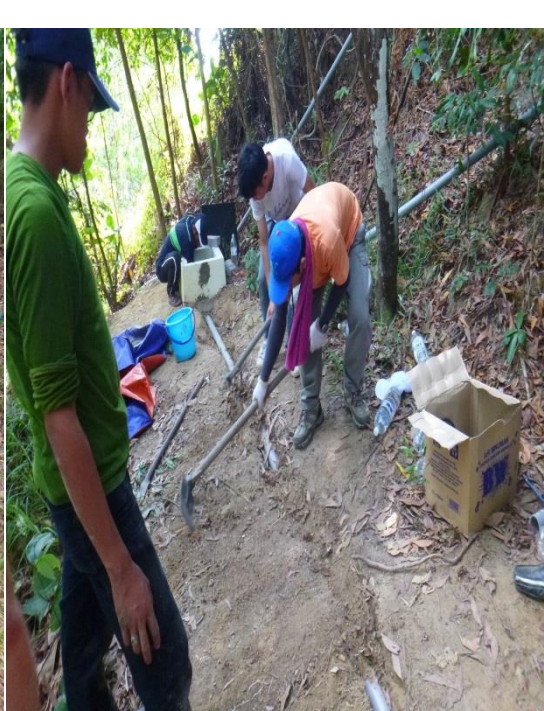
MAGDAS installation at Pontianak, Indonesia





MAGDAS installation at Jayapura and Biak, Indonesia





MAGDAS installation at UMS, Sabah, Malaysia



Daily space weather report



Outreach activities



International students visit



MAGDAS training, Sudan



Junior school students visit

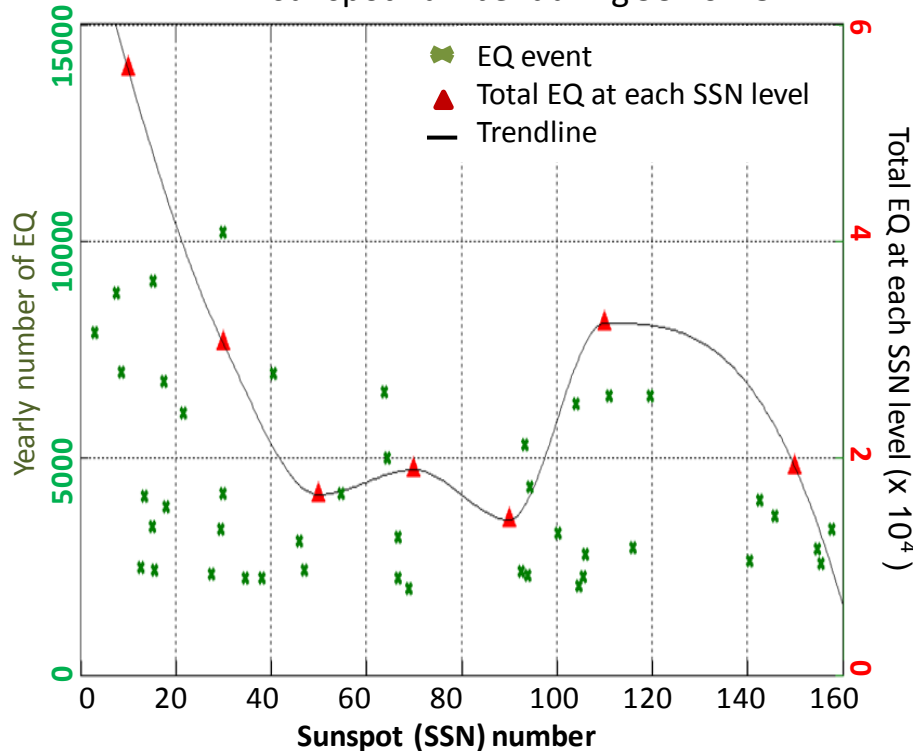


ISWI-MAGDAS School, Bandung

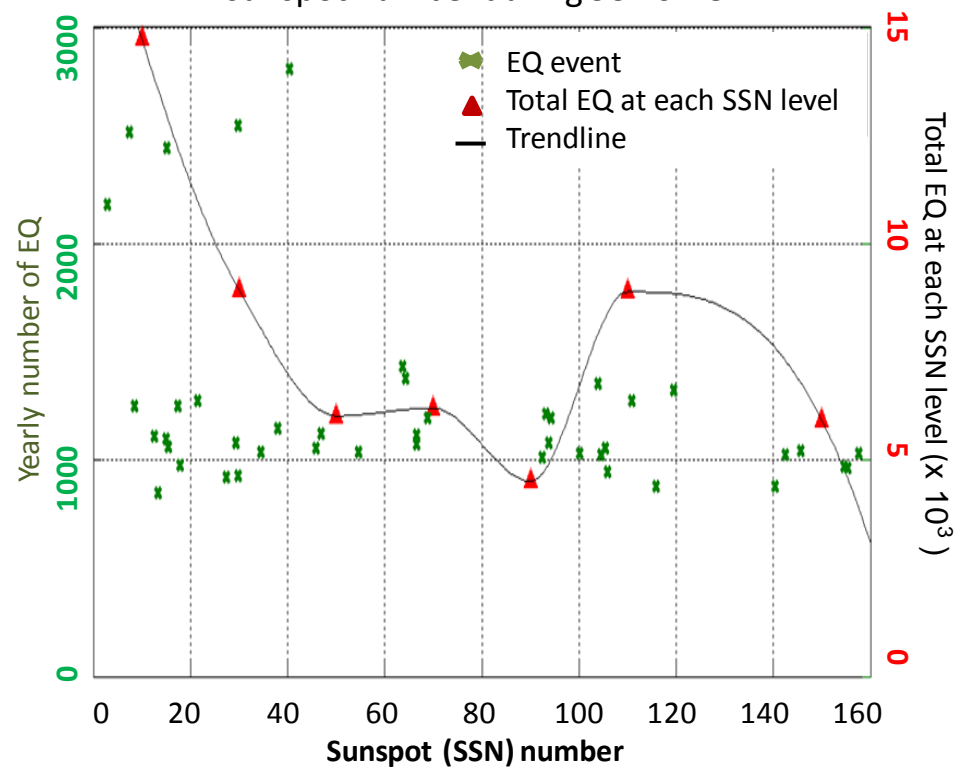


3.1.3 Variation of Earthquake depth with Solar cycle

Earthquake at epicenter depth < 40 km with sunspot number during SC 20-23

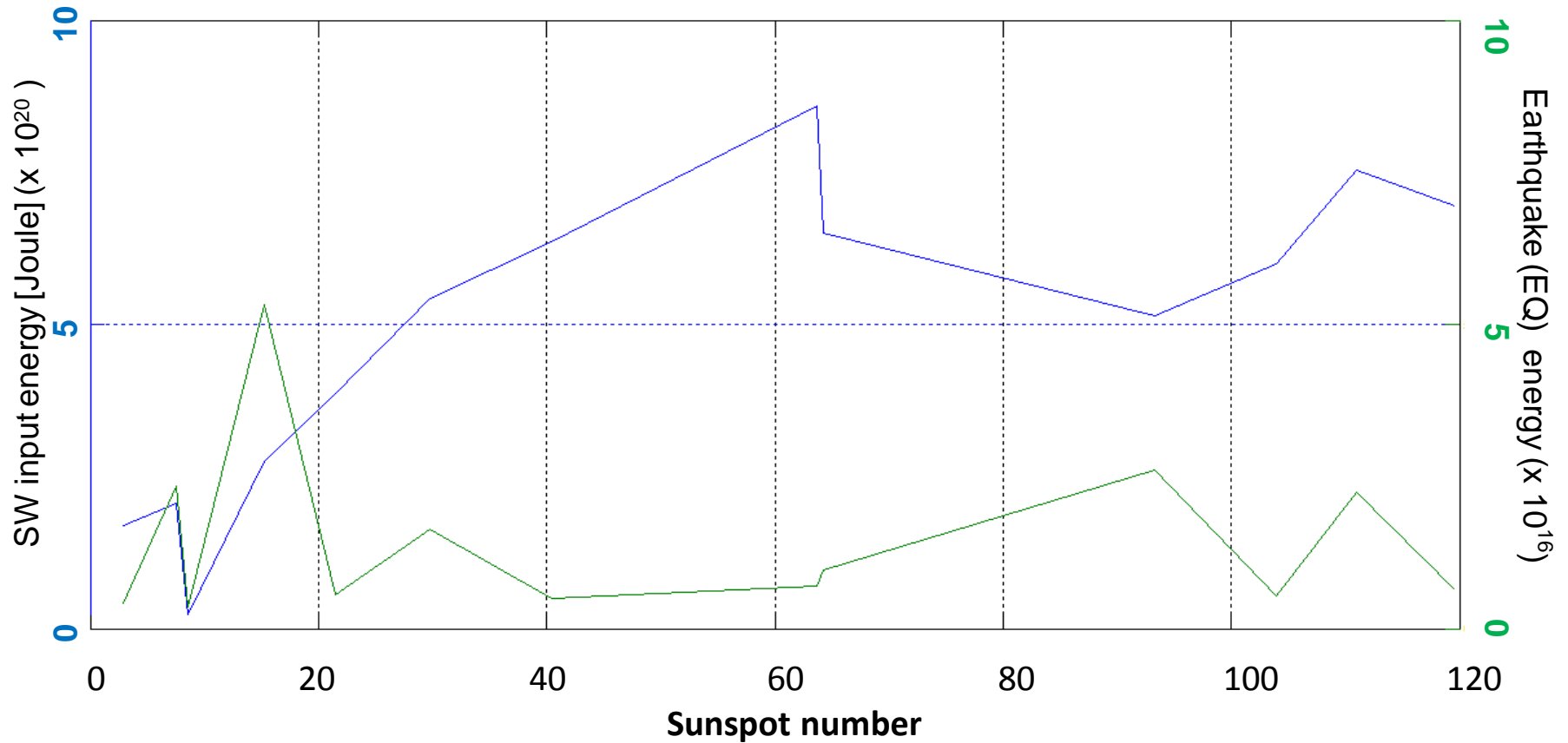


Earthquake at epicenter depth 40-100 km with sunspot number during SC 20-23

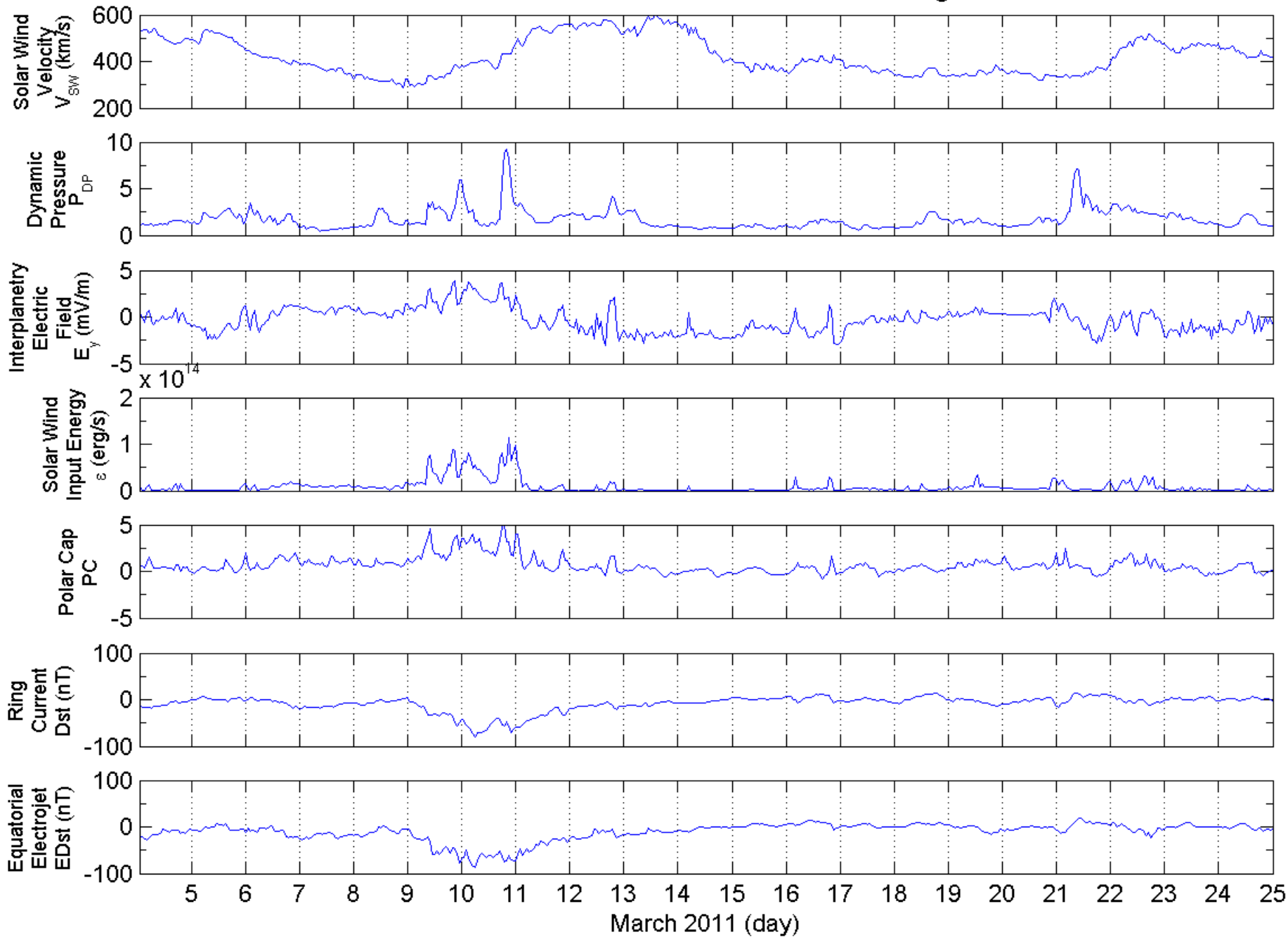


- Each sunspot number (SSN) level is categorized for every 20 SSN
- Highest number of EQ (both ranges) are observed during lowest range of SSN (0-20)
- A small increase in the number of EQ (both ranges) at SSN level 100-120.

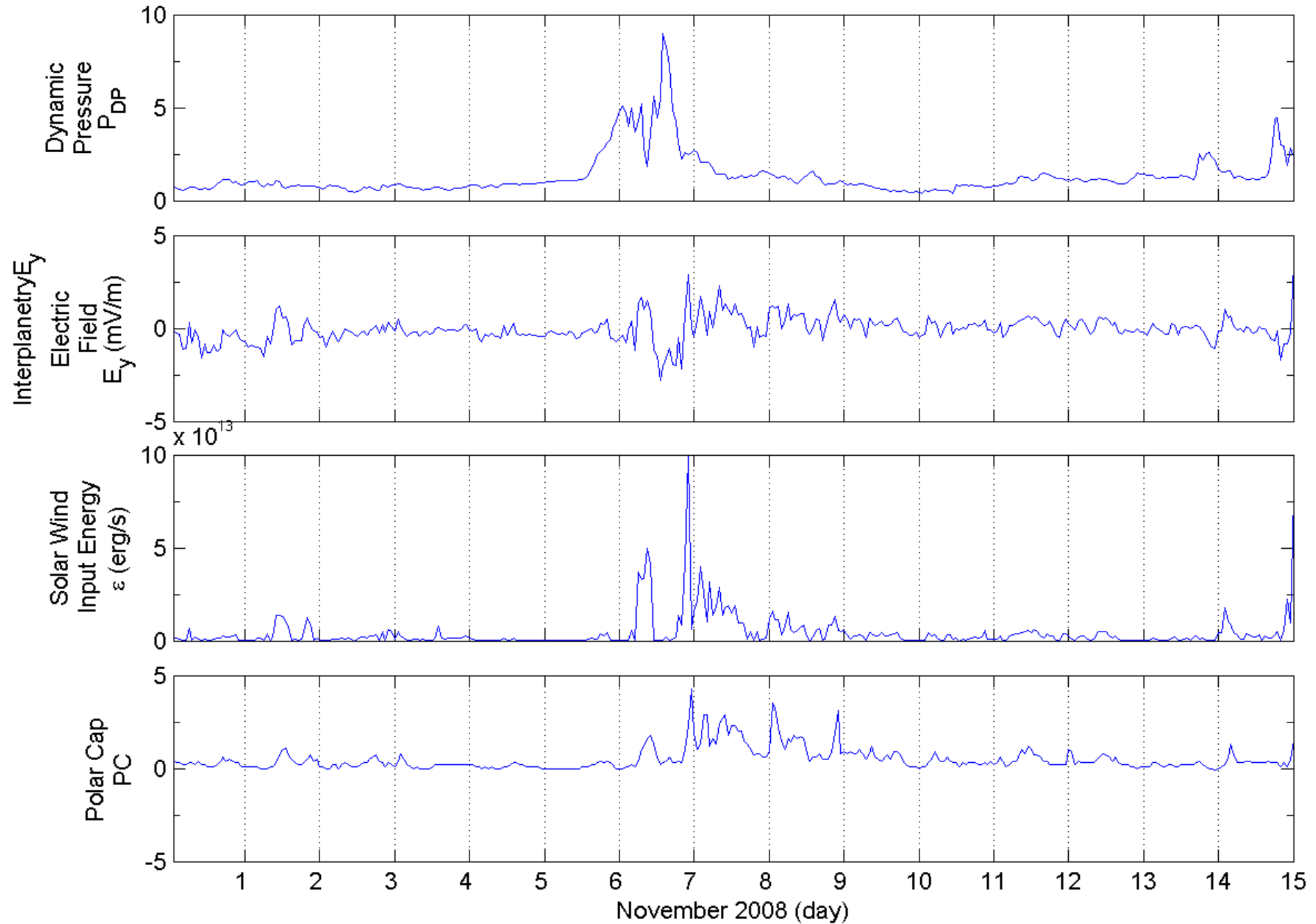
Variation of annual solar wind input energy and earthquake energy (epicenter depth 40-100 km) during SC 23



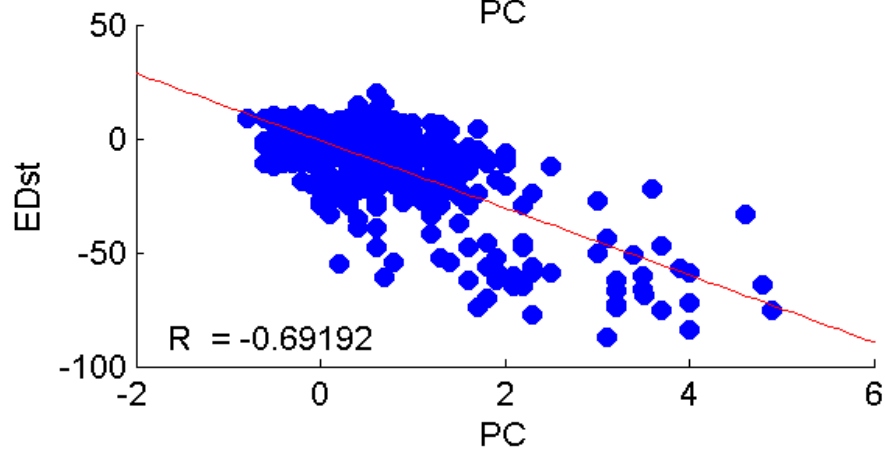
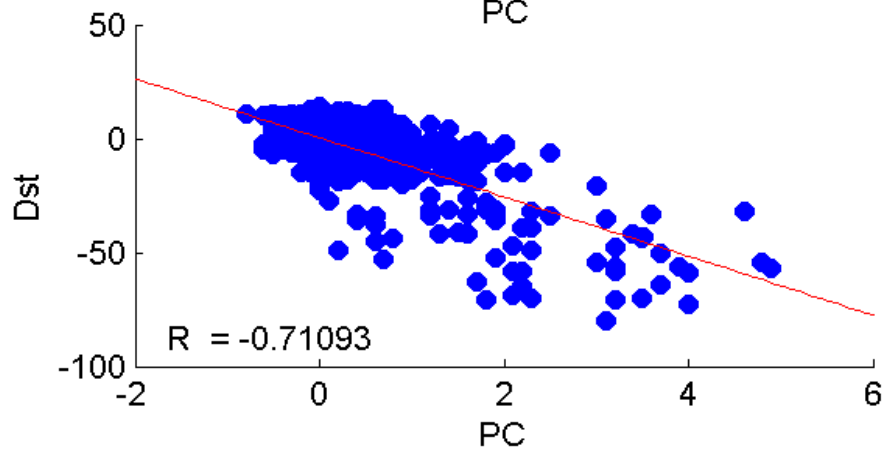
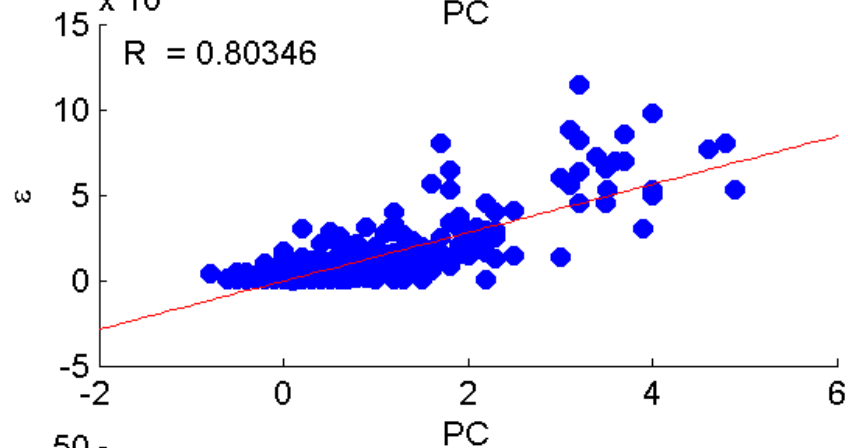
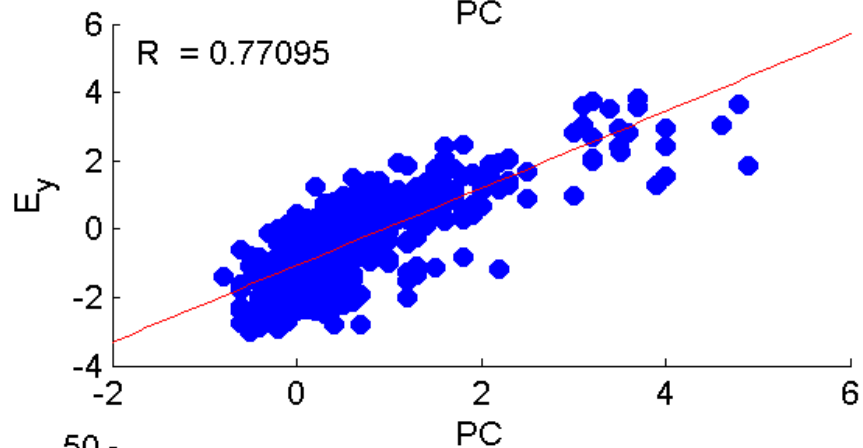
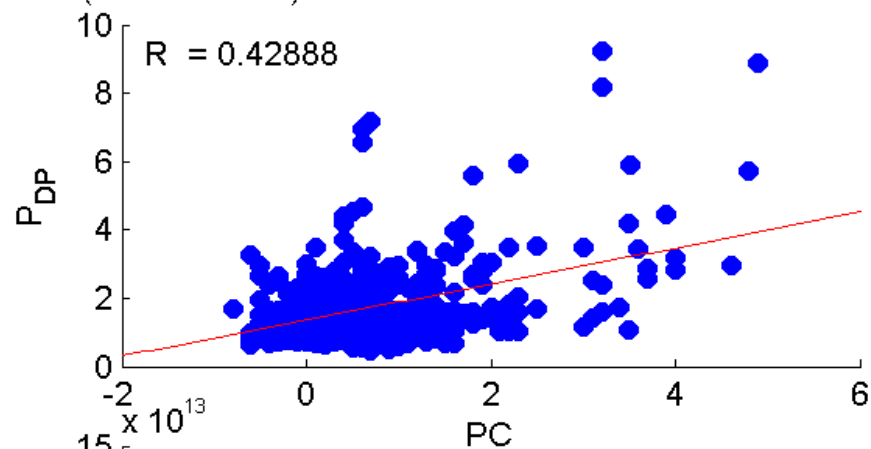
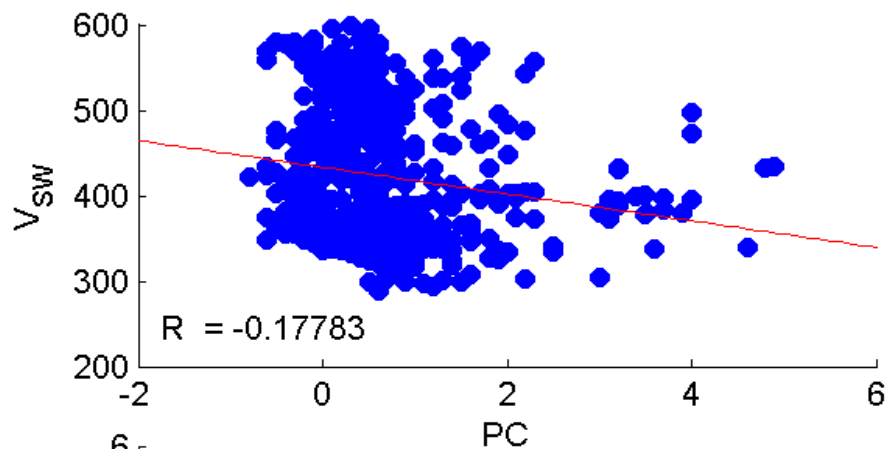
Correlation between Solar Wind Parameters and Geomagnetic Indices



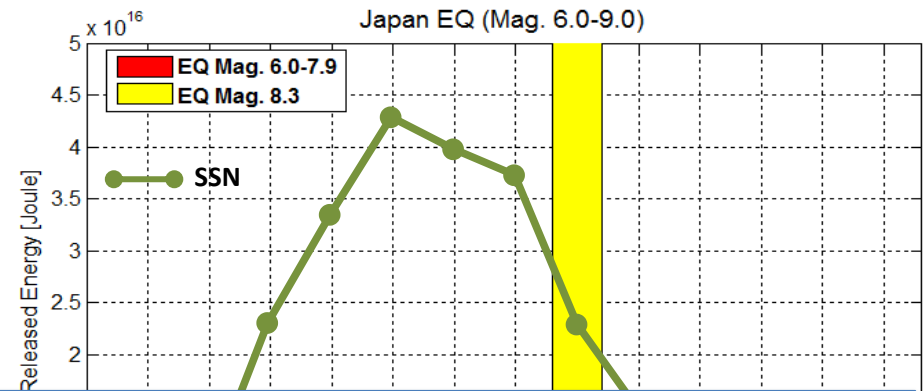
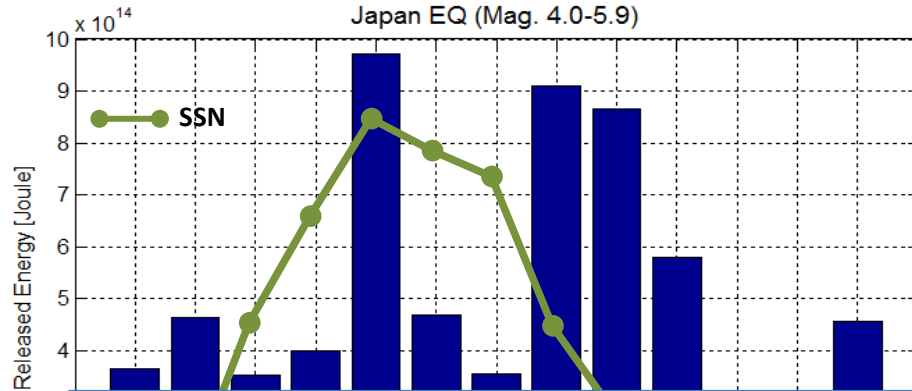
Correlation between Solar Wind Parameters and PC index



Correlation Coefficient (20110305-25)

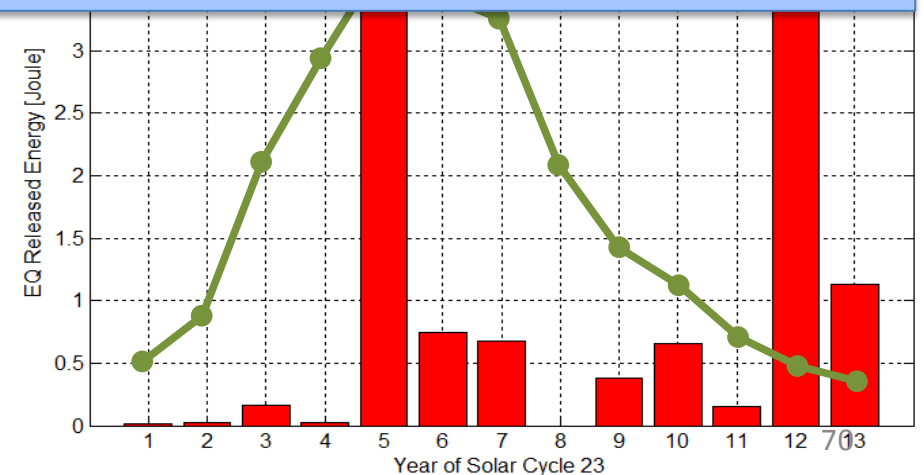
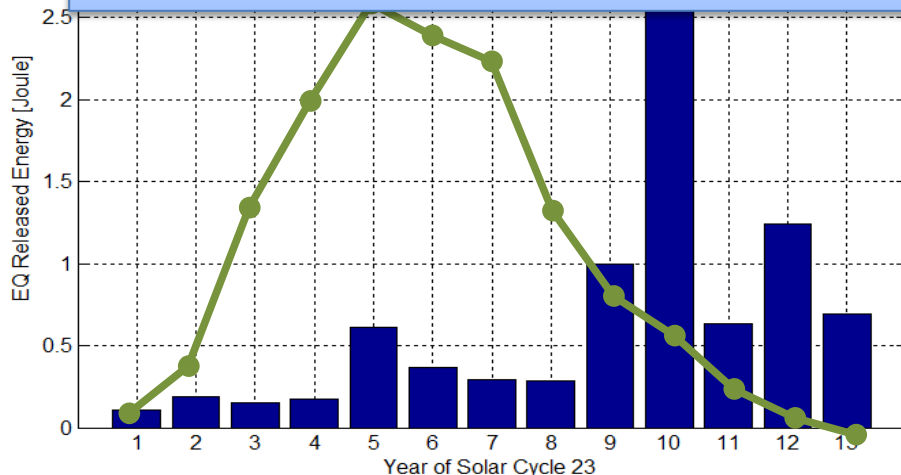


Distribution of Regional EQ Energy (SC23): Japan & Sumatra

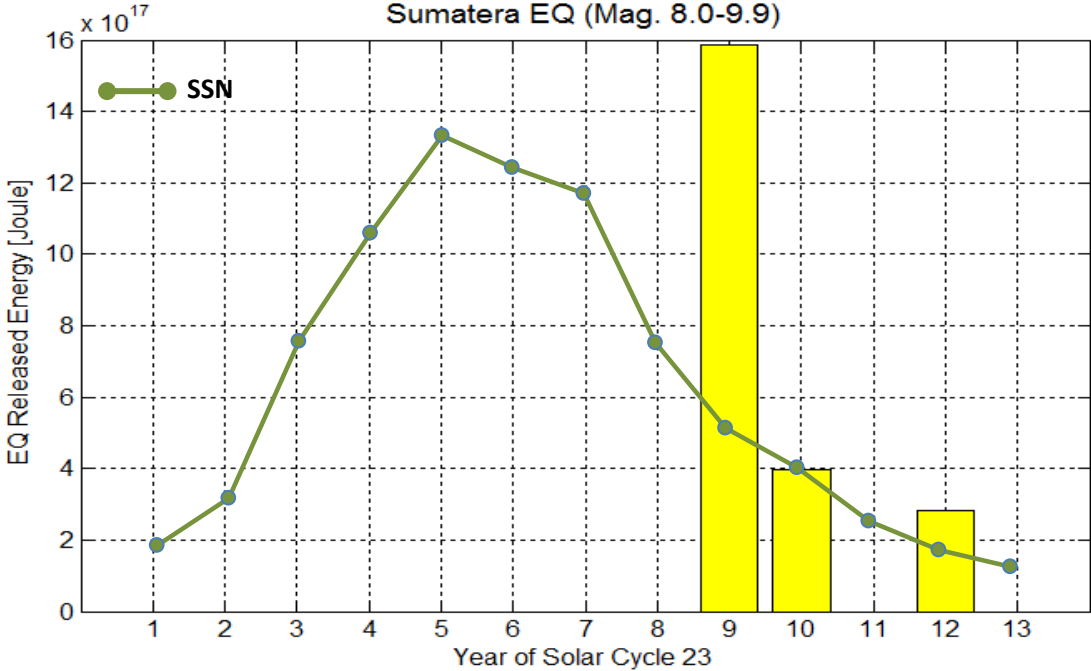


◆ The amount of EQ released energy generally shows two-peak trends, one coinciding with maximum SC period, and the second one on the descending phase of SC.

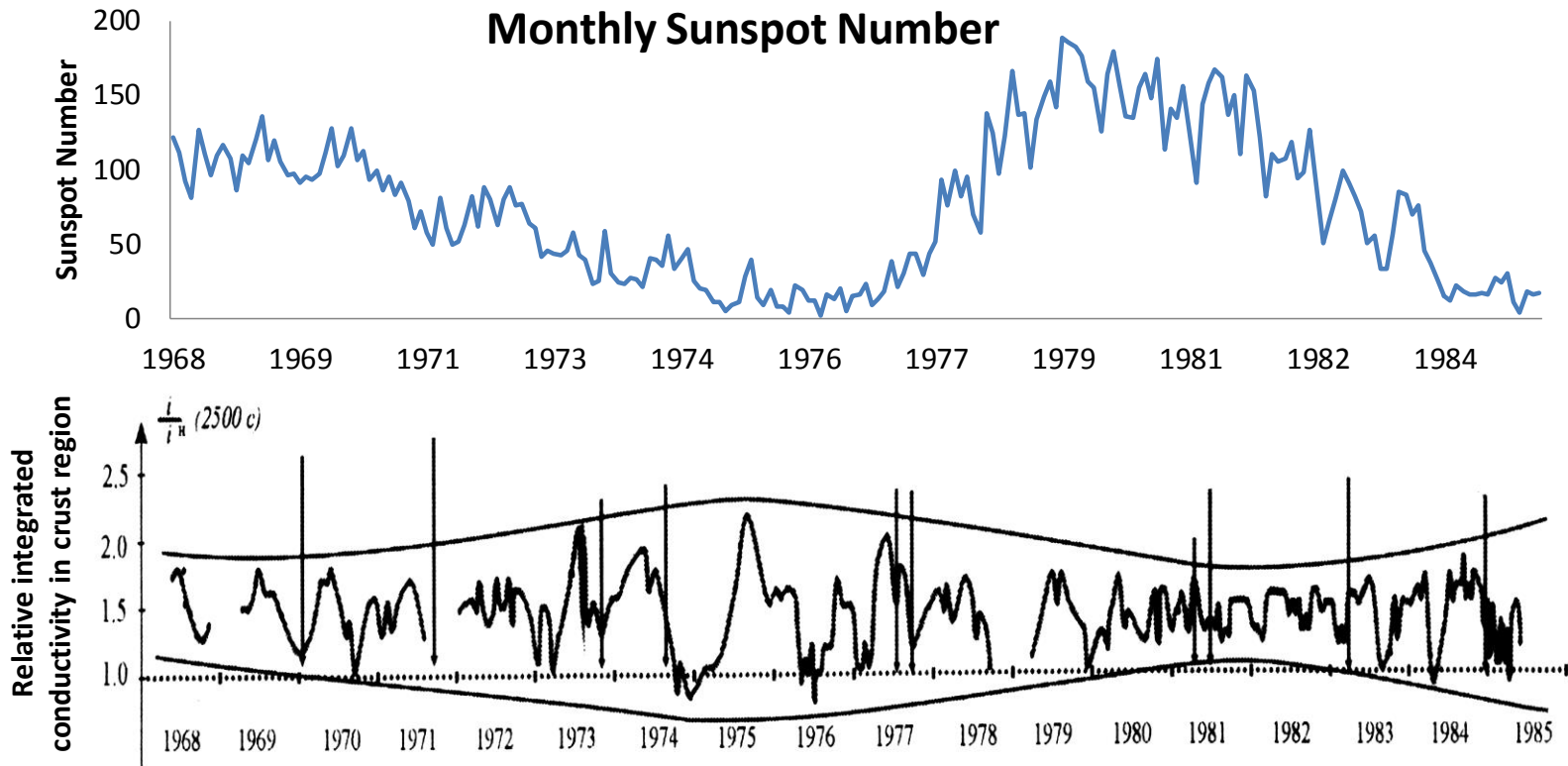
◆ Main EQ energy released during the descending and min SC.



Distribution of Regional EQ Energy: Sumatera (cont..)

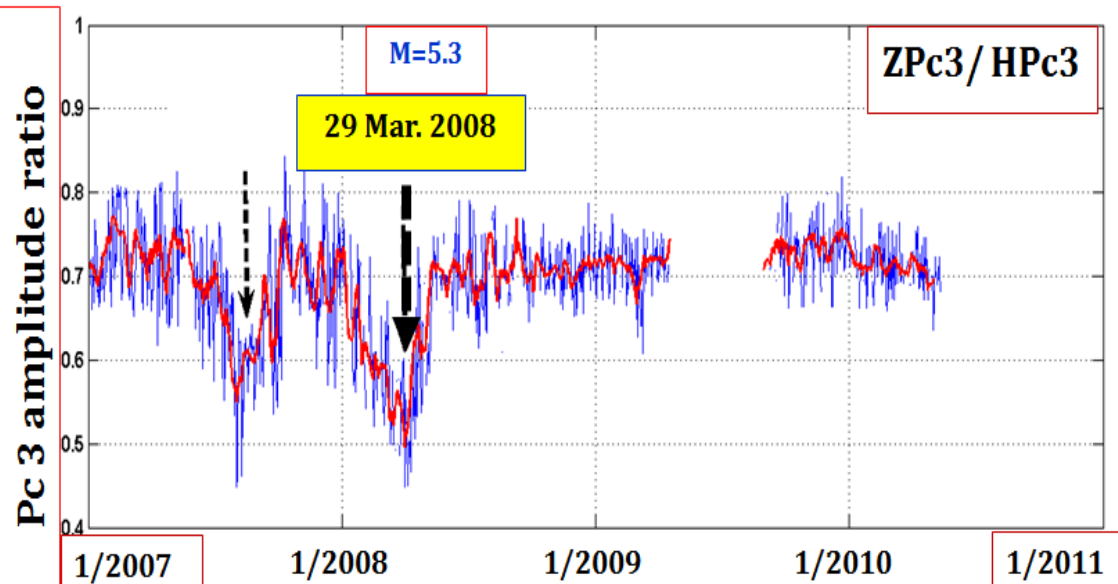
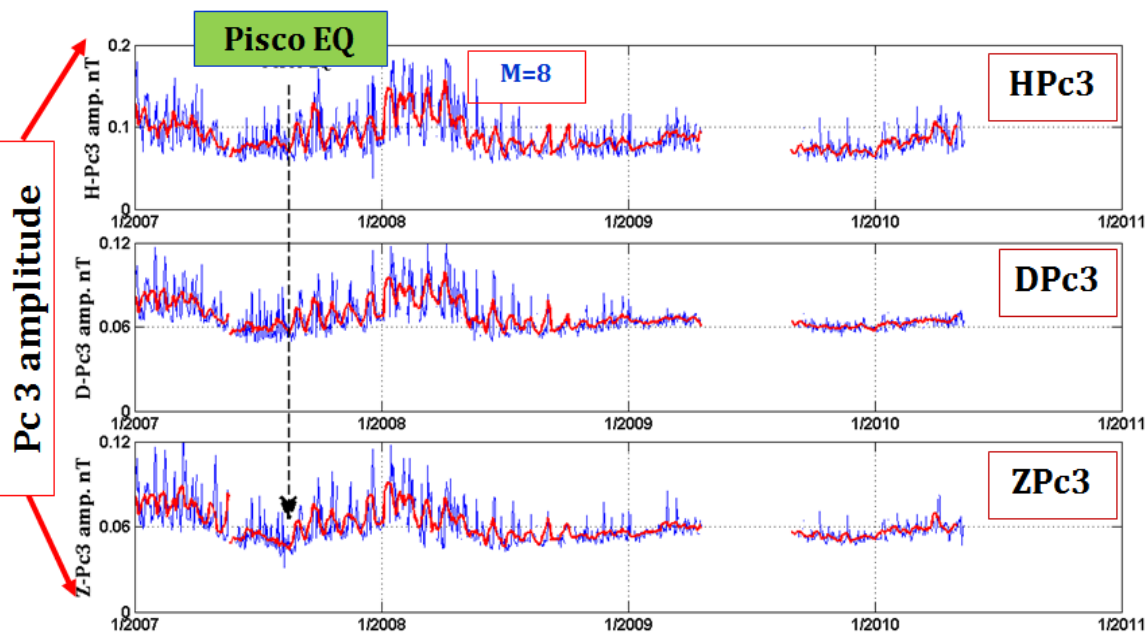


1.3 Relative Integrated Conductivity in crust region with Sunspot Number



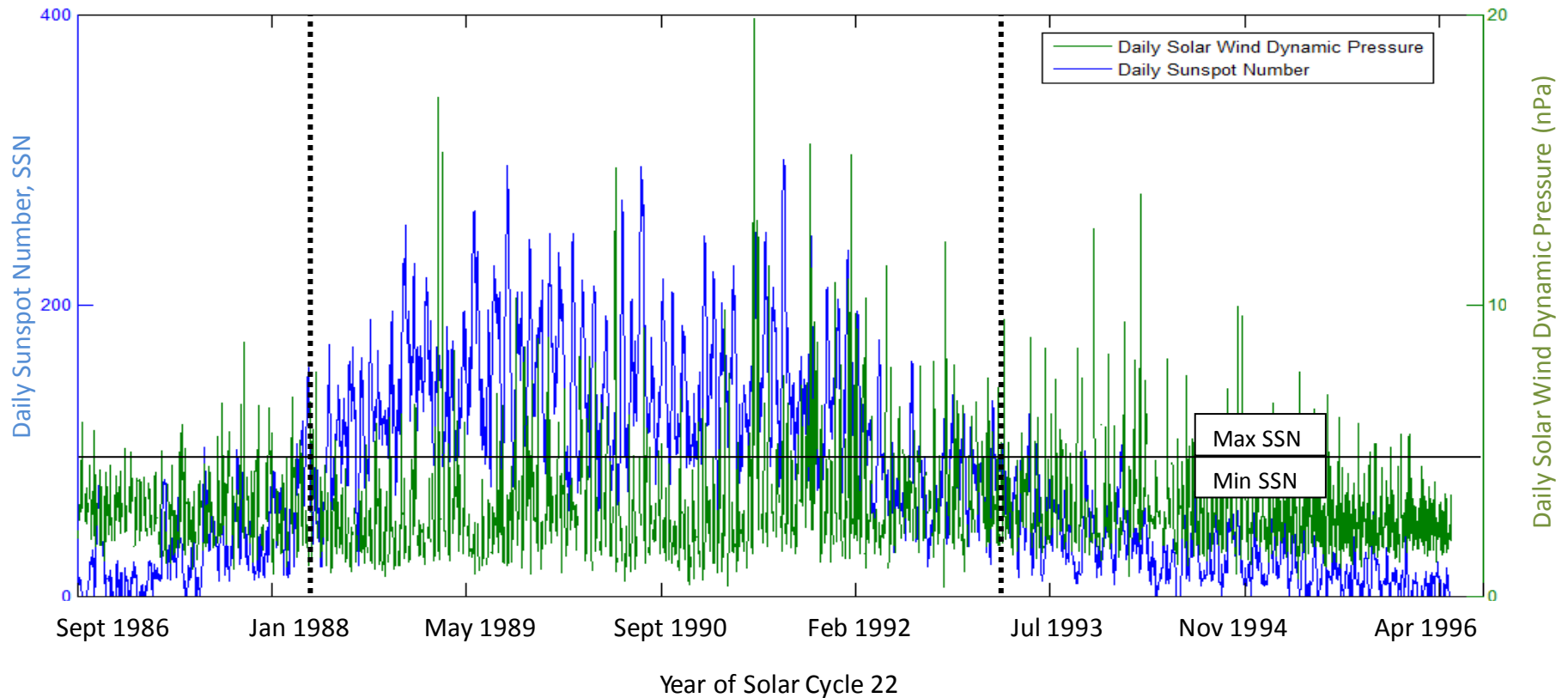
The time variation of the reduced density of telluric current east-west direction from 1968 to 1985 (for the period of 2500 sec). The arrows indicate the moments of crustal earthquakes with magnitude $M > 4$, the length of the arrows is proportional to the magnitude [V. M. Nikiforov, 2010]

Anomalous ULF emissions during EQ events (Emad et. al, 2012)



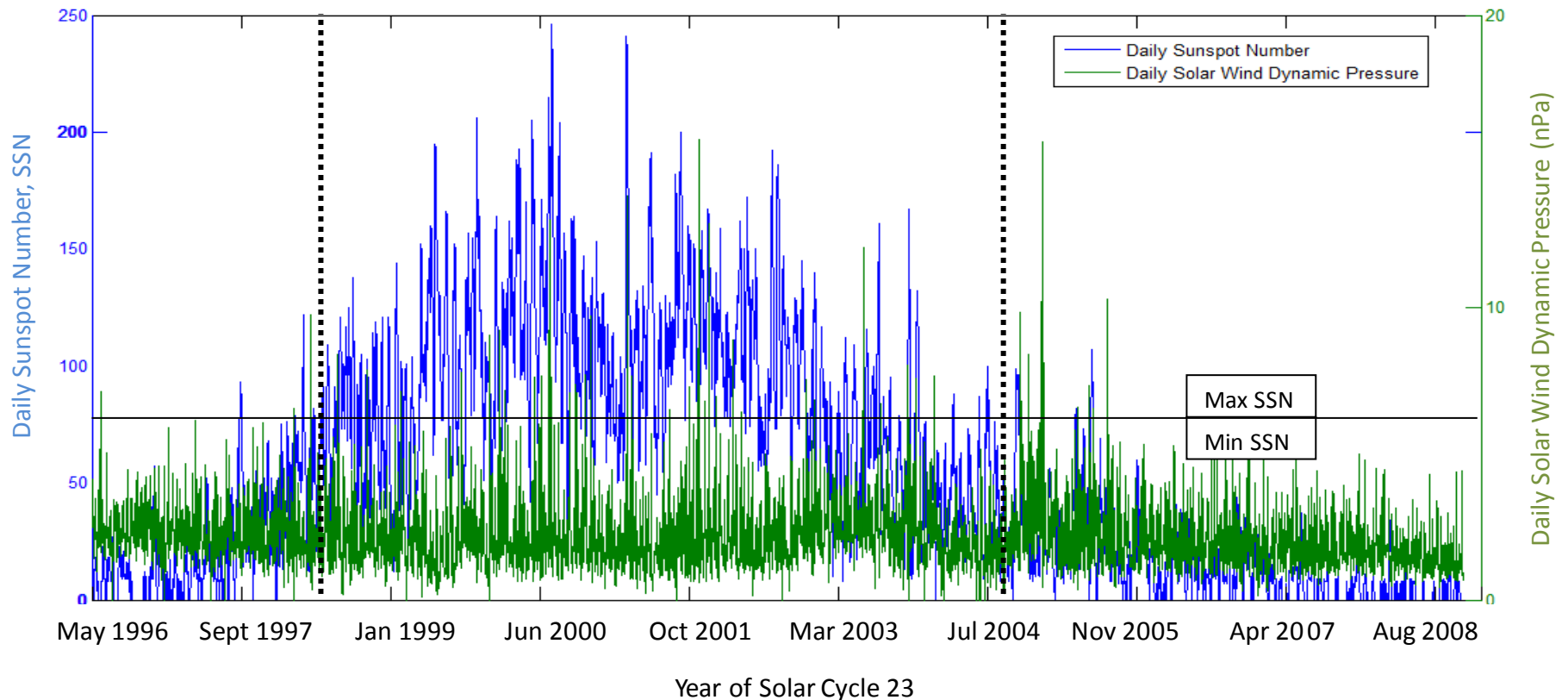
- Higher variation in the daily average of Pc3 amplitude (10-45s) detected a few months before the EQ events; on 15 Aug 2007 and 29 Mar 2008.
- The Pc3 amplitude ratio (ZPc3/HPc3) also shows a good agreement with higher depression ratio for both EQ events.

Superposition of Daily Sunspot Number and Solar Wind Dynamic Pressure during SC 22



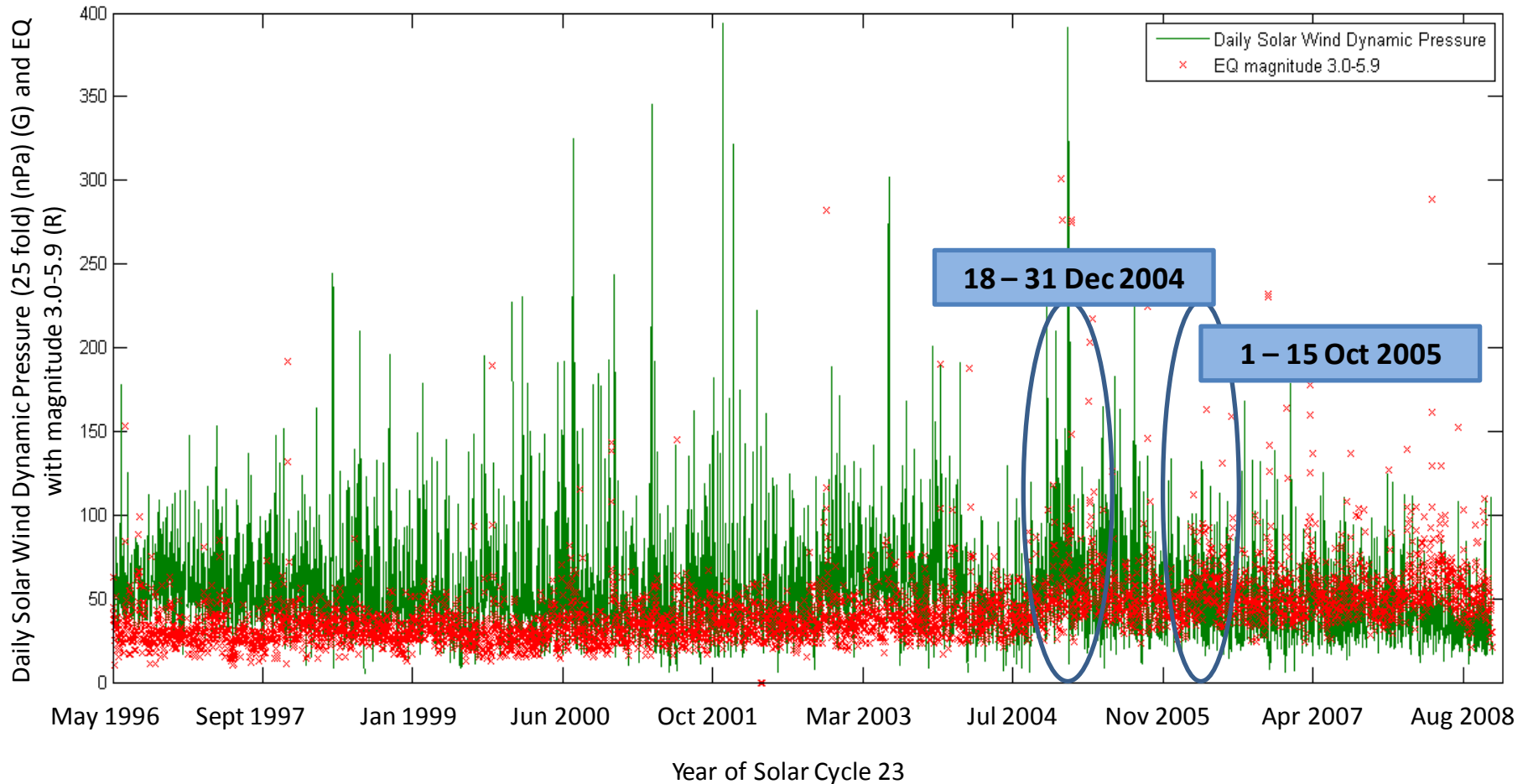
- The average solar wind dynamic pressure during maximum SC is 2.1 nPa and for minimum SC is 2.2 nPa.
- Number of event ≥ 3 nPa maximum SC are 458 events and for minimum SC are 520 events.

Superposition of Daily Sunspot Number and Solar Wind Dynamic Pressure during SC 23



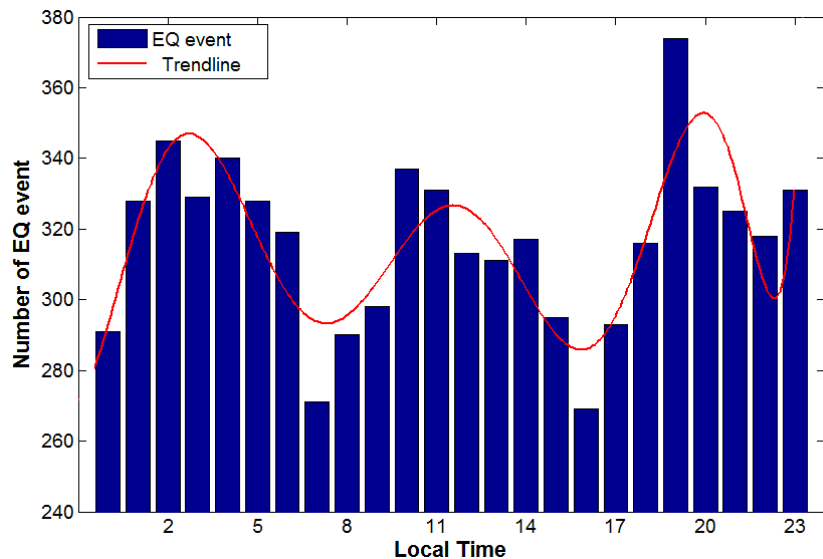
- The average solar wind dynamic pressure during maximum SC is 2.2 nPa and for minimum SC is 2.1 nPa.
- Number of event ≥ 3 nPa maximum SC are 445 events and for minimum SC are 394 events.

2.4.1 Relationship of Solar Wind Dynamic Pressure with Earthquakes – analyzed events

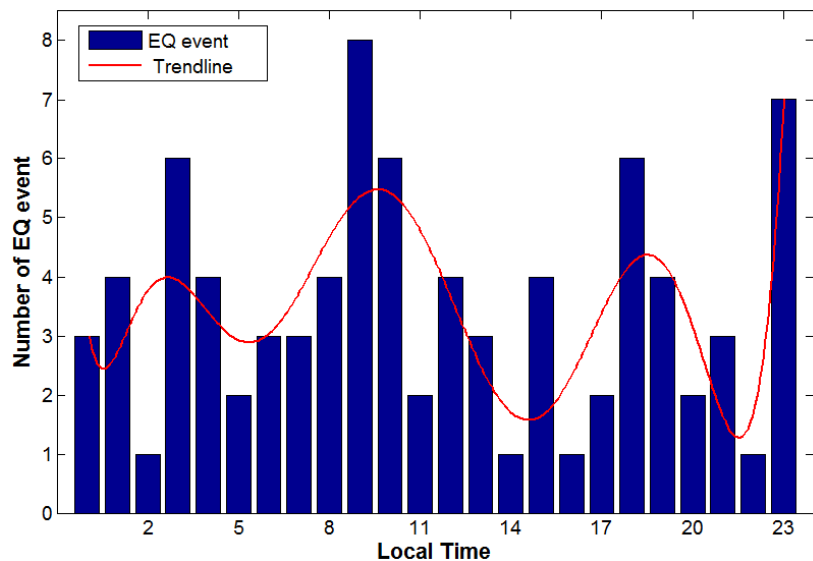


- **Additional statistics: 5 – 25 March 2011**

Overall trends of Diurnal Japan EQ (Mag. 3.0 – 9.9) with Local Time during SC 23

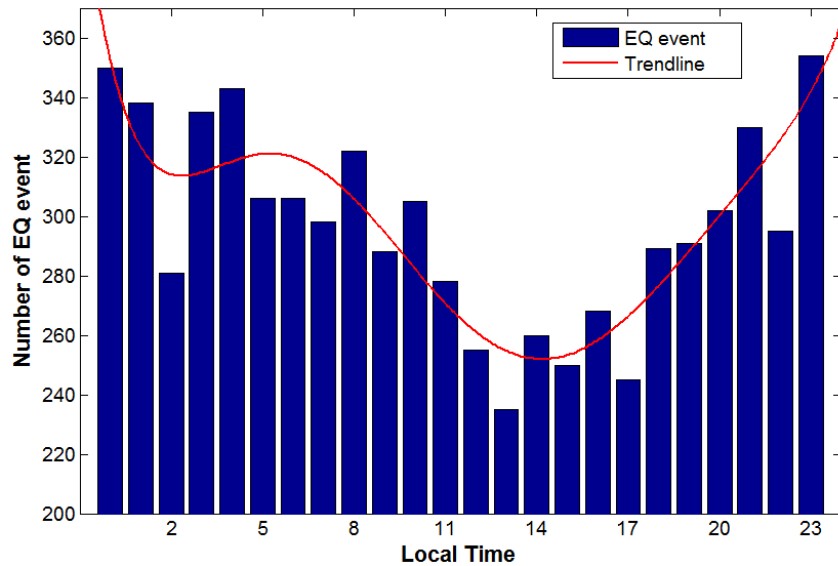


● For diurnal Japan low EQs magnitude, we detected 3 peaks of EQs triggered which are during; early morning, afternoon and night time
 ● dusk to dawn and dawn to dusk, both experiencing minimum number of EQs
 ● It's shows there is possible connection with day and night time terrestrial parameters, i.e Sq current.
 ● Further details analysis needed to prove this hypothesis



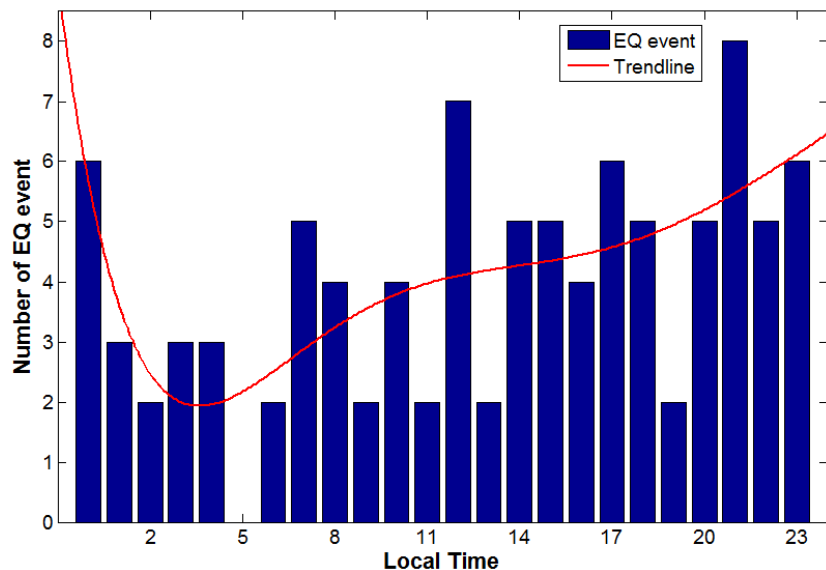
● The higher magnitude of Japan EQs also shows the similar pattern with lower EQs magnitudes
 ● The similarity of diurnal variation with lower EQs magnitudes shows the same triggering mechanism for EQs at higher magnitudes
 ● Further analysis also needed to prove this hypothesis

Overall trends of Diurnal Sumatera EQ (Mag. 3.0 – 9.9) with SW parameters



• For diurnal Sumatera low EQs magnitude, we detected 2 peaks of EQs triggered which are during; dusk to dawn and from dawn to dusk

• For further analysis, we are currently analyzing the local Sq current and looking into a few possible mechanisms which possibly connecting them, i.e. Lorentz forces and tidal forces of the sun

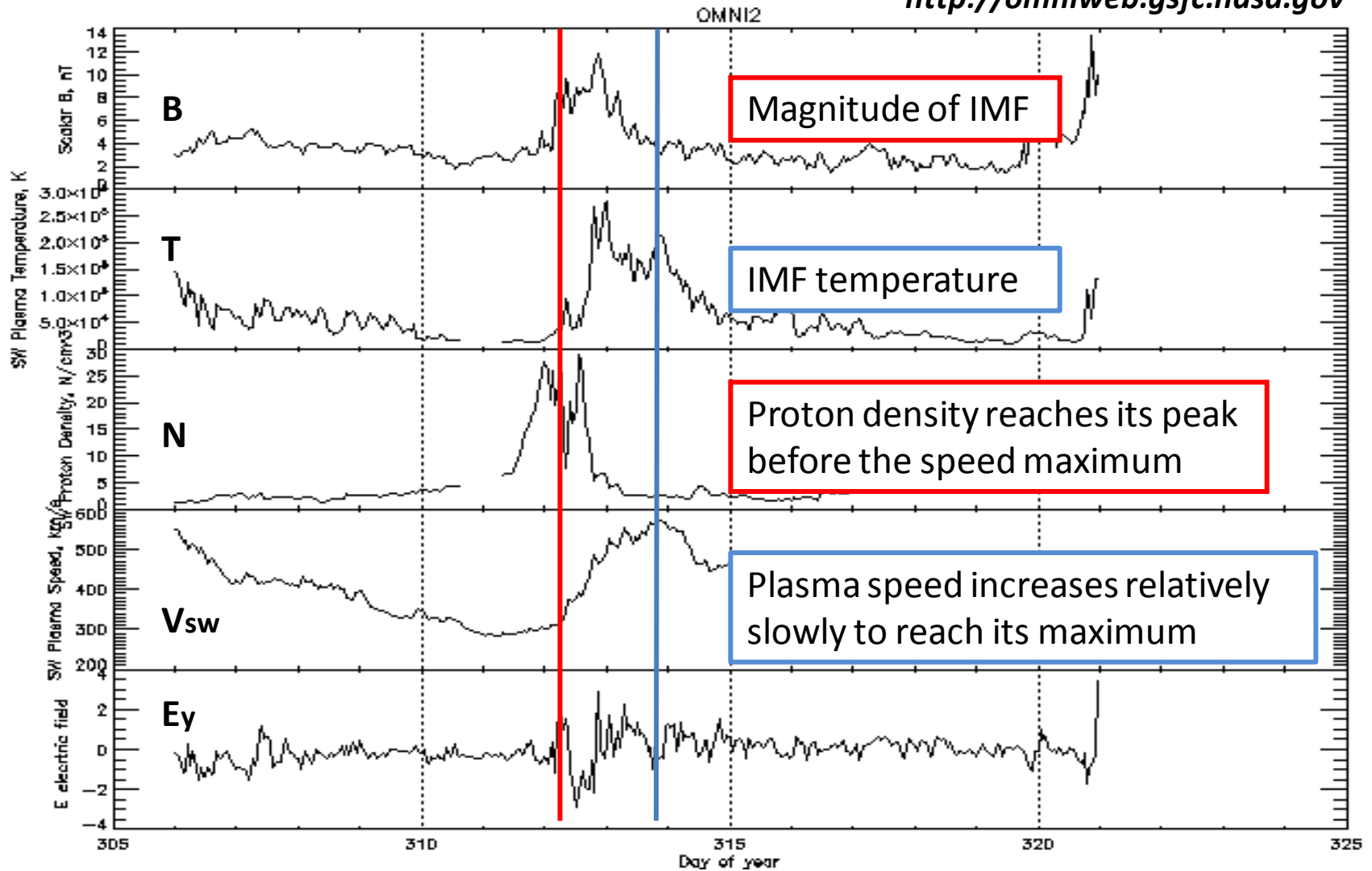


• The plots for higher Sumatera EQs in contrast with the lower EQ magnitudes range.

• We are suggesting for longer period of diurnal EQs analysis due to the activeness of triggered EQs in this subduction zone

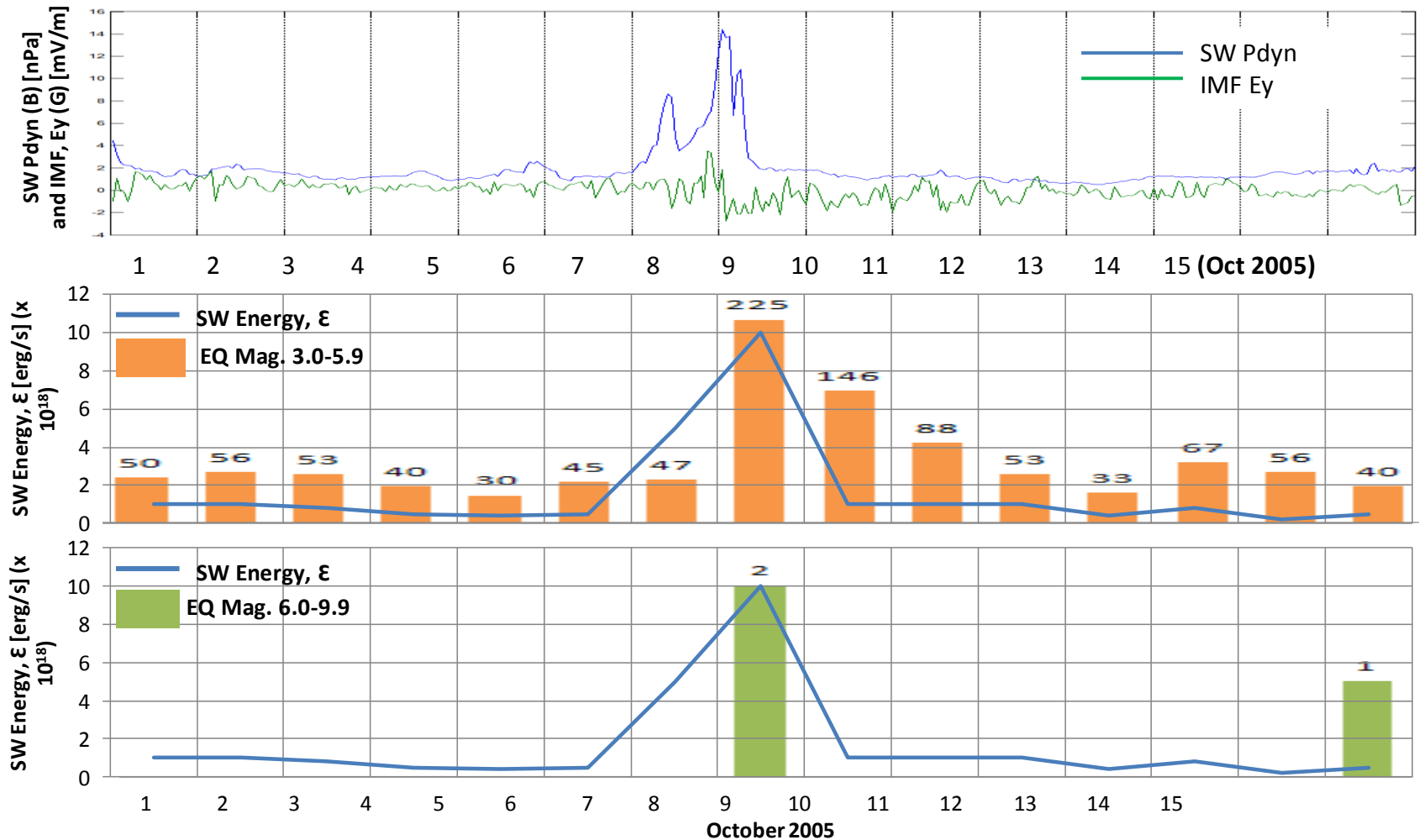
Coronal Hole (CH)-HSSW

<http://omniweb.gsfc.nasa.gov>



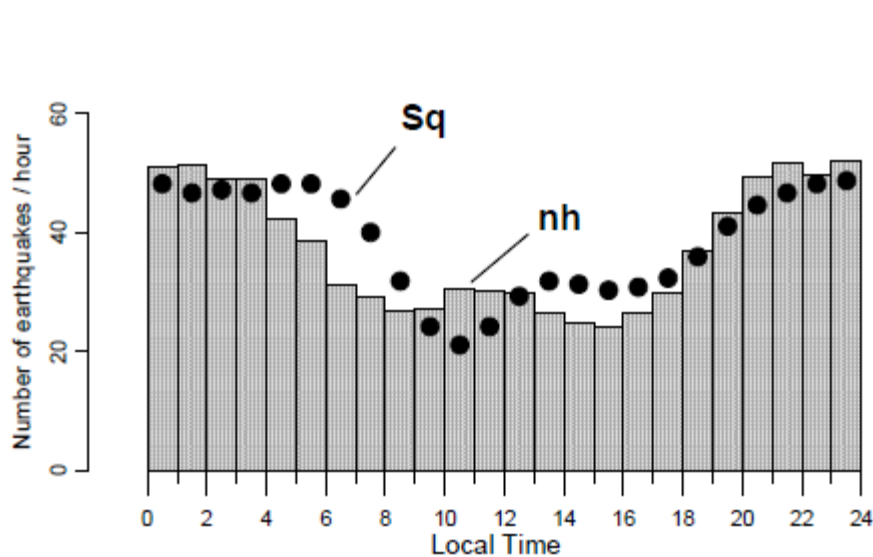
A typical CH-HSSW (detected on 8 Nov 2008). Observation period is from 1 Nov to 15 Nov 2008.

2.4.3 Relationship of Solar Wind Energy with Earthquakes: 1 – 15 October 2005



- SW Pdyn and IMF Ey show a highest variation on 8 Oct 2005 with more than 12 nPa and -2 mV/m respectively; on the same day where the SW energy detected a high rise.
- On the same day, the number of EQ increases almost 5 times from the previous days.

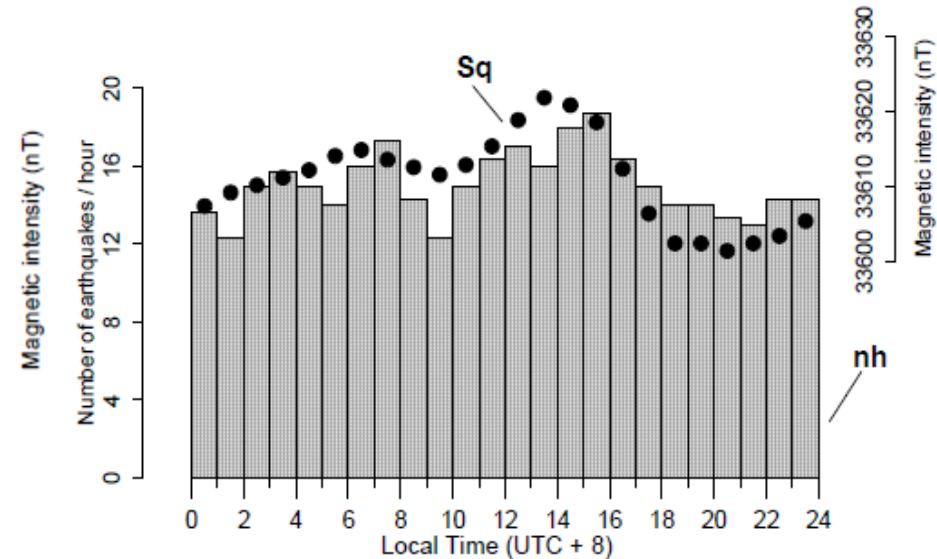
2.1 Diurnal changes of earthquake and geomagnetic Sq-variations (G. Duma & Y. Ruzhin, 2002)



Region: Austria

Period: 1901 – 1990

EQ magnitude: $2.5 \leq M \leq 5.0$



Region: East China

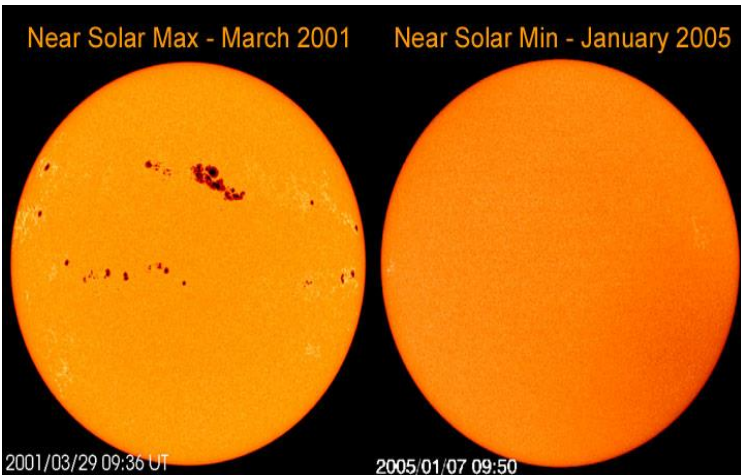
Period: 1900 – 1992

EQ magnitude: $M \geq 6.0$

- The number of earthquake (nh) corresponds to the variation of geomagnetic Sq-variations (Sq).
- The Sq current system is mainly controlled by solar radiation
→ **Possible Solar – Seismicity coupling**

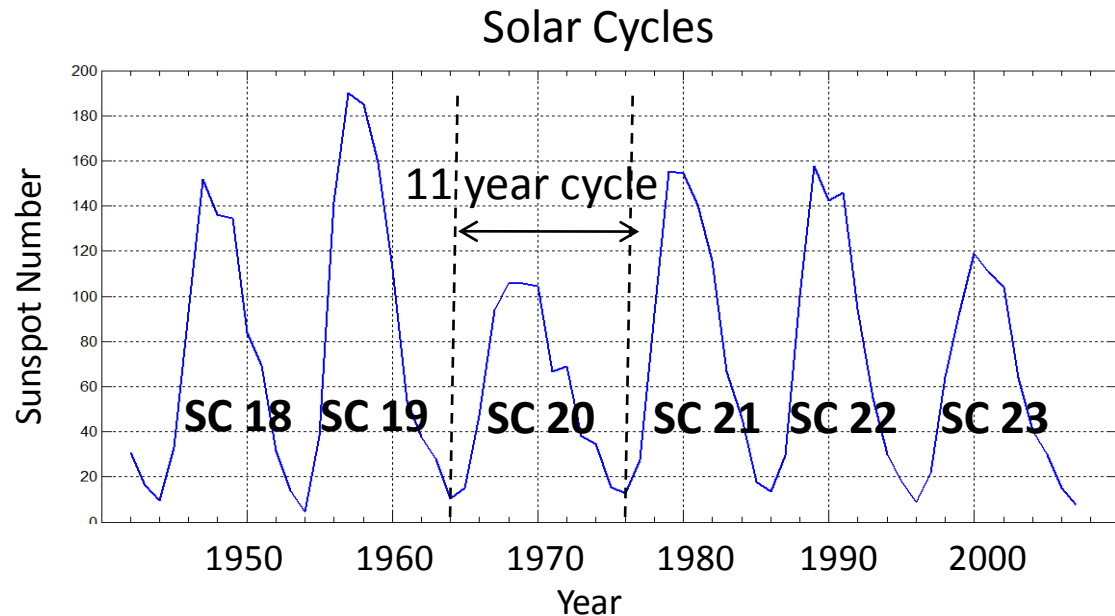
3.1 Variation of Solar Cycle and Earthquake

- Solar cycle (SC) represents the number of sunspot observed on the sun which has 11-year cycle (average).



Sunspots observed by NASA

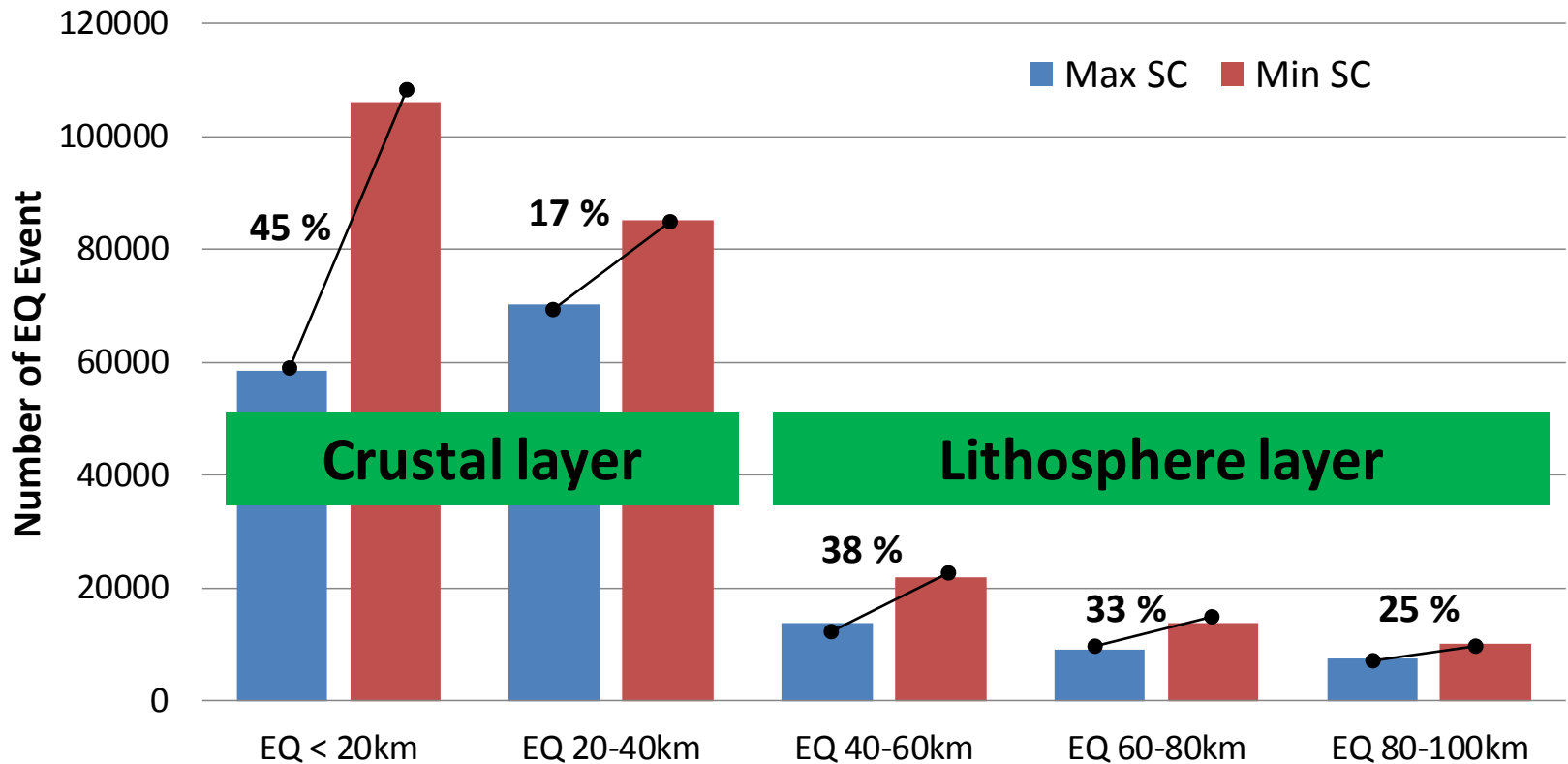
Source: <http://sohowww.nascom.nasa.gov/>



Objective:

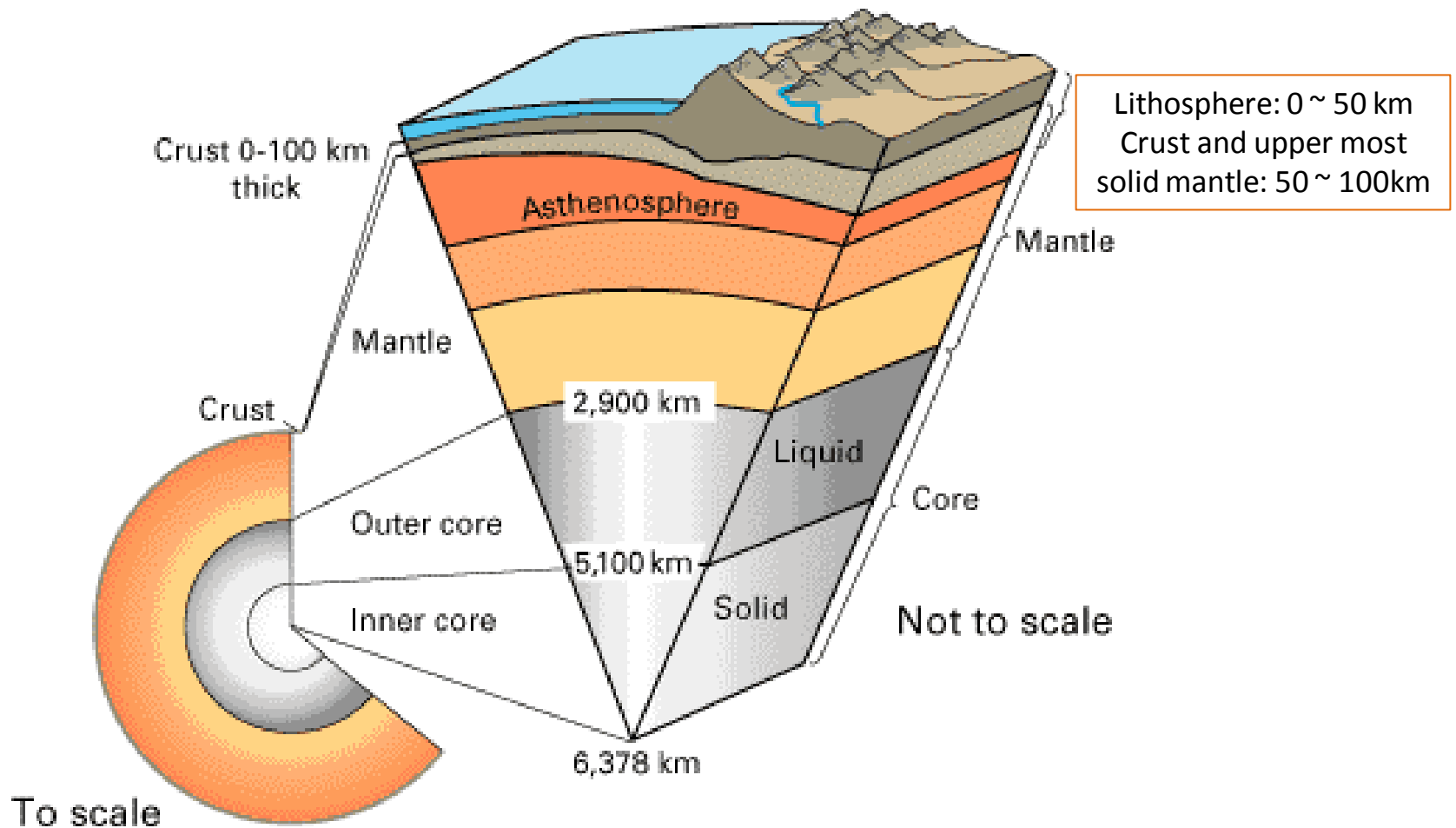
To investigate the relationship between solar activity (solar cycles) and earthquake events (globally and locally) at different magnitudes and epicenter depth.

3.1.6 Occurrences of EQ at Different Depth during SC 20 to 23



- Higher number of EQs occurred at 0 to 40 km depth during the solar minimum phase, and a few events at deeper-depth from 40 to 100km.
- The existence of dilatancy fracture ($\rho = 20-50 \Omega\text{m}$) at crustal layer also possible to contribute higher number of shallow depth earthquakes.

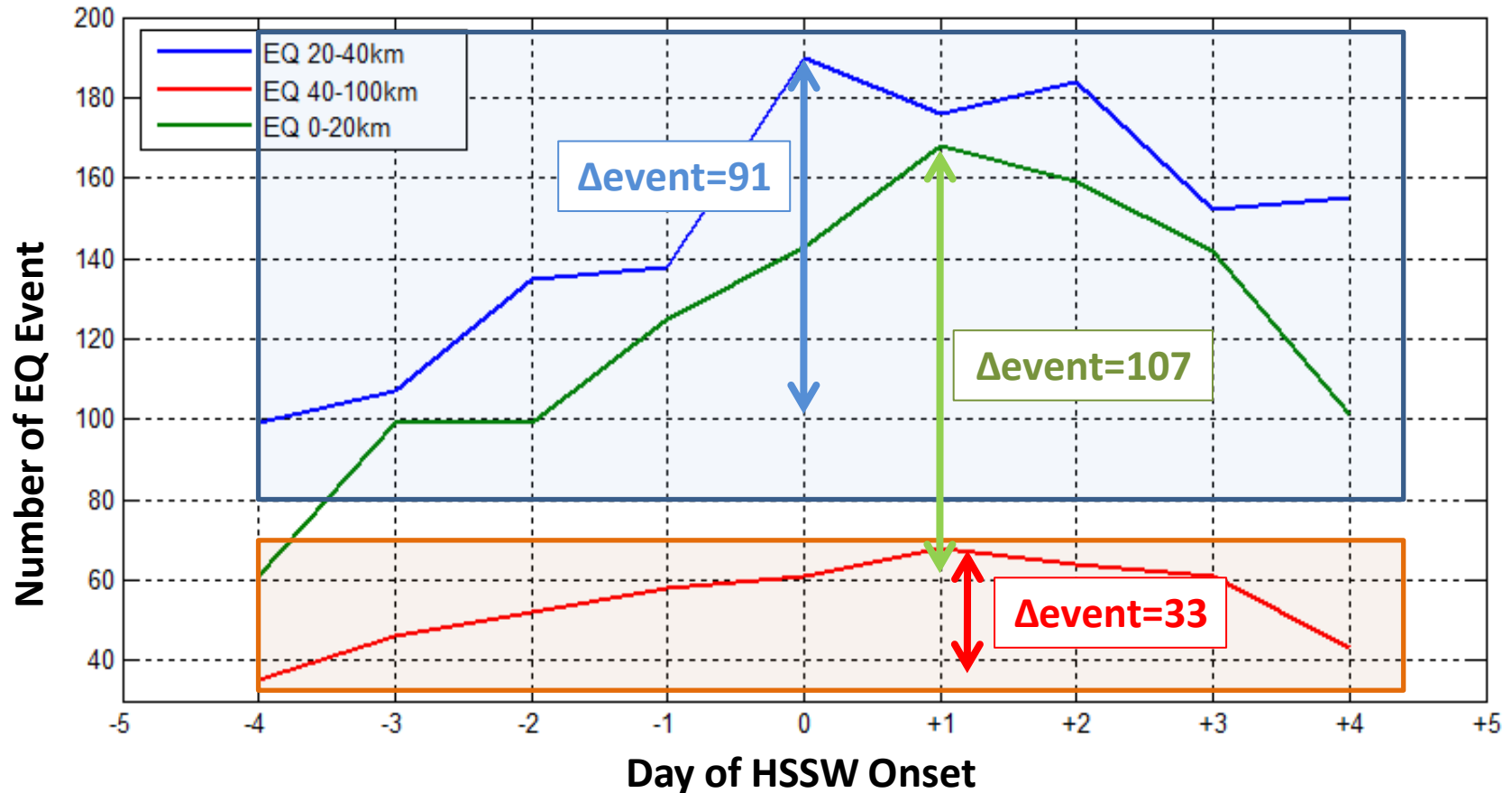
Inside the Earth



Source: *Inside the Earth* available at <http://pubs.usgs.gov>

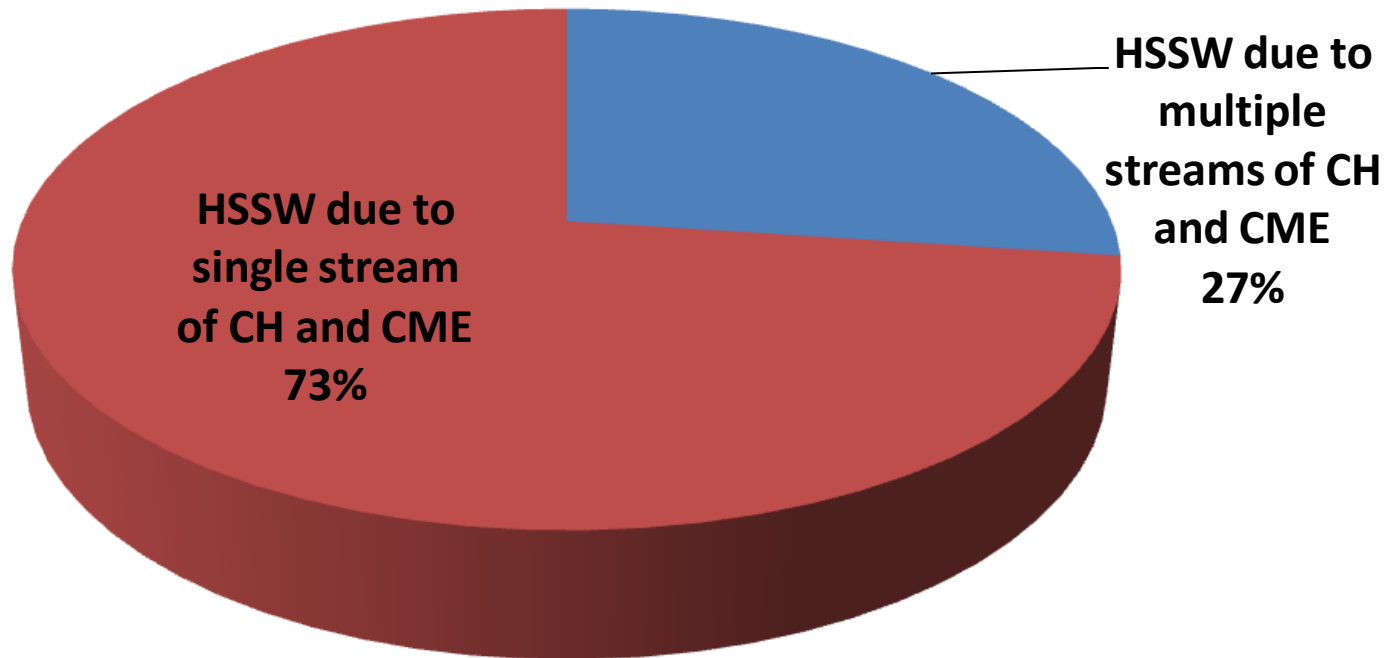
Analysis of HSSW Dependence on EQ at Different Depth

Relationship of EQ Onset with HSSW



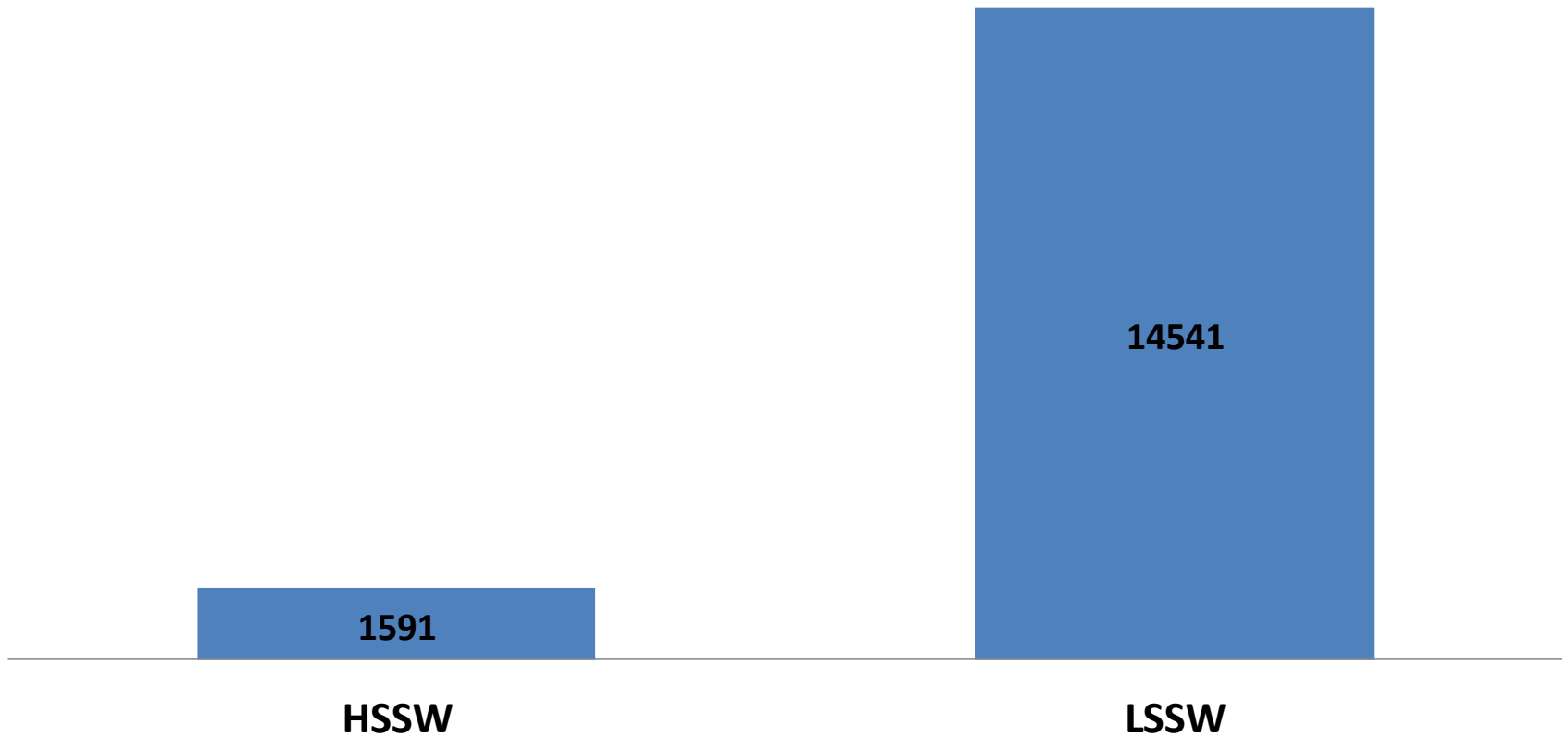
- The shallow earthquakes; from 0 to 40km show a higher correlation with HSSW on the day to 3 days after the HSSW arrived to the earth compared to deep earthquakes.

Percentage of HSSW due to Multiple and Single Stream



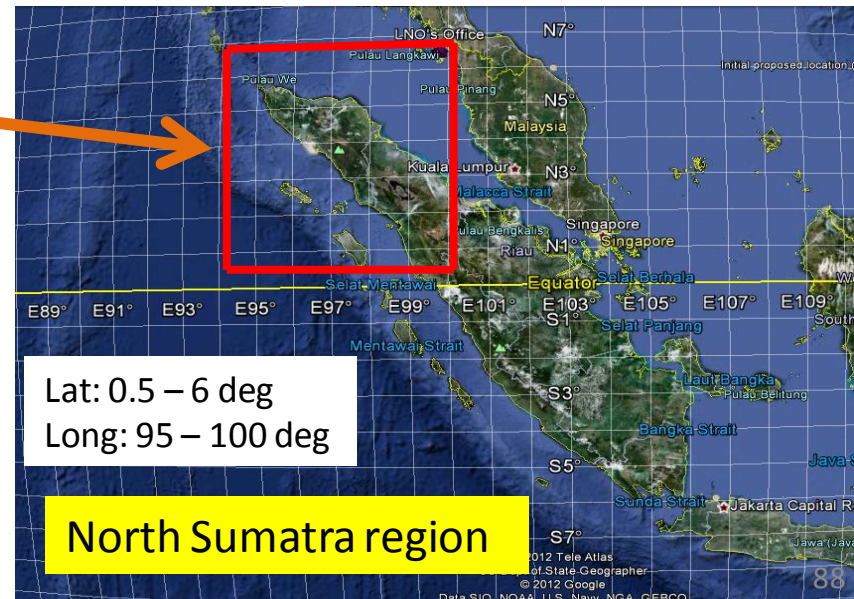
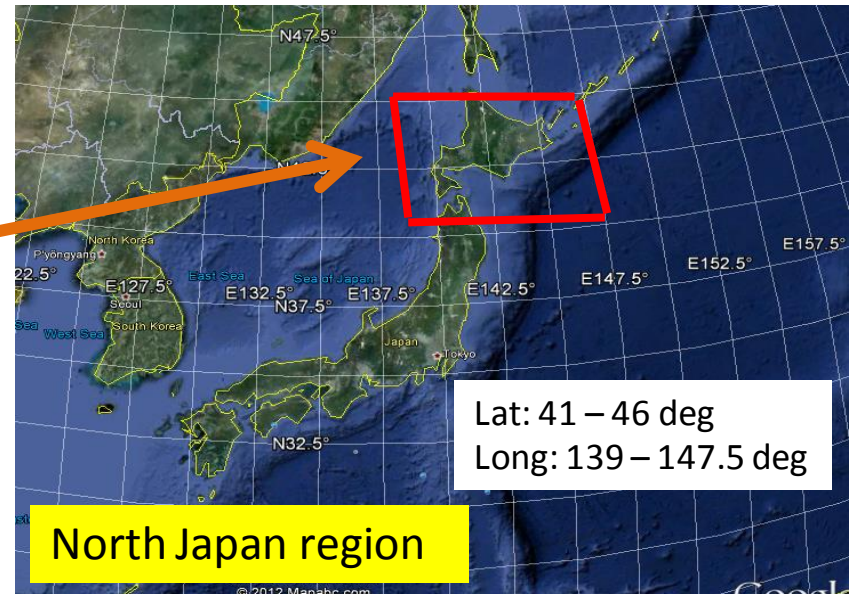
- 432 HSSW events (out of 1591) detected caused by multiple streams of solar wind.
- **80 %** of these multiple stream-HSSW occurred before the earthquake events with magnitude 6.0-9.9.
- It maybe due to higher energy from multiple stream-solar wind propagated to lower atmosphere.

Fraction of Daily Solar Wind for SC 20-23



Scope of analysis

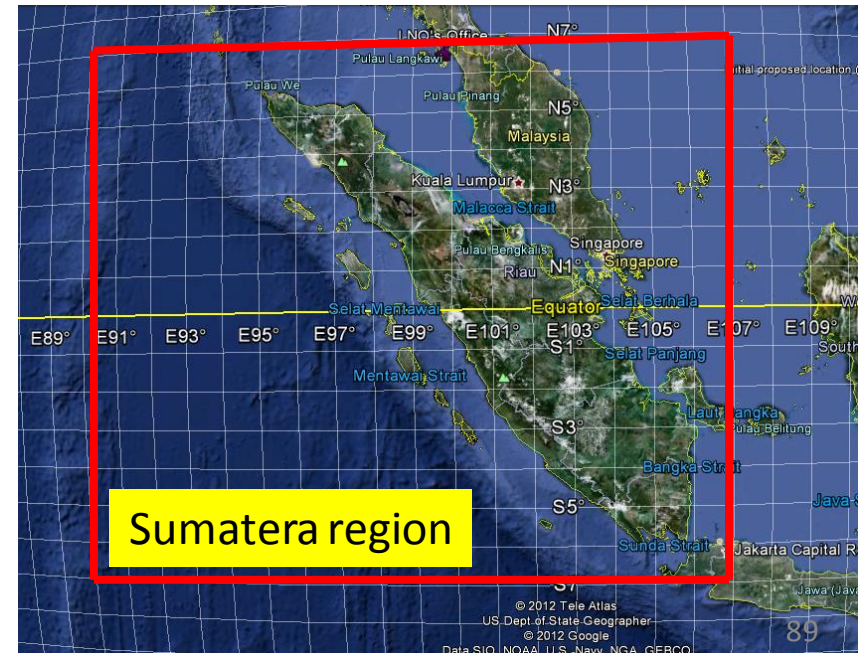
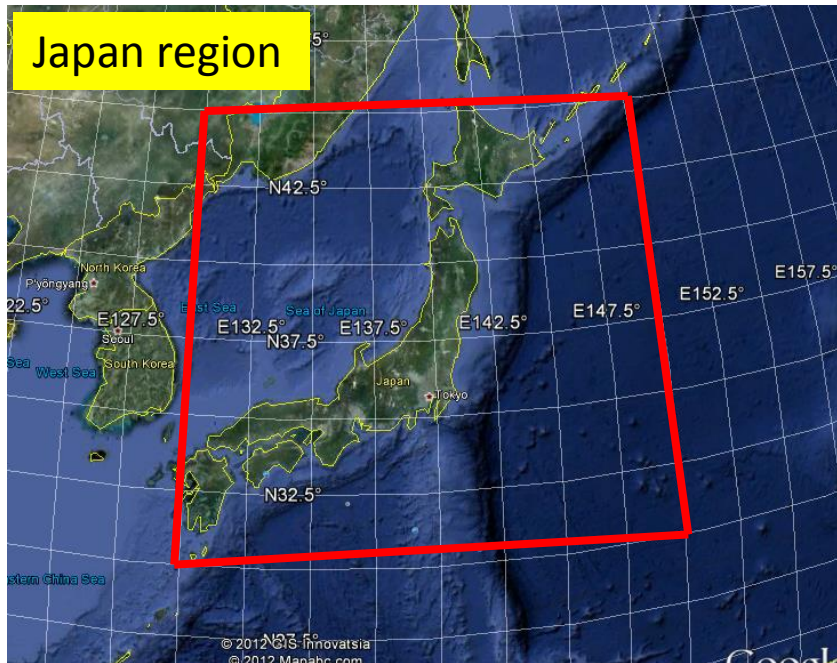
MAGDAS 210° MM Chain



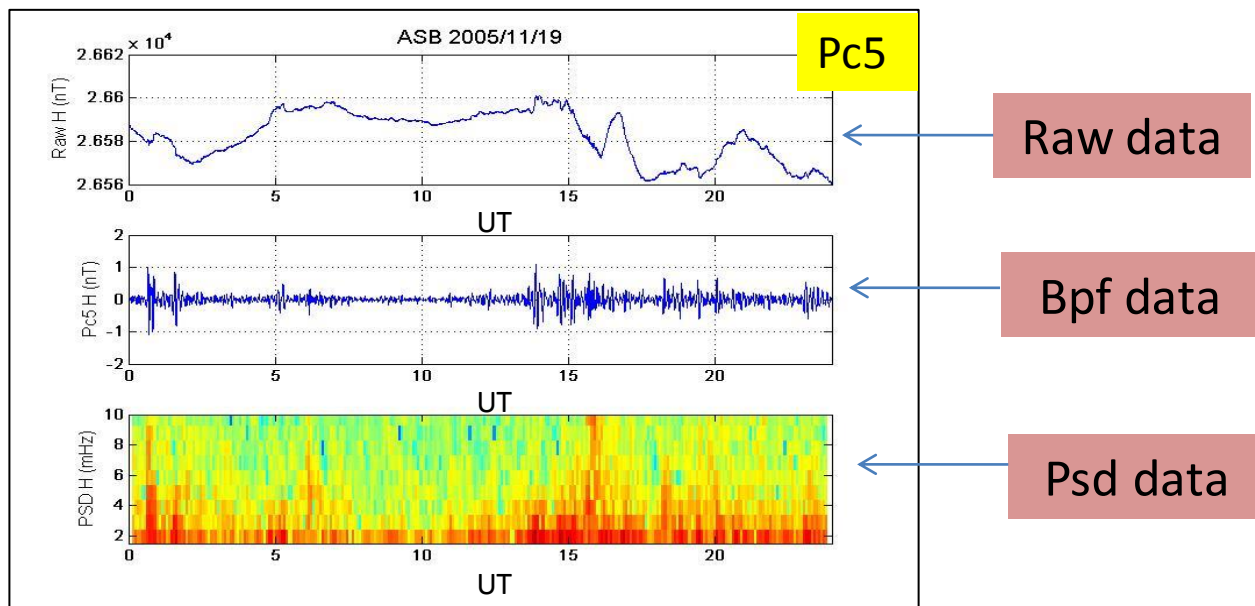
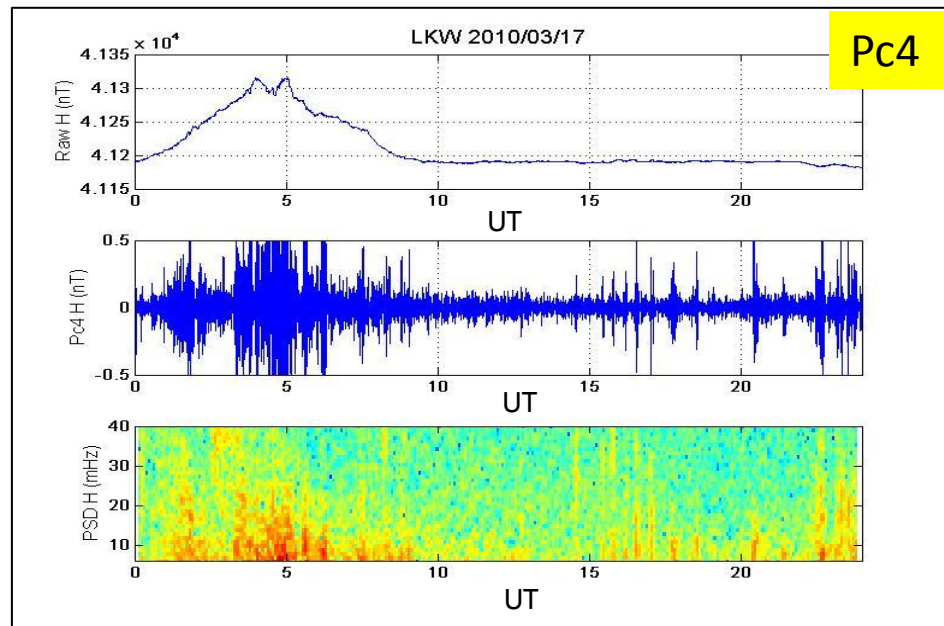
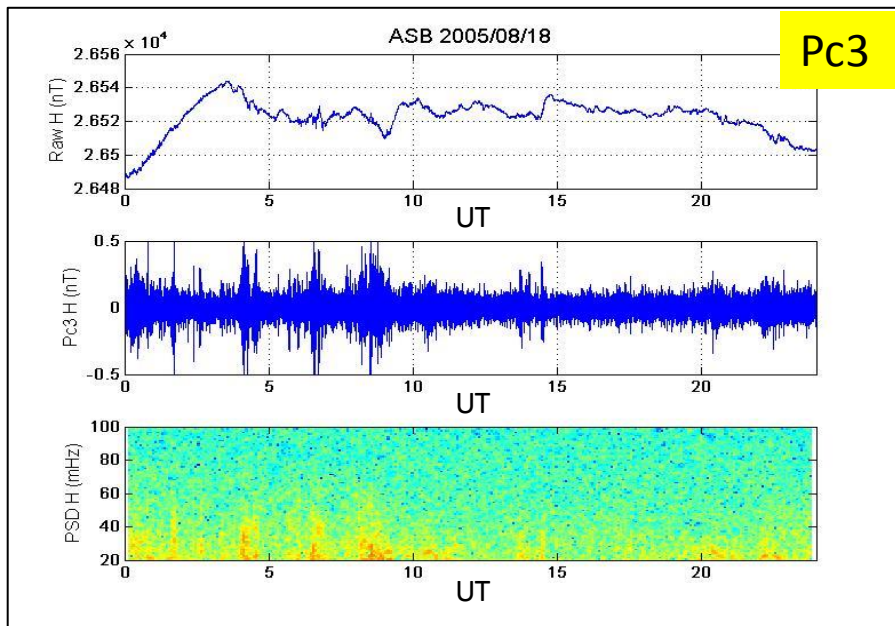
Analysis on Regional EQ events with solar parameters

Scope of analysis:

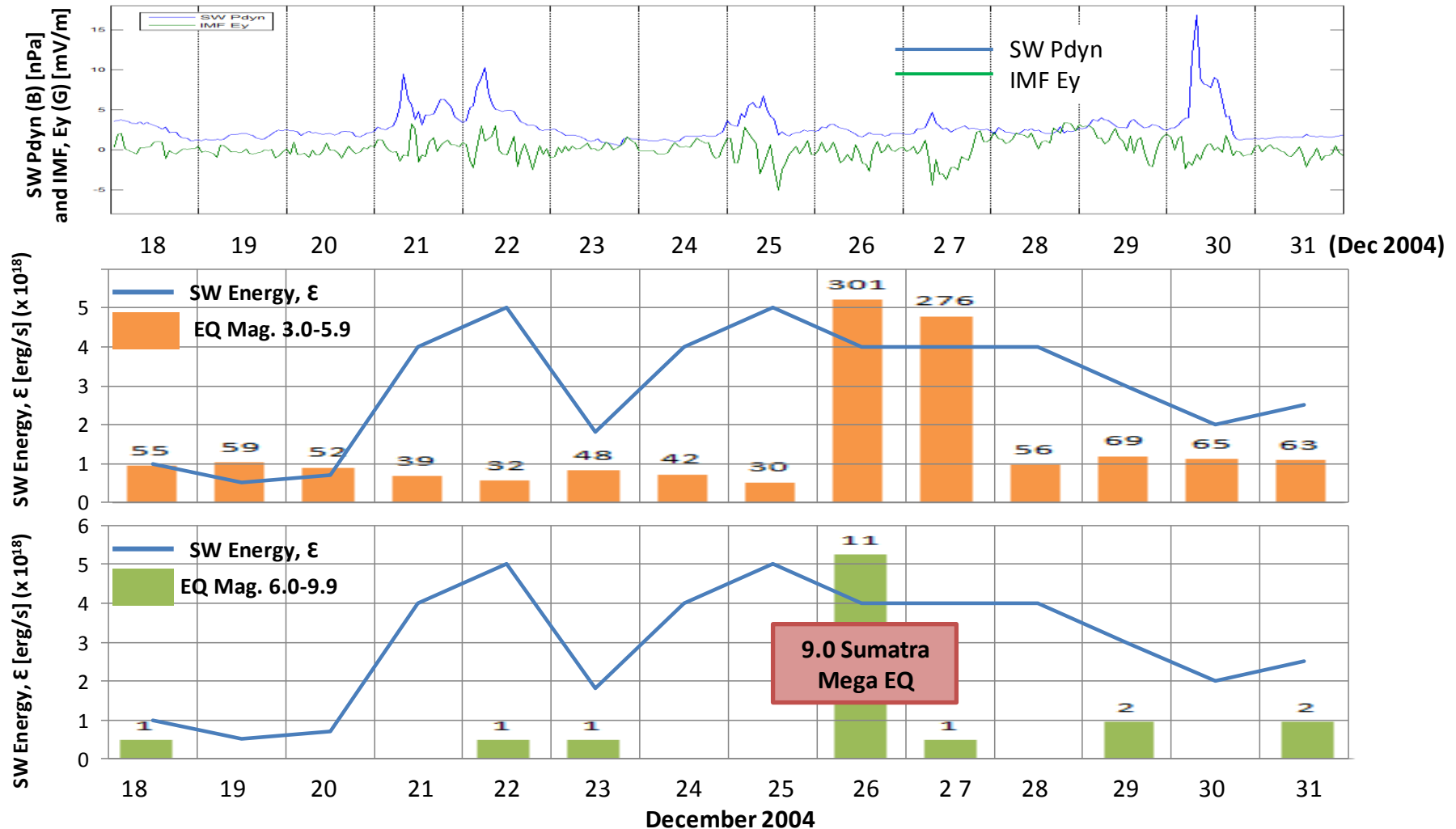
- Period of analysis: SC 23
- Regions of analyzed EQ events:
 - 1) Japan (Lat: 30 to 45 deg, Long: 129 to 149 deg)
 - 2) Sumatera (Lat: -7 to 7 deg, Long: 90 to 107 deg)
- Solar wind parameters:
 - 1) Solar wind kinetic energy Flux (SW Fkin)
 - 2) Solar wind input energy (epsilon, ϵ)



3.3.2 Typical Pc3, Pc4 and Pc5 recorded at LKW and ASB stations

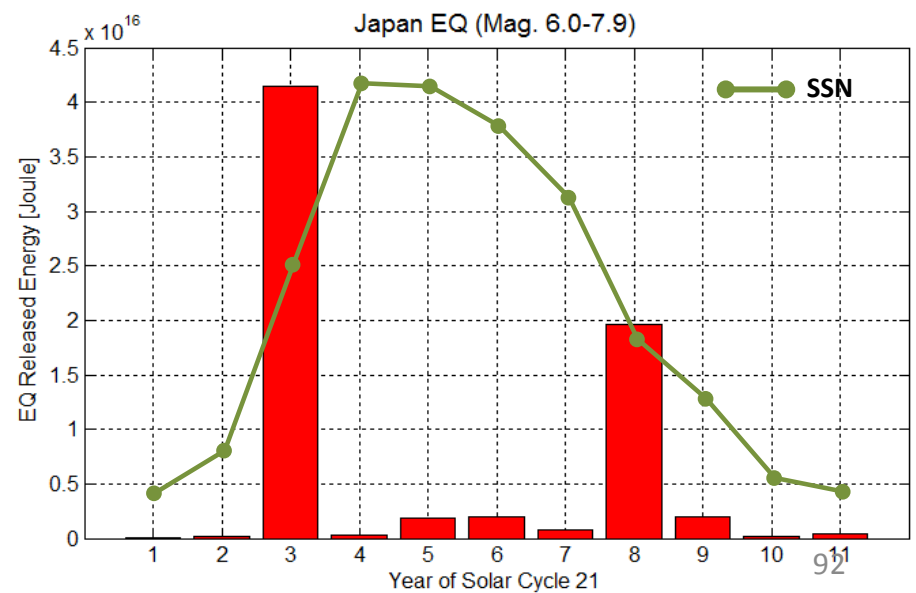
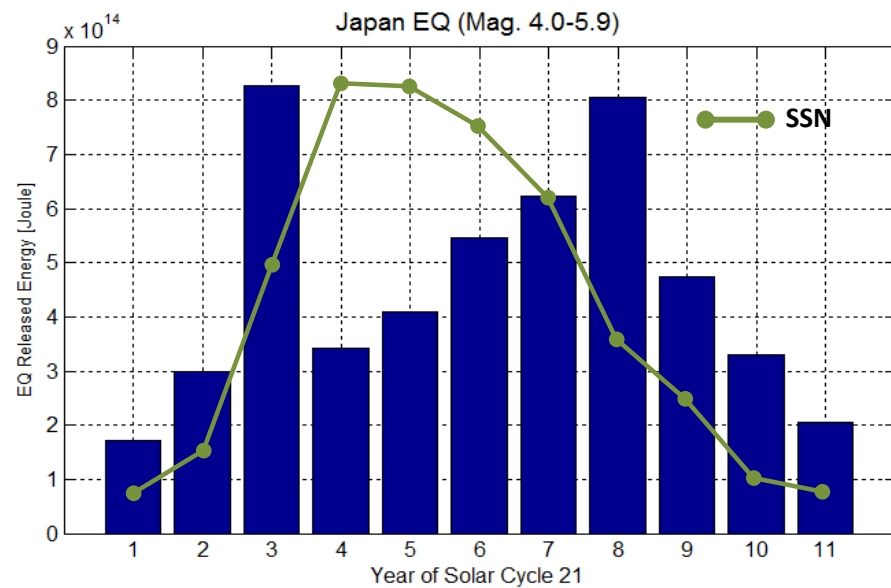
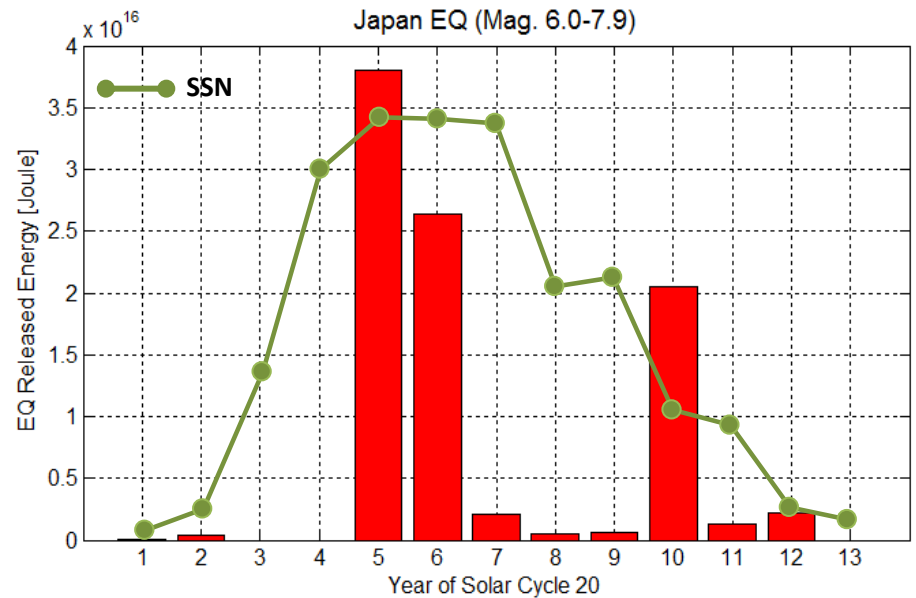
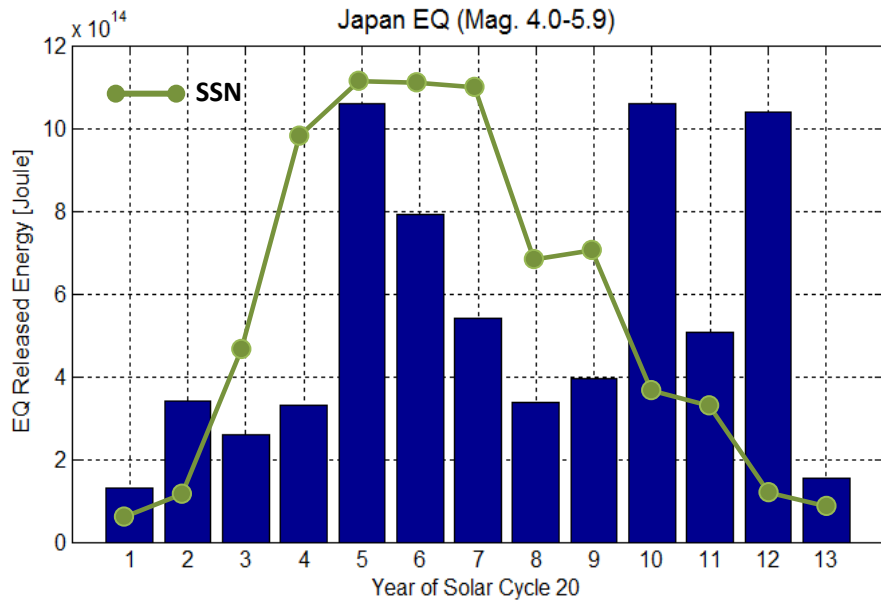


3.2.3.3 Relationship of Solar Wind Input Energy with EQ: 18 – 31 December 2004

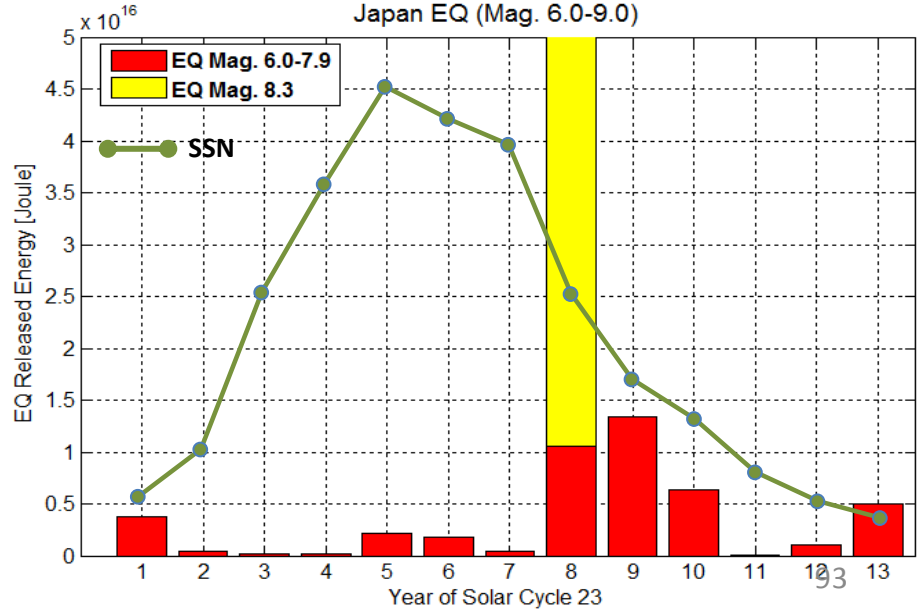
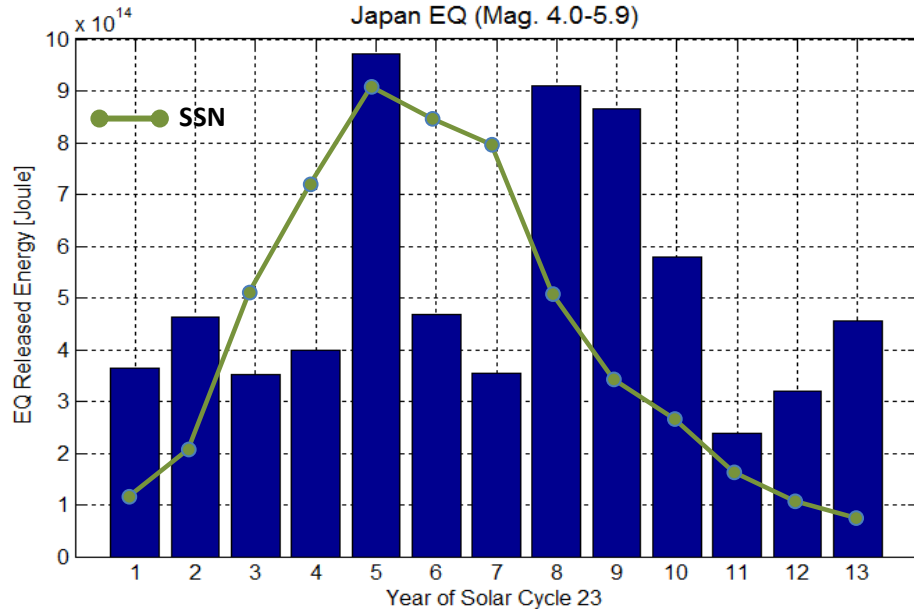
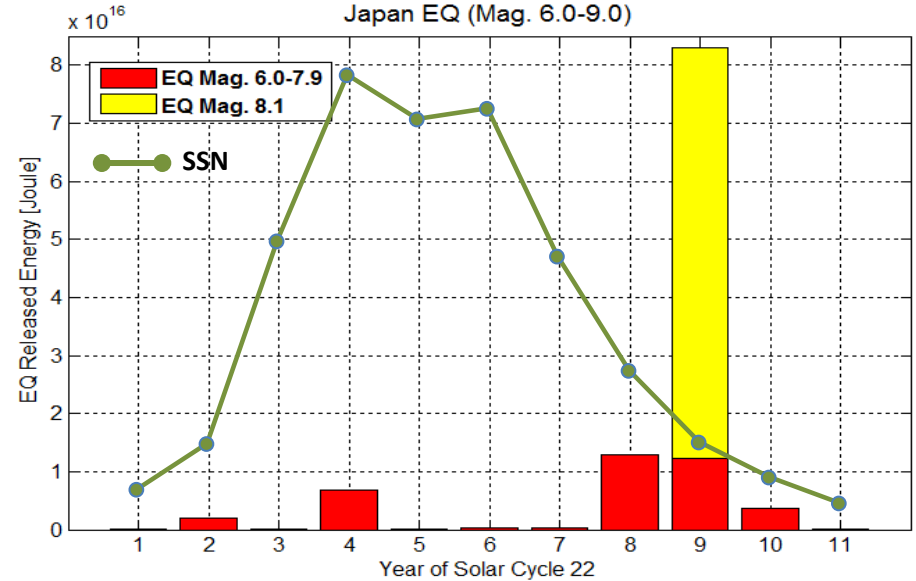
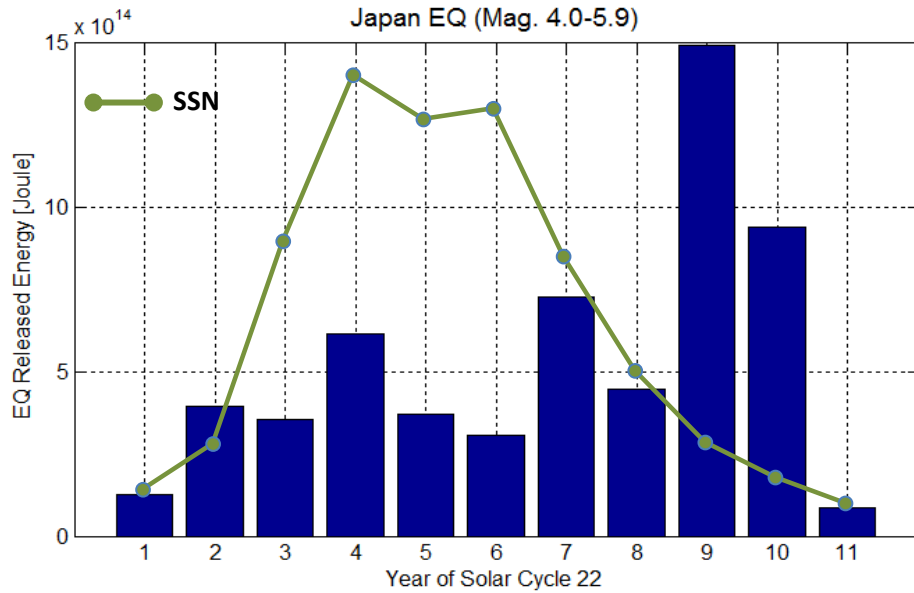


- SW energy starts to increase 5 days before the increasing number of EQ, on the same day of higher fluctuations of SW Pdyn and IMF Ey. The SW energy keeps in higher phase when the number of EQ reached its maximum on 26 Dec 2004.

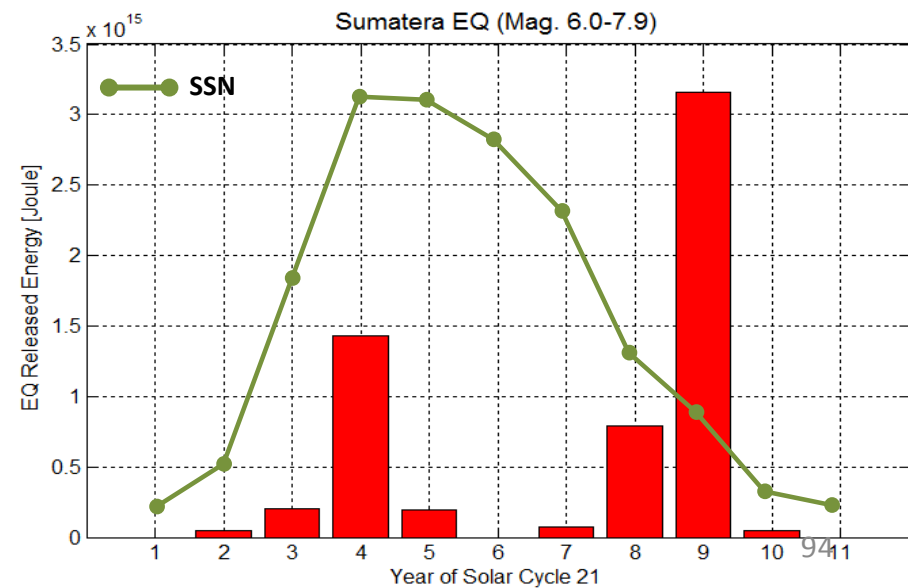
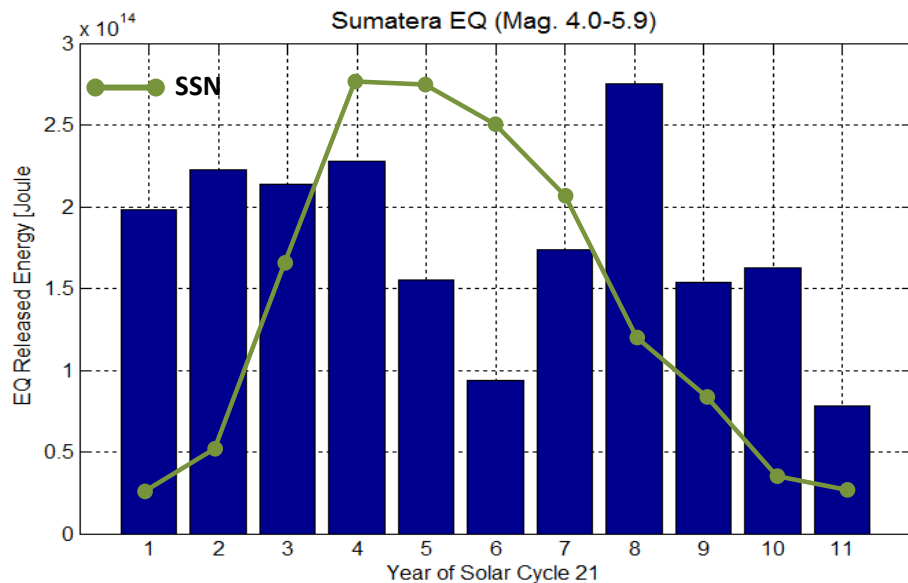
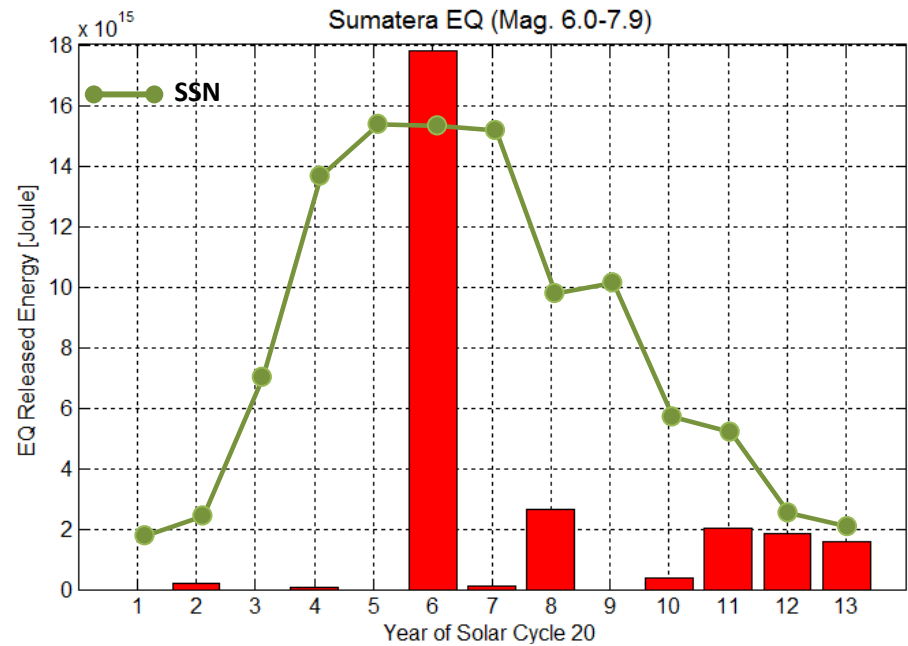
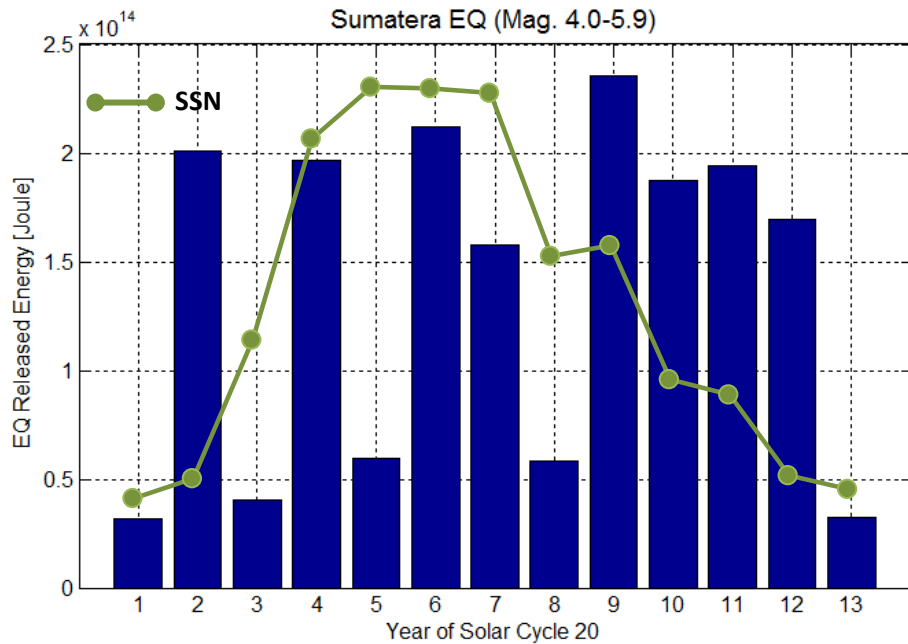
3.1.4 Distribution of Regional EQ Energy: Japan



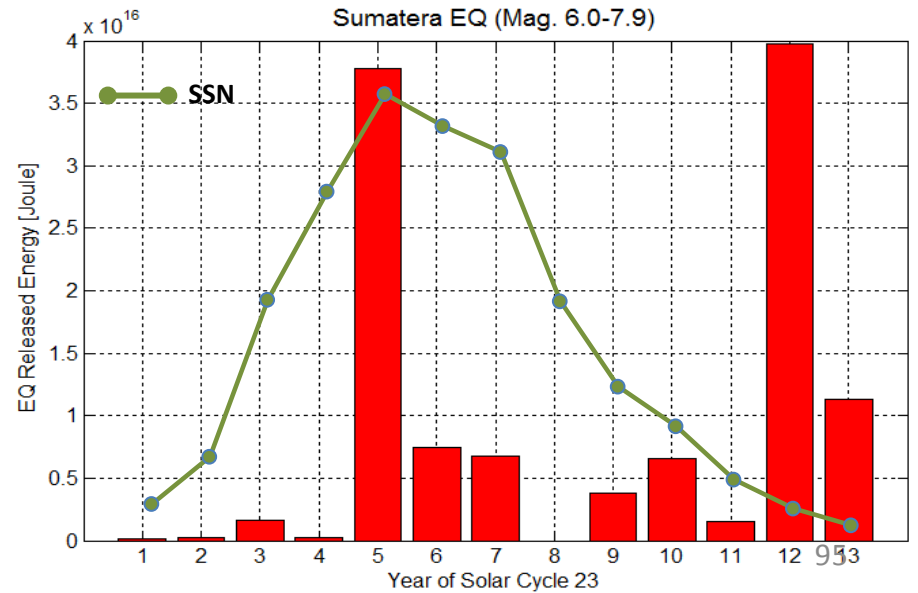
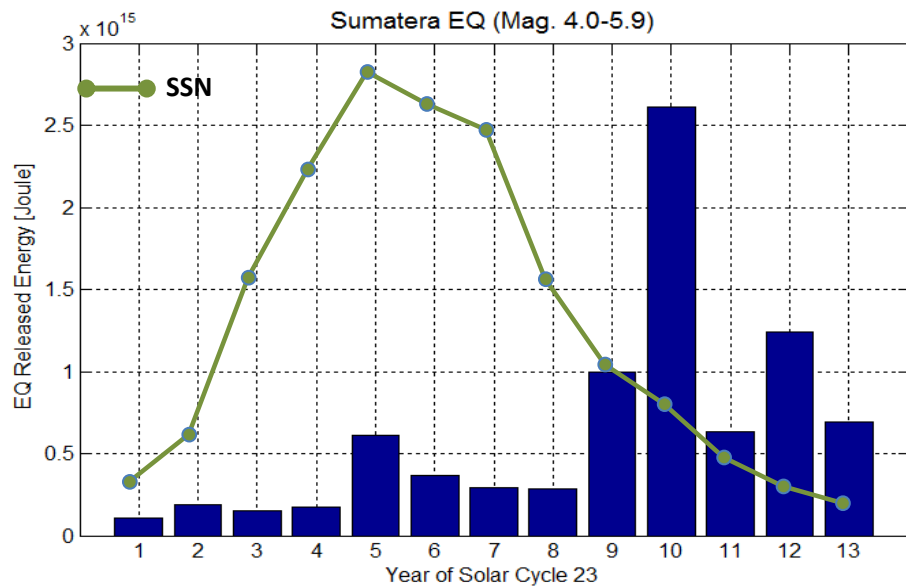
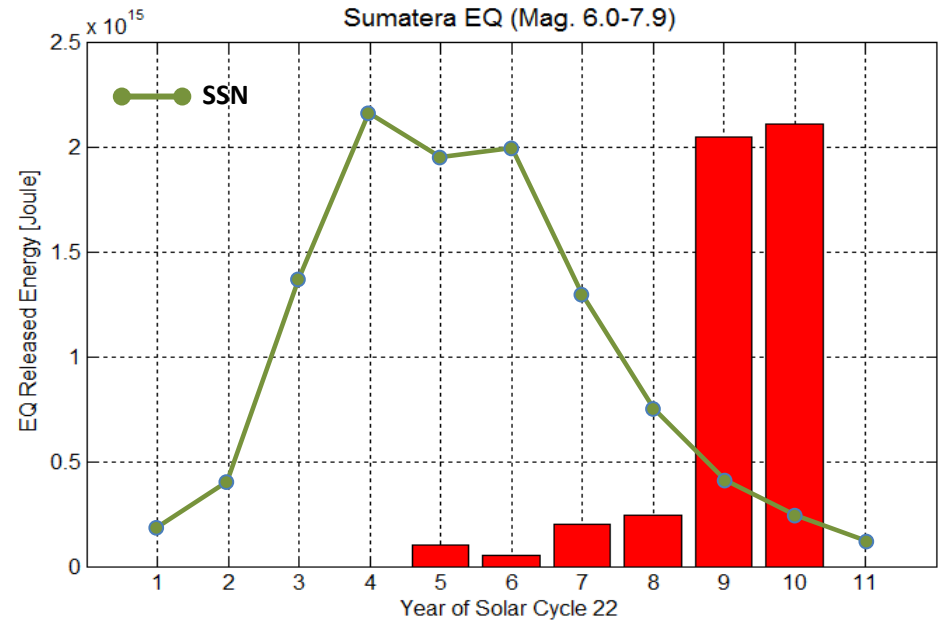
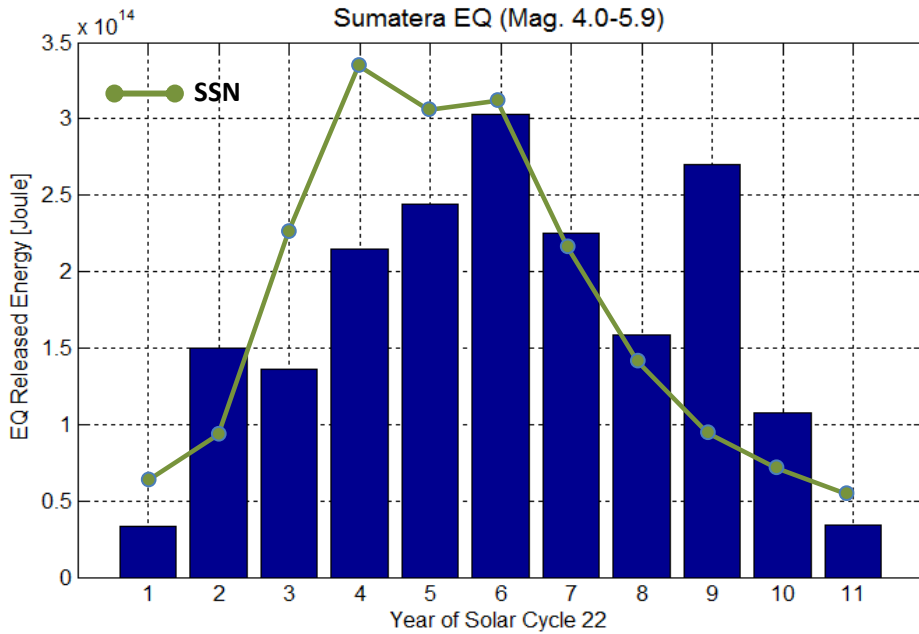
3.1.4 Distribution of Regional EQ Energy: Japan (cont..)



3.1.5 Distribution of Regional EQ Energy: Sumatra

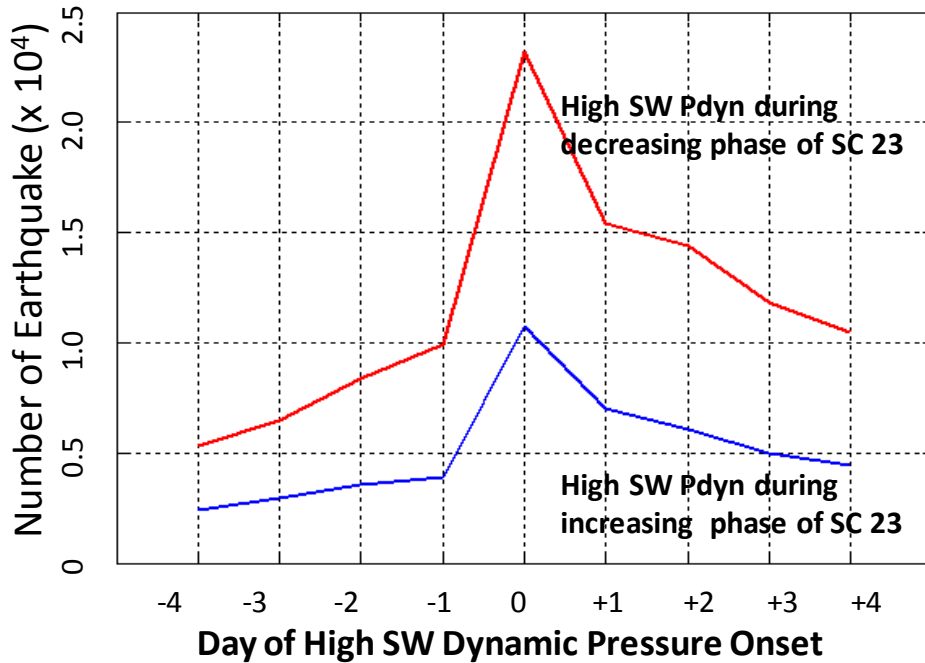


3.1.5 Distribution of Regional EQ Energy: Sumatra (cont..)

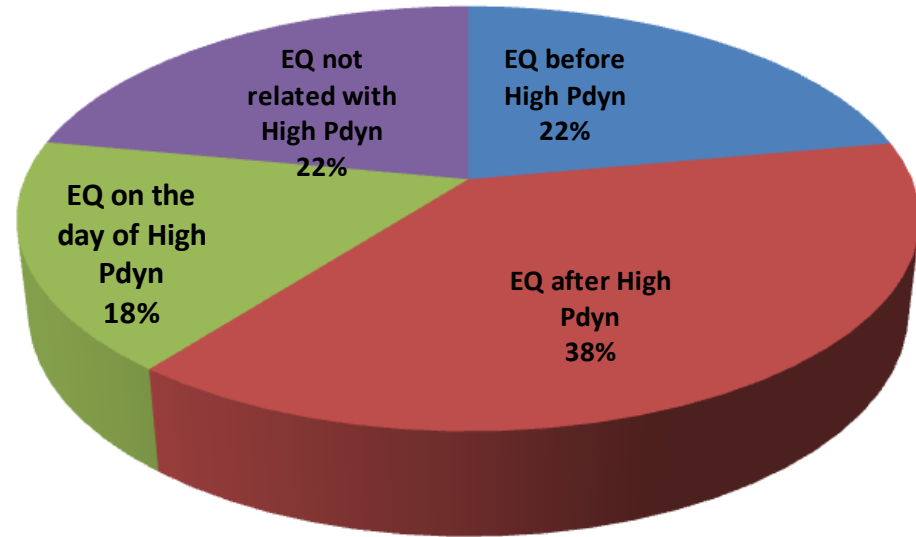


3.2.2.2 Day to day variation of High Solar Wind Dynamic Pressure with Earthquakes Magnitude 3.0-5.9

High SW Pdyn and EQ (Mag. 3.0-5.9) during SC 23



Average Fraction Correlation of Solar Wind High Dynamic Pressure and EQ (Mag. 3.0-5.9)

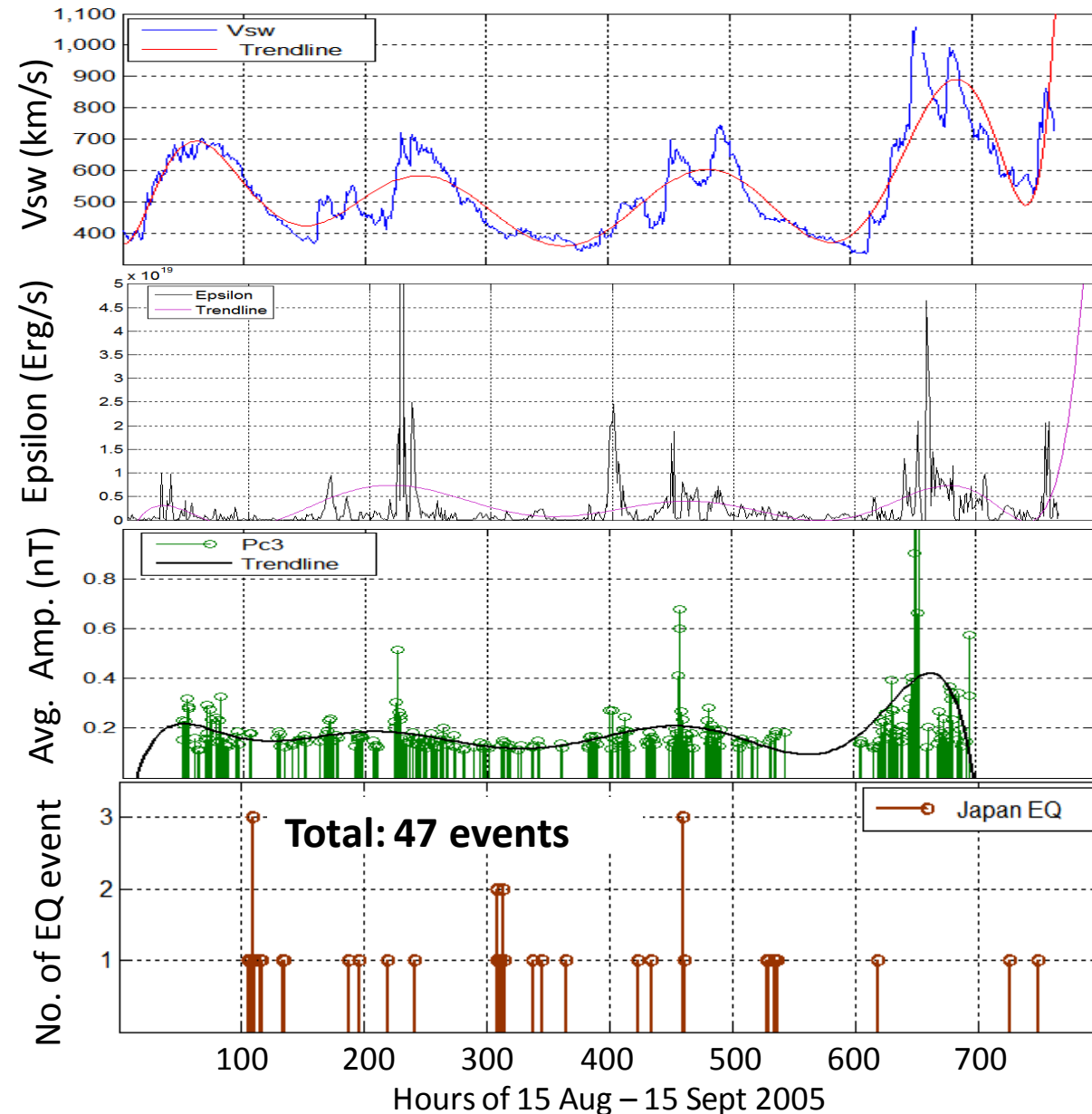


Total EQ: 13,6574 events
Total High Pdyn: 968 events

Total EQ: 57,483 events
Total High Pdyn: 316 events

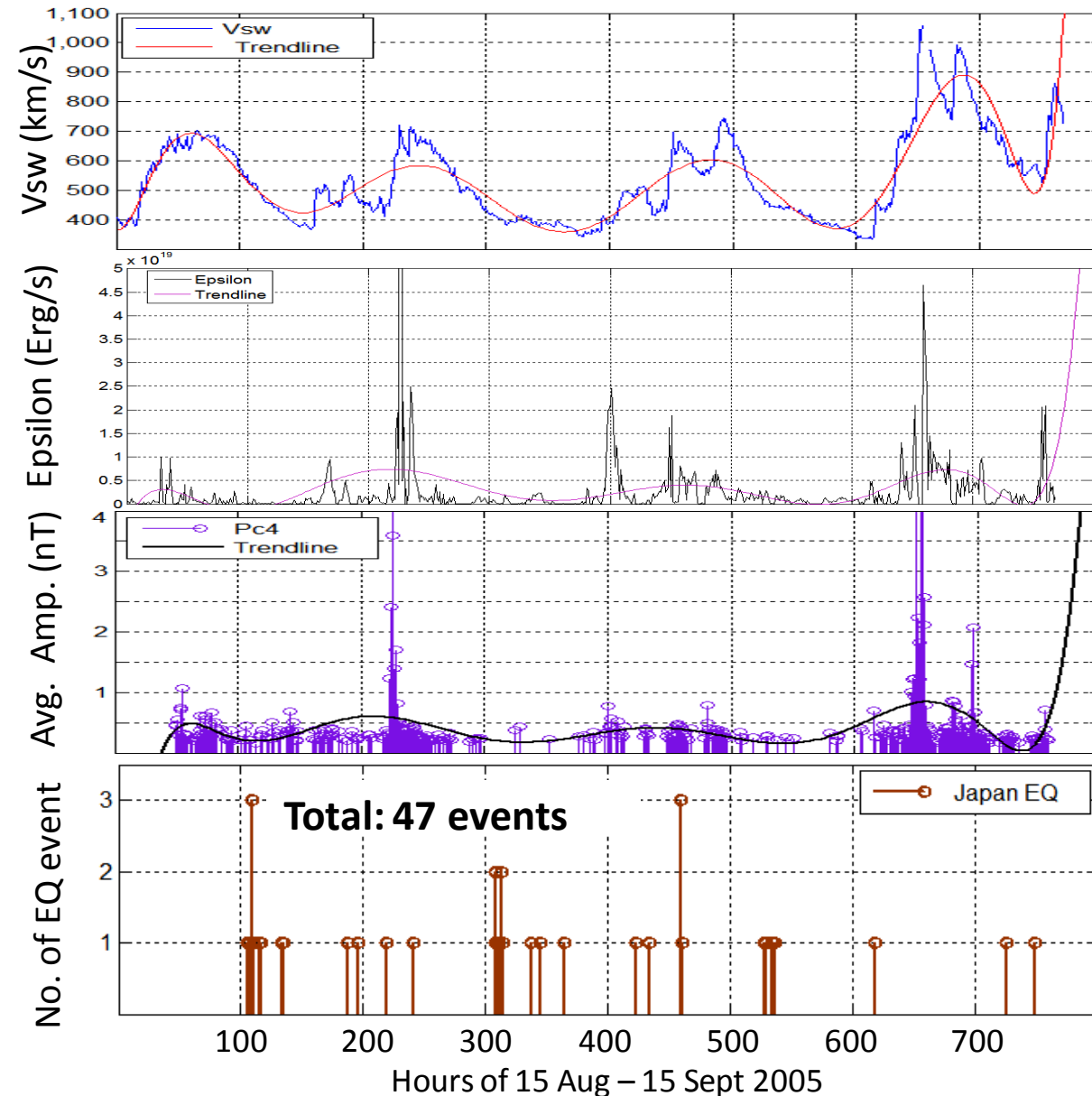
- 18 % of EQ recorded on the day of high SW Pdyn pressure detected; gives the maximum number of earthquakes occurred.
- 56 % of EQ events observed on the day and 4 days after the arrival of high SW Pdyn.

3.3.3 Relationship of Vsw and magnetic pulsations (Pc3) at North Japan (15 Aug-15 Sept 2005)



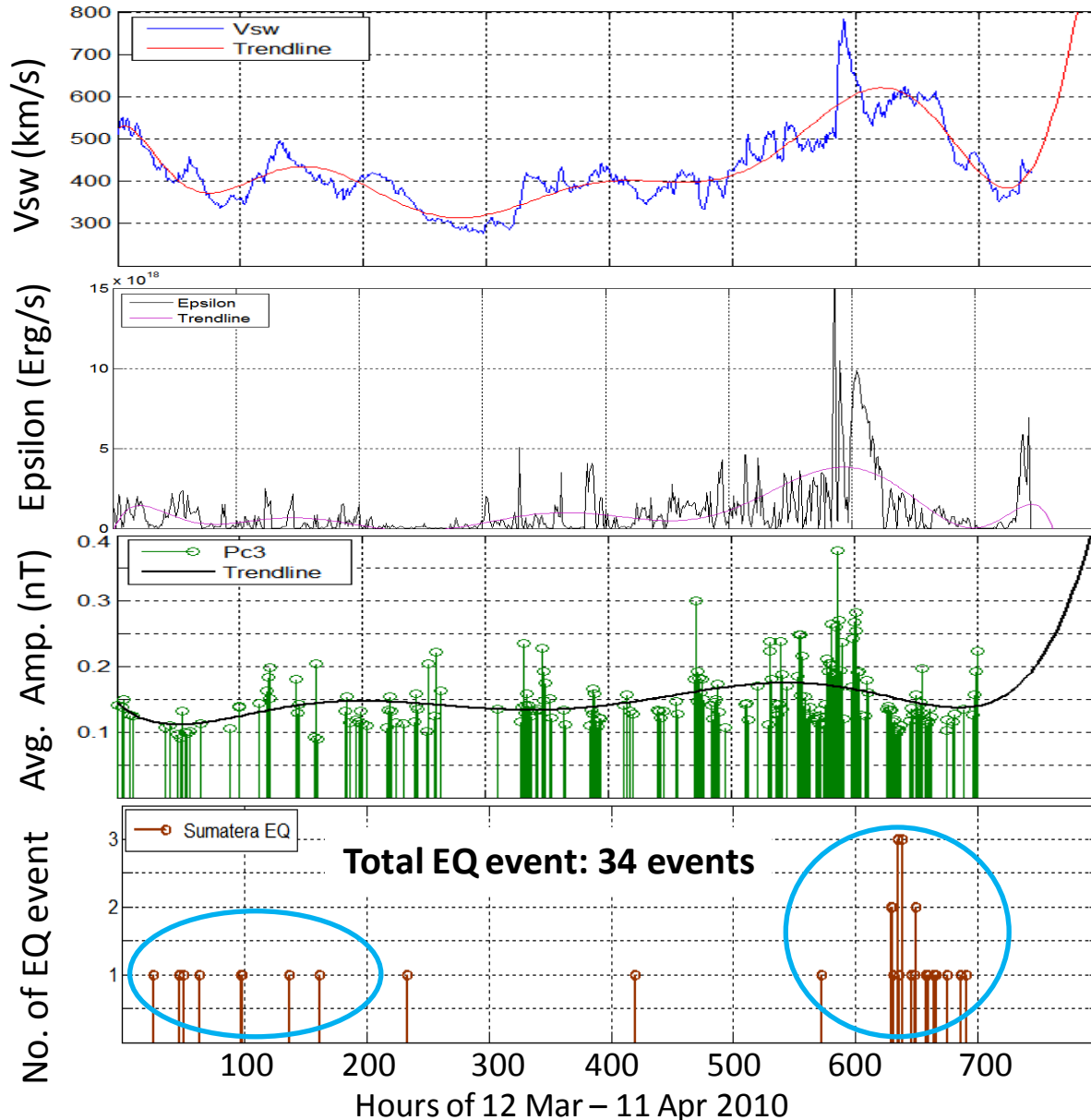
- ◆ Recorded Pc3 show enhancements in average amplitude (≥ 0.2 nT) during higher speed of solar wind (≥ 500 km/s)
- ◆ EQ events doesn't show significant correlations with Pc3; but further analysis required to confirm this hypothesis.

3.3.4 Relationship of Vsw and magnetic pulsations (Pc4) at North Japan (15 Aug-15 Sept 2005)



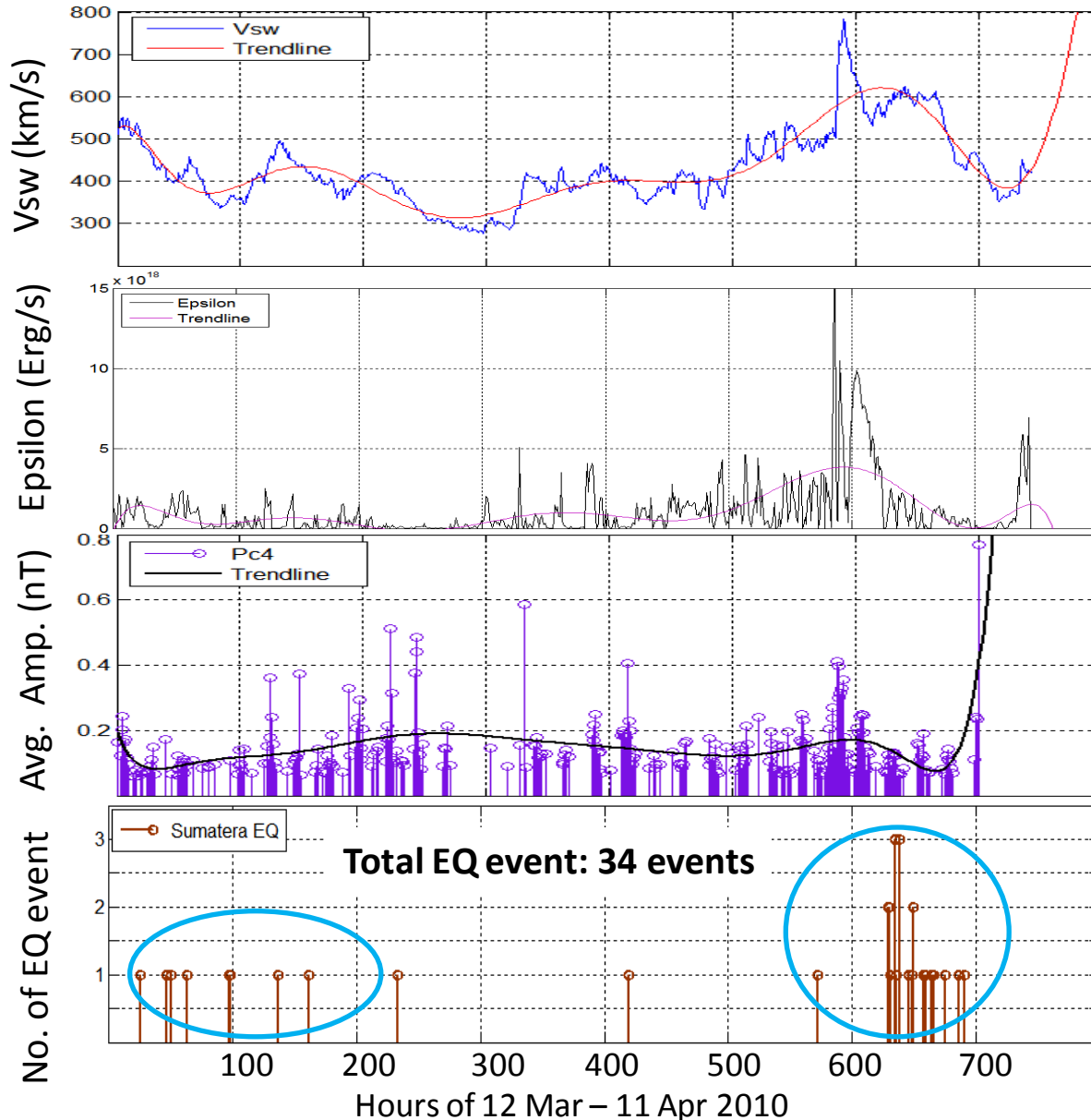
- ◆ The increase of Vsw (≥ 500 km/s) generally will enhance the average amplitude of Pc4 to ≥ 0.4 nT.
- ◆ EQ events seem to occur at higher average amplitude of Pc4.

3.3.7 Relationship of Vsw and magnetic pulsations (Pc3) at North Sumatra (12 Mar – 11 Apr 2010)



- ◆ Average amplitude of Pc3 increase to more than 0.15 nT during $V_{sw} \geq 400$ km/s.
- ◆ More EQ events occurred at higher V_{sw} , meanwhile for correlation with Pc3, it needs further analysis.

3.3.8 Relationship of Vsw and magnetic pulsations (Pc4) at North Sumatra (12 Mar – 11 Apr 2010)



◆ Based on the Pc4 trend line, there is no clear dependency of Pc4 with Vsw.

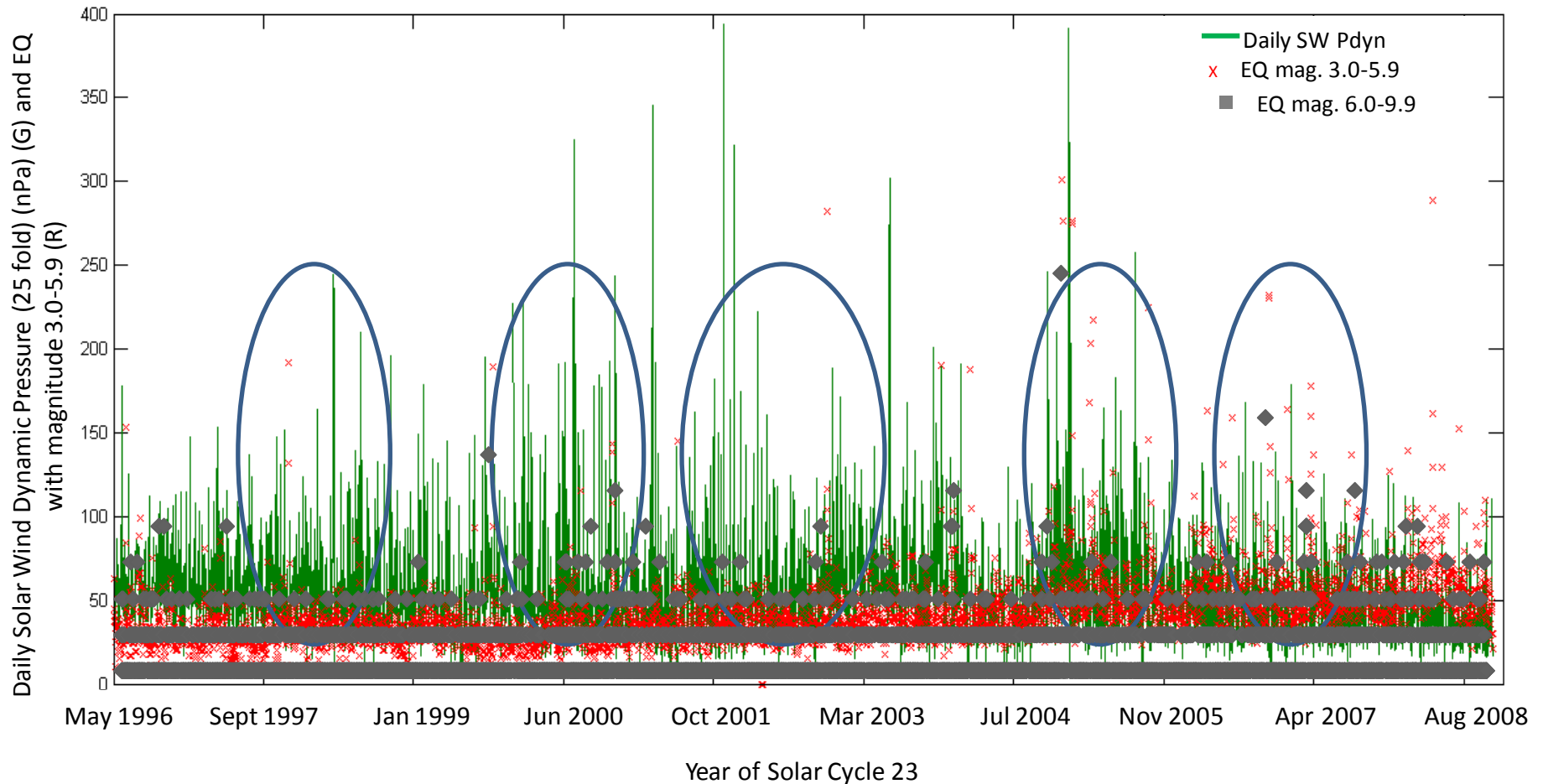
3.2.1 Relationship of EQ with HSSW

- To investigate the relationship of earthquake occurrence with high speed solar wind (HSSW).

High Speed Solar Wind (HSSW)

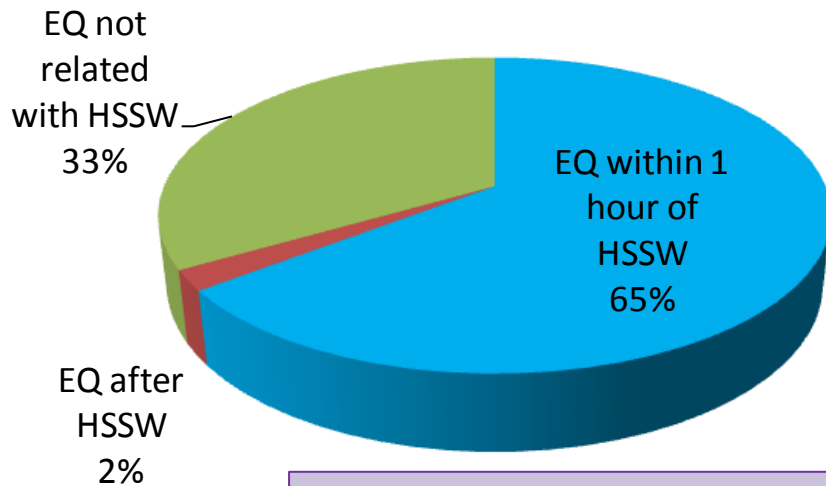
- Solar wind has different origins in the solar coronal; coronal holes (CH) and coronal mass ejections (CME) or both (multiple streams).
- A HSSW is mainly characterized based on four factors [*Lindblad and Lundstedt, 1981; Mavromichalaki et. al, 1988; and V. Gupta and Badruddin, 2010*]:
 - i. Considerable enhancement in V_{SW} ($\Delta V_{SW} \geq 100$ km/s)
 - ii. High temperature (T in K)
 - iii. High variation of proton density (N in cm^{-3}) and
 - iv. High magnitude of IMF (B in nT).

3.2.2.1 Superposition of Daily Solar Wind Dynamic Pressure and Earthquakes during SC 23



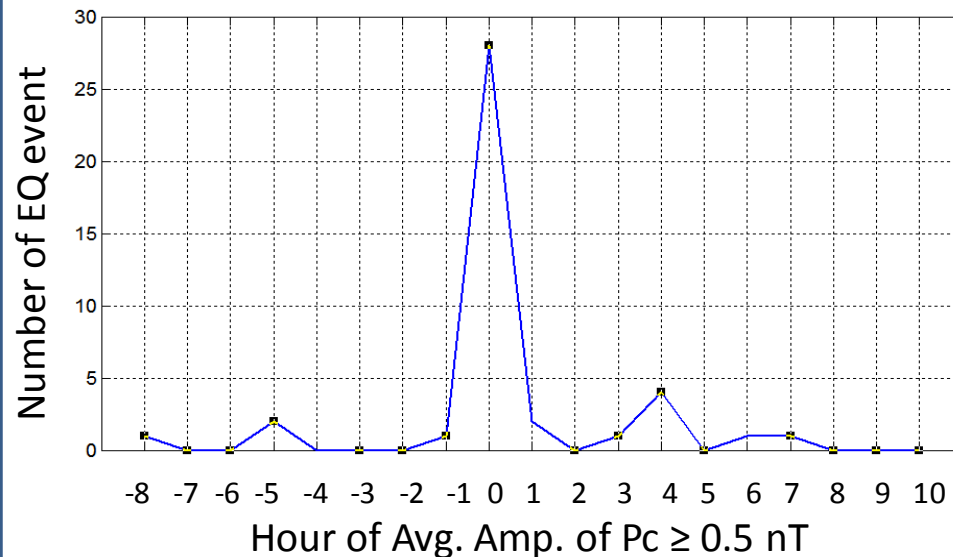
- Number of earthquakes for both magnitude ranges tend to increase during higher solar wind dynamic pressure.

3.3.6 Analysis of North Japan EQ with HSSW (≥ 500 km/s) and Magnetic Pulsation (≥ 0.5 nT)



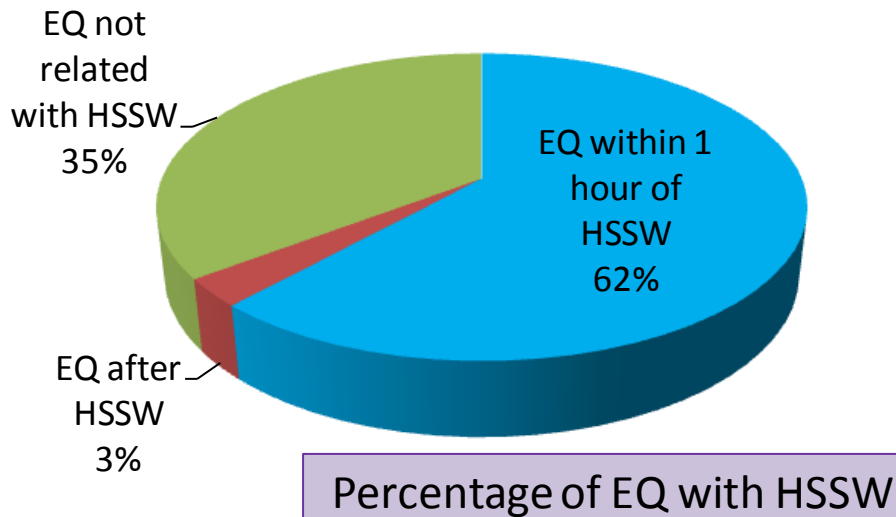
Percentage of EQ with HSSW

- ◆ The analysis was done within 4 hours before and after the HSSW.
- ◆ During the analyzed period, from 47 EQ events, 31 events (65%) occurred within 1 hour after the arrival of HSSW.
- ◆ 33% of EQs occurred at more than 4 hours the arrival of HSSW .

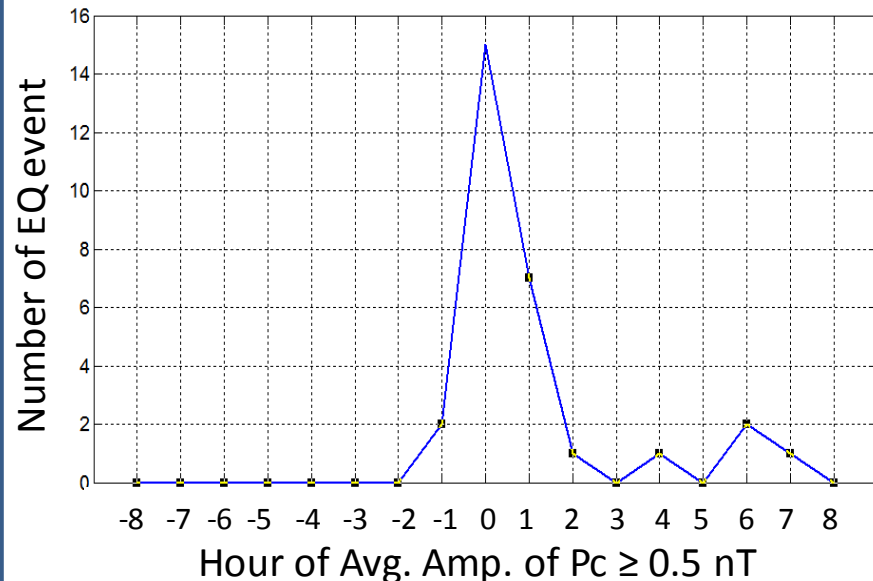


- ◆ Hour-to-hour analysis of the EQ events with magnetic pulsation shows **maximum number of EQ occurred on the same hour** of recorded Pc at ≥ 0.5 nT.
- ◆ In total, 79% (37/47) of EQ events occurred within 7 hours after magnetic pulsation ≥ 0.5 nT.

3.3.10 Analysis of North Sumatra EQ with HSSW (≥ 500 km/s) and Magnetic Pulsation (≥ 0.5 nT)



- ◆ The analysis was done within 4 hours before and after the HSSW.
- ◆ During the analyzed period, from 34 EQ events, 21 events (62%) occurred within 1 hour after the arrival of HSSW.
- ◆ 35% of EQs occurred at more than 4 hours the arrival of HSSW .



- ◆ Hour-to-hour analysis of the EQ events with magnetic pulsation shows **maximum number of EQ occurred on the same hour** of recorded Pc at ≥ 0.5 nT.
- ◆ In total, 79% (27/34) of EQ events occurred within 7 hours after magnetic pulsation ≥ 0.5 nT.

3.2.3.2 Estimation of the amount of earthquake released energy and SW input energy (\mathcal{E})

Average daily EQs release energy: $0.5 \sim 1 \times 10^7$ Joule [Kanamori, 1977]

Average SW input energy: 4×10^{18} Ergs/s [Akasofu, 1981]

Within 1 day: 4×10^{18} Ergs/s \times 1 day \times 24 hours \times 60 min \times 60 sec

$$= 4.3 \times 10^{22} \text{ Erg/s}$$

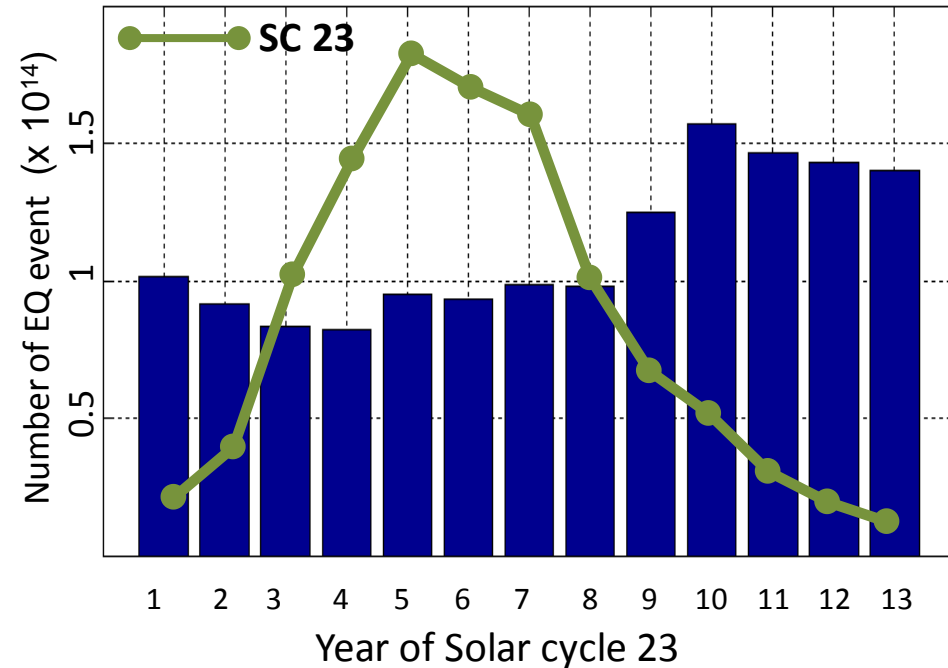
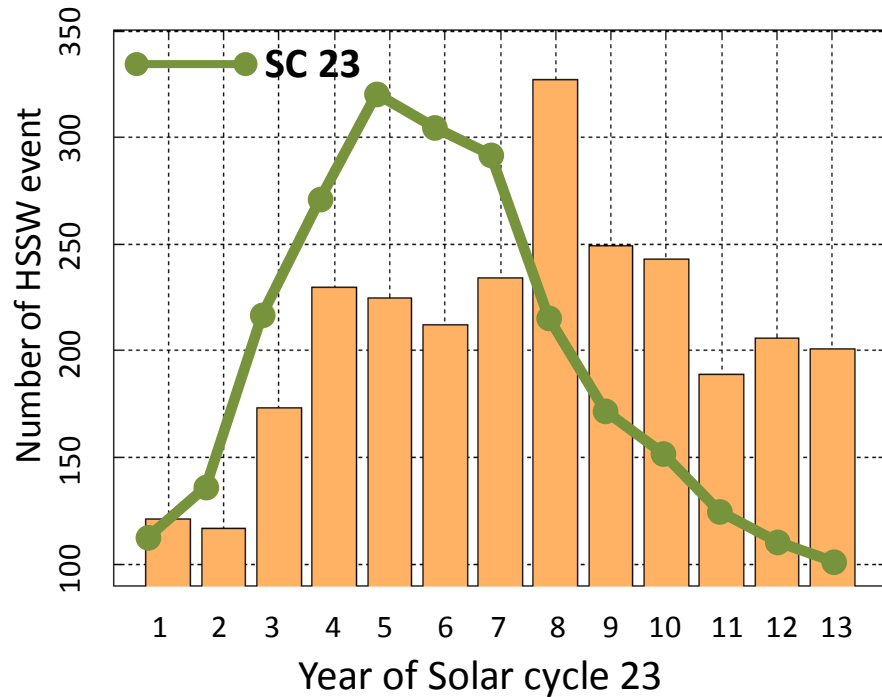
$$= \underline{4.3 \times 10^{15} \text{ Joule}}$$

By comparison:

Average EQs energy ($0.5 \sim 1 \times 10^7$ Joule) \ll Average SW input energy (4.3×10^{15} Joule)

Hence, it could be enough energy in Solar wind to be one of the energy source of earthquakes.

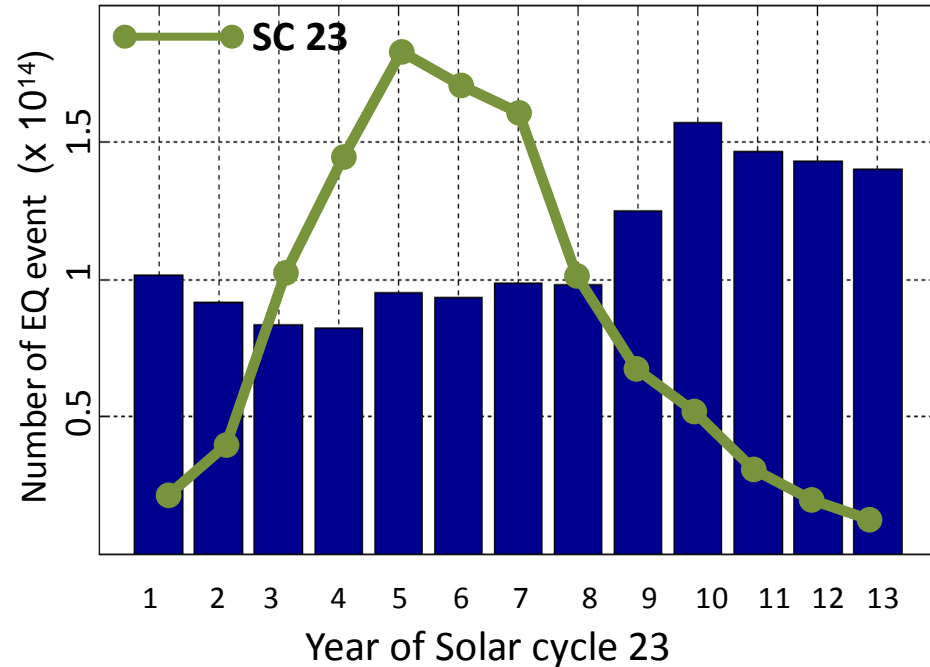
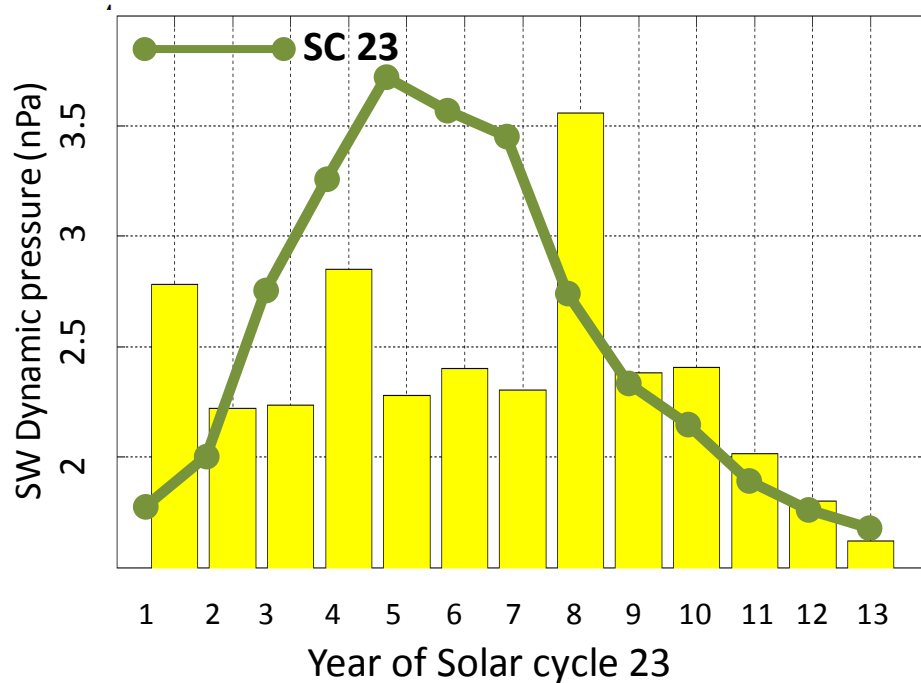
3.2.1.1 High Speed Solar Wind Events (HSSW) (SC 23)



◆ The general trends of EQ released energy are similar with the trends of detected HSSW.

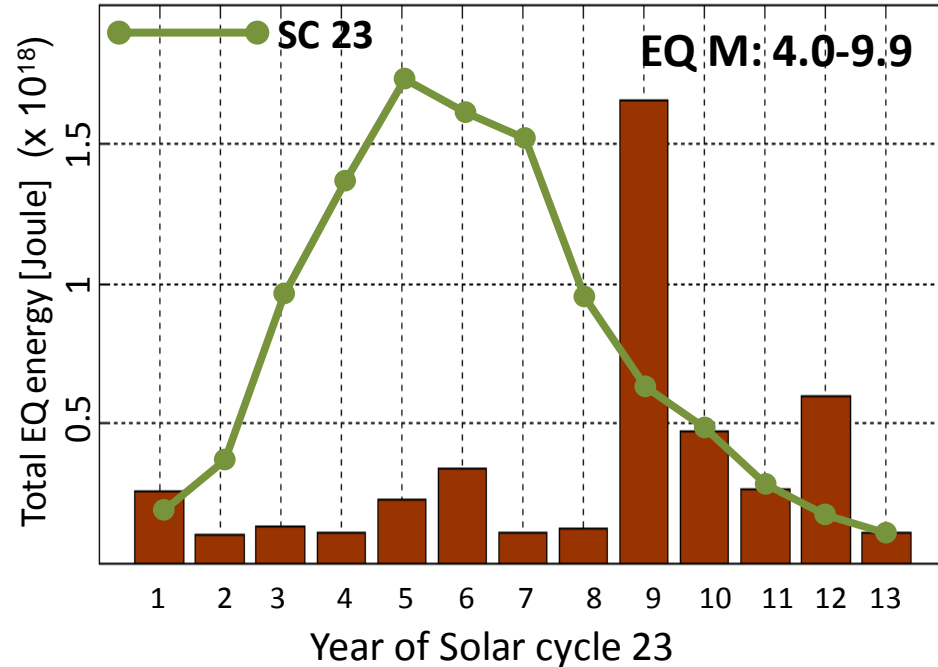
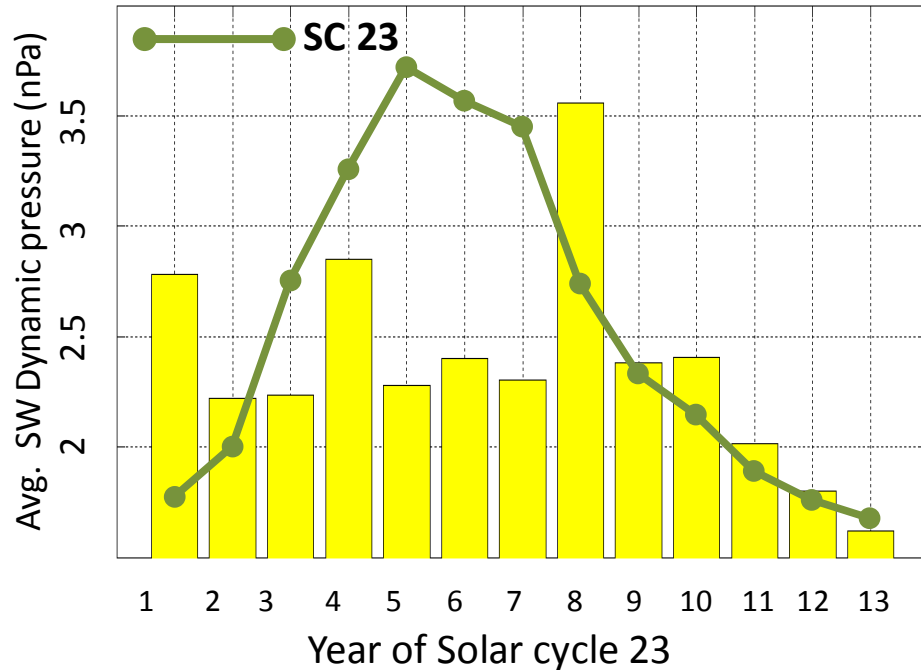
◆ Hence, further analysis is needed to clarify this relationship by considering earth's magnetic pulsations as one of the possible connecting factor between solar activity and seismic event.

3.2.2 Relationship of EQs with High Solar Wind Dynamic Pressure



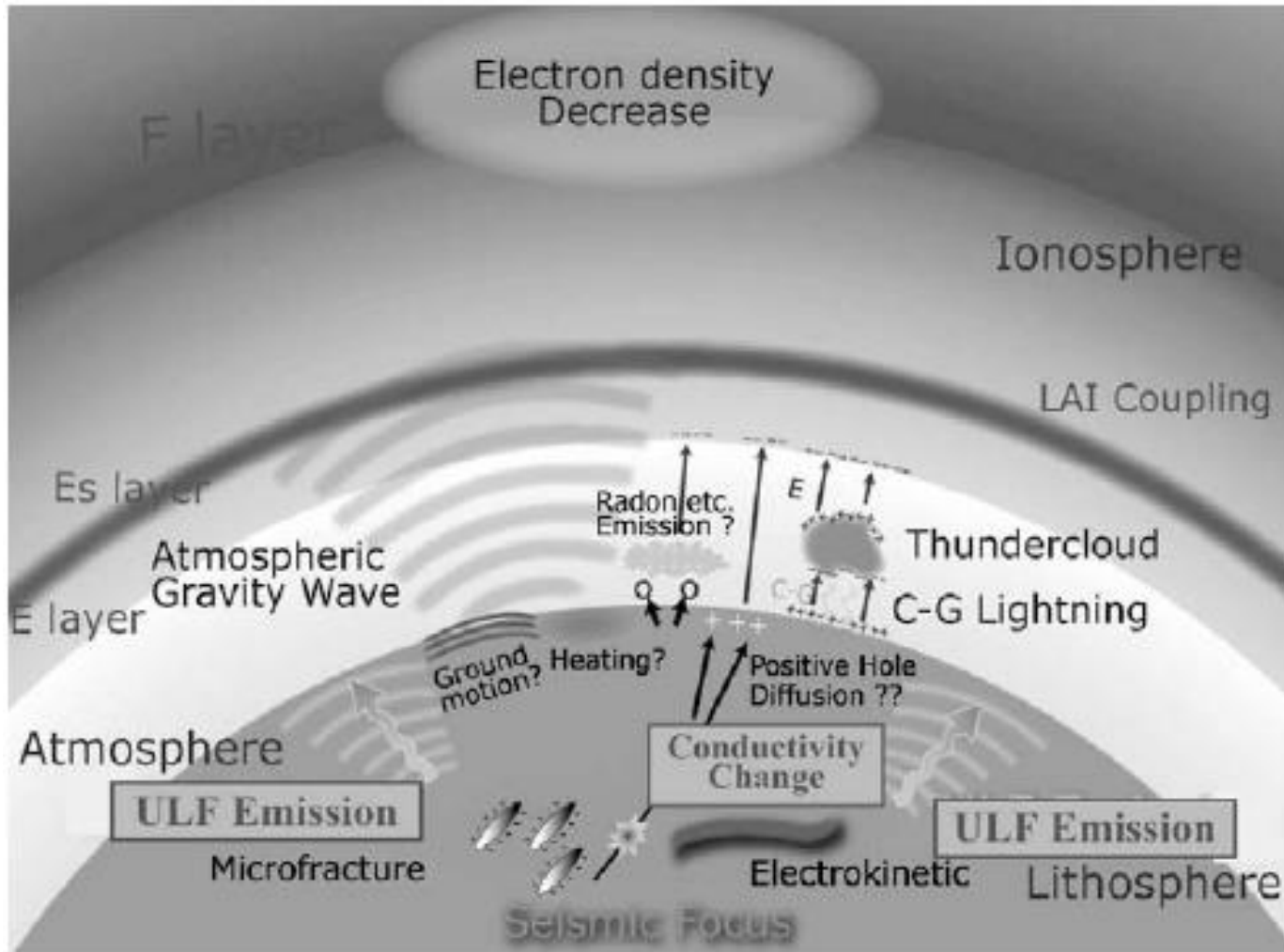
- ◆ Higher amplitude of solar wind dynamic pressure occurred during descending phase of SC 23
- ◆ The number of earthquake is higher during descending phase of SC 23; the same trend with solar wind dynamic pressure.

3.2.2 Relationship of EQs with High Solar Wind Dynamic Pressure



- ◆ Higher amplitude of solar wind dynamic pressure occurred during descending phase of SC 23
- ◆ The amount of earthquake released energy is higher during descending phase of SC 23; the same trend with solar wind dynamic pressure.

Three models of ULF anomalies associated with EQs



[ULF emissions](#)

[Conductivity change](#)

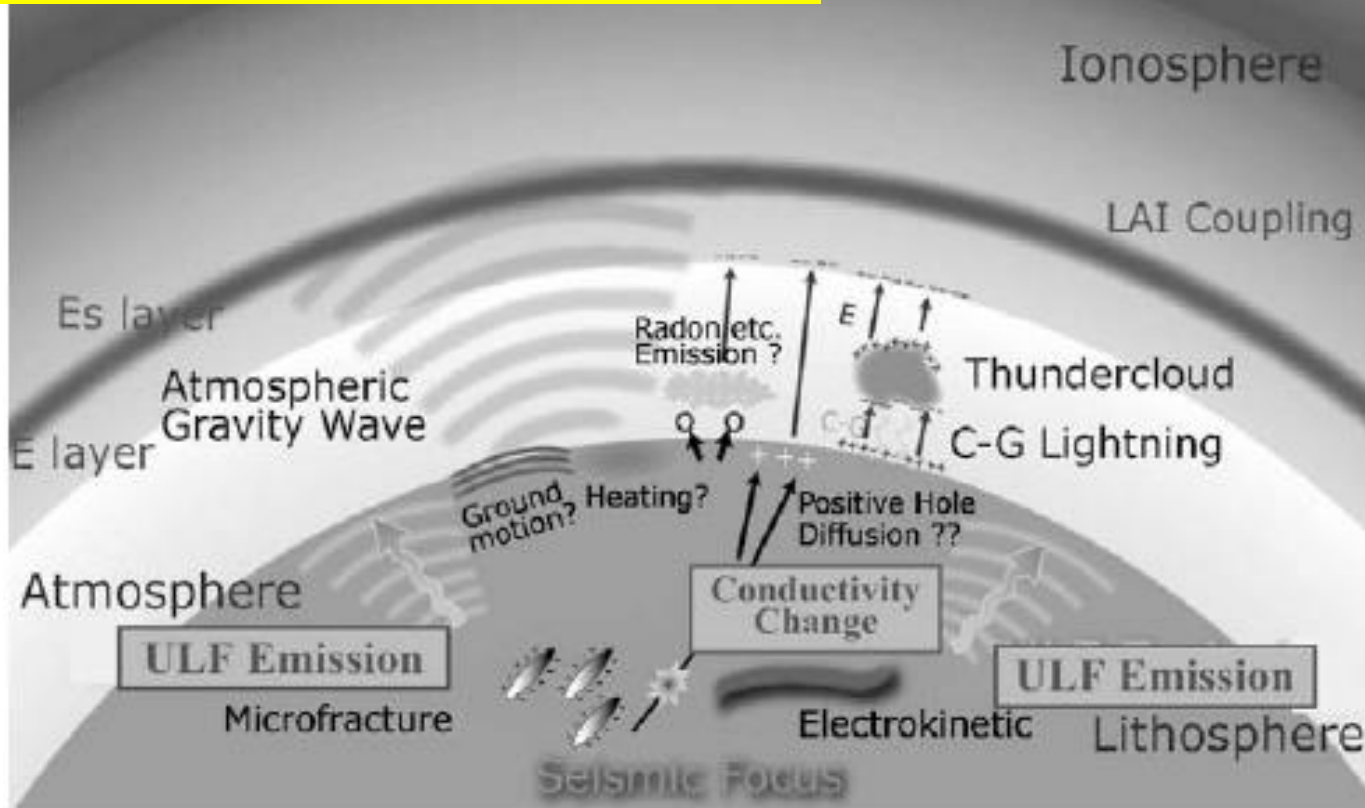
[Electrokinetic effects](#)

Courtesy of Hattori, 2006 and Yumoto et al., 2009

Three models of ULF anomalies associated with EQs

ULF emissions [Molchanov et al., 1995, 2003]

- Due to charges created from microfracturing prior to EQ.



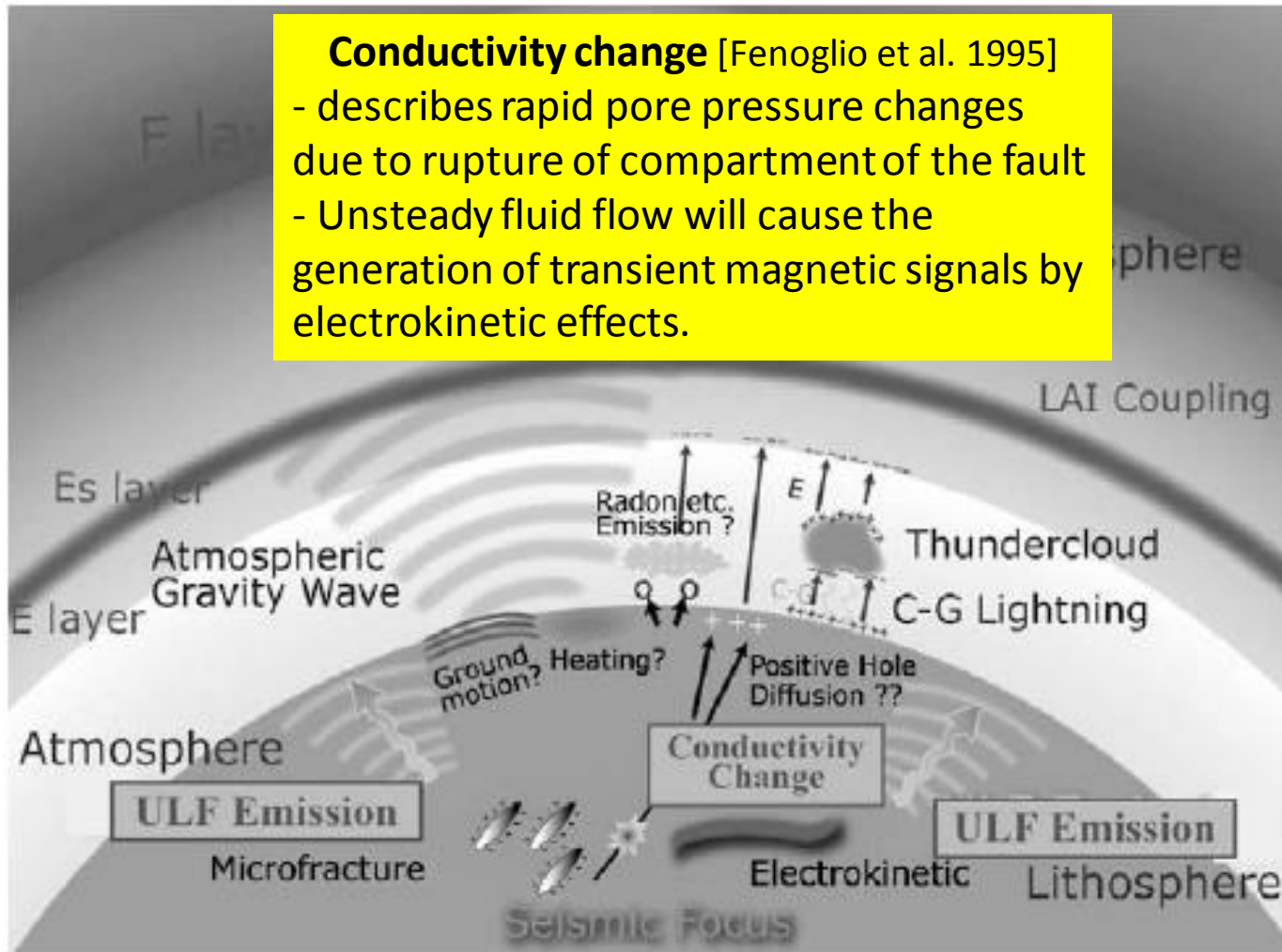
ULF
emissions

Conductivity
change

Electrokinetic
effects

*Courtesy of
Hattori, 2006
and Yumoto et
al., 2009*

Three models of ULF anomalies associated with EQs



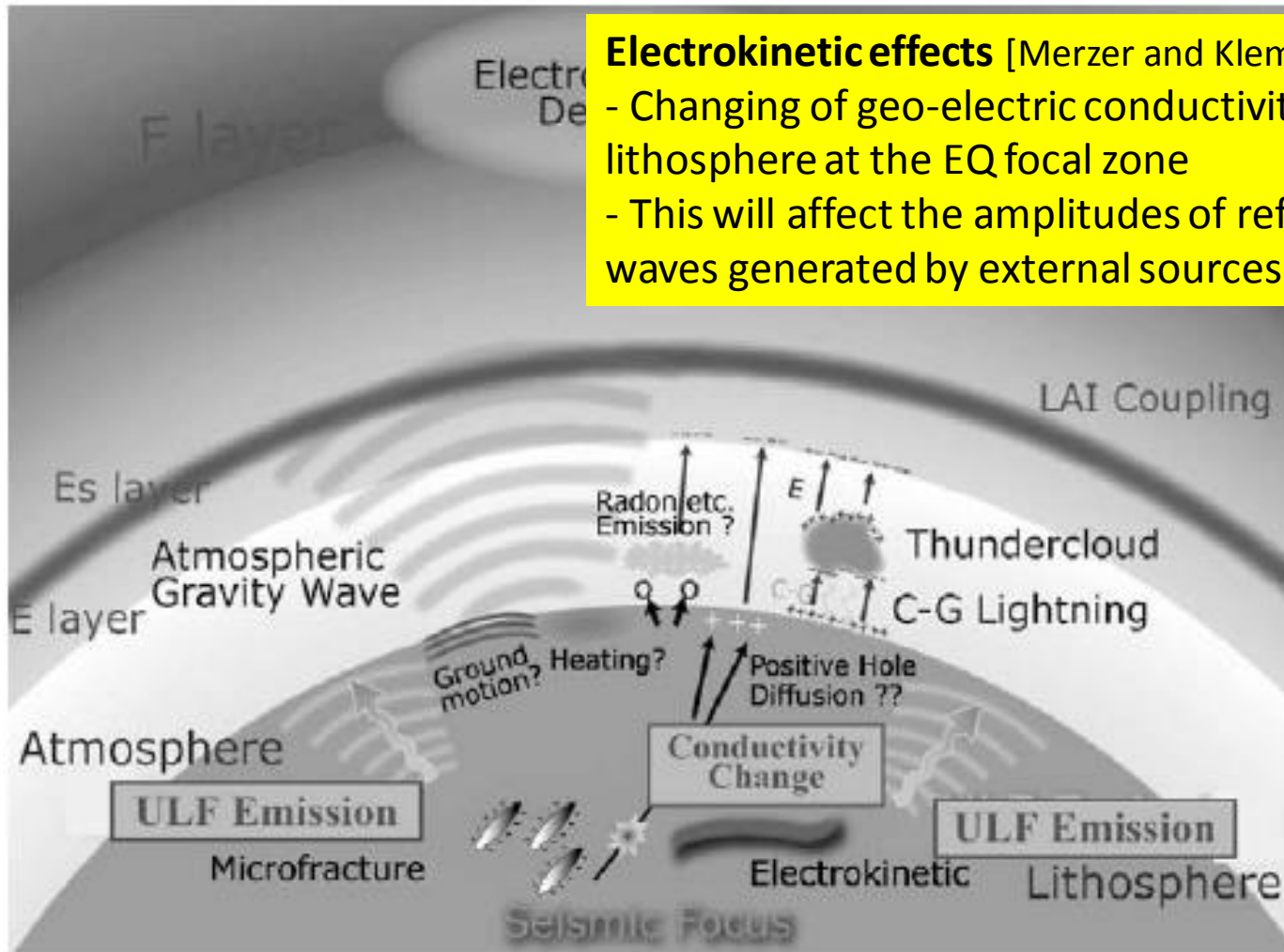
[ULF emissions](#)

[Conductivity change](#)

[Electrokinetic effects](#)

Courtesy of Hattori, 2006 and Yumoto et al., 2009

Three models of ULF anomalies associated with EQs



Electrokinetic effects [Merzer and Klemperer, 1997]

- Changing of geo-electric conductivity in the lithosphere at the EQ focal zone
- This will affect the amplitudes of reflected EM waves generated by external sources.

[ULF emissions](#)

[Conductivity change](#)

[Electrokinetic effects](#)

Courtesy of Hattori, 2006 and Yumoto et al., 2009